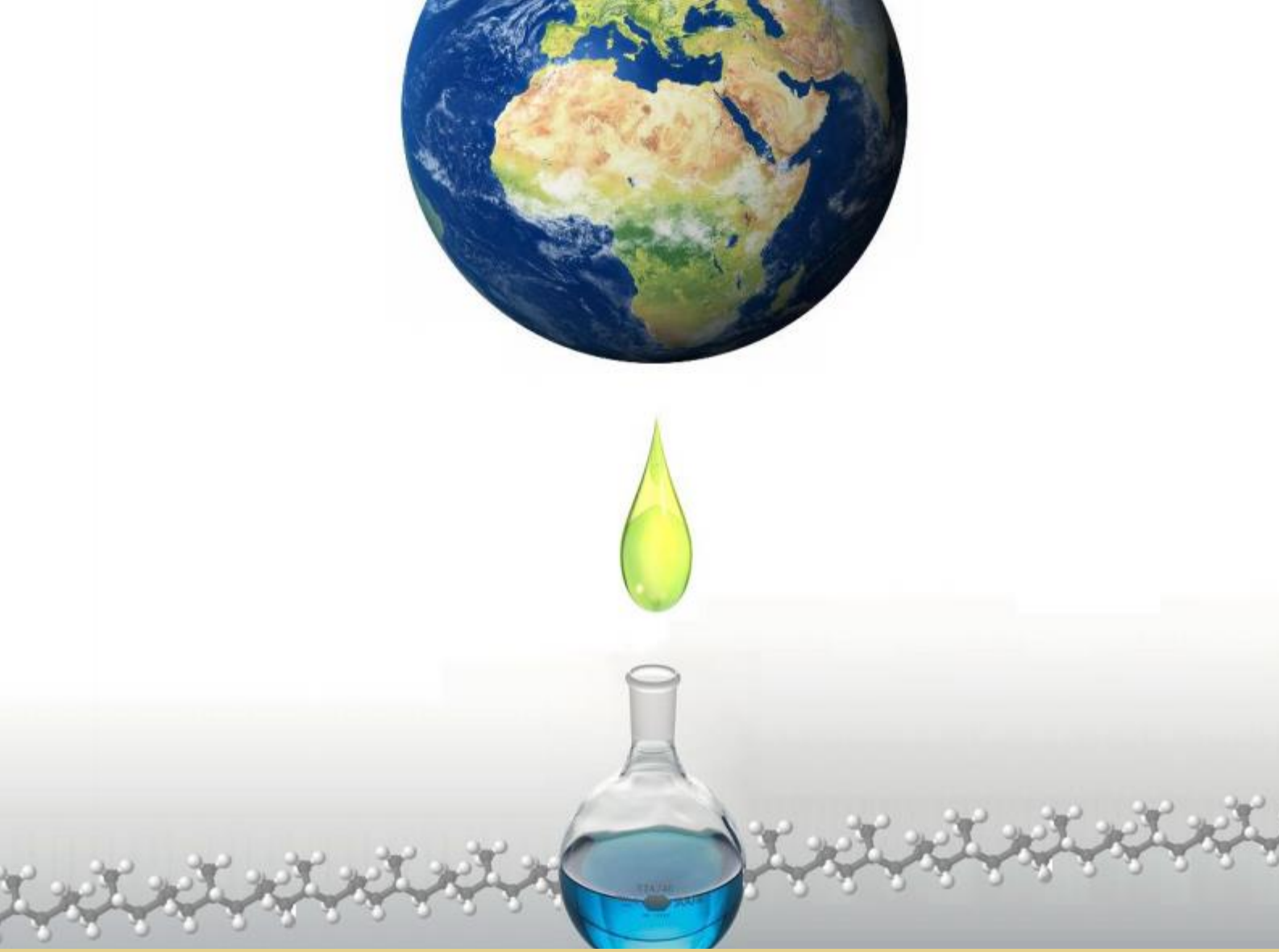

Pedro Manuel Maximiano Santos

Green Solvents for Reversible Deactivation Radical Polymerization

Thesis in the scientific area of Chemical Engineering, supervised by Professors Jorge Fernando Jordão Coelho and Arménio Coimbra Serra and submitted to the Department of Chemical Engineering, Faculty of Science and Technology, University of Coimbra

September 2015

· U C ·

UNIVERSIDADE DE COIMBRA

Pedro Manuel Maximiano Santos

Green Solvents for Reversible Deactivation Radical Polymerization

Thesis for the Master degree in the scientific area of Chemical Engineering, submitted to the Department of Chemical Engineering, Faculty of Science and Technology, University of Coimbra

Supervisors:

Prof. Dr. Jorge Fernando Jordão Coelho

Prof. Dr. Arménio Coimbra Serra

Host institutions:

CEMUC, Department of Chemical Engineering, Faculty of Sciences and Technology of the University of Coimbra

Coimbra

2015

· U C ·

UNIVERSIDADE DE COIMBRA

“What we know is a drop. What we don´t know is an ocean.”

(Sir Isaac Newton)

Acknowledgements

First and foremost I would like to acknowledge Professors Jorge Coelho and Arménio Serra for their guidance and all their advices, without which this work would not be possible, and for integrating me in the polymer research group at CEMUC, which I am proud to be a part of. I would also like to give my deepest thanks to the members of this research group, in particular to investigators Carlos Abreu, Fábio Branco, Joana Mendes, Joana Góis, João Costa and Patrícia Mendonça, for their invaluable assistance and mentorship during all my time in the laboratory.

Finally a special thanks to my parents and my closest friends, in particular Adriana Carecho, Andreia Timóteo, Célia Pedro, Cristiana Sousa, Diana Bregieiro, João Seiça, João Vareda, Maria Motta, Marisa Vieira and Sara Costa, for their emotional support and companionship on a daily basis throughout the 5 years of this course.

Abstract

Reversible Deactivation Radical Polymerization, RDRP, is a rapidly expanding topic in the field of polymer chemistry (in particular the 3 main RDRP methods: NMP, ATRP and RAFT), due to its unique ability to synthesize polymers with well-defined structures (predetermined molecular weights and low polydispersities), compositions and end functionalities. These methods, although very robust and versatile, are still largely based on toxic organic solvents (such as THF, DMF, DMSO, DCM...), which are not only harmful to the environment (one of the reasons behind recent legal restrictions to their use in the polymer industry) but also to human health. This last aspect hampers the broad use of the final polymers in the field of biomedicine, where RDRP methods find very extensive applicability. Despite the recent introduction of green solvents, such as water, alcohols, ionic liquids and supercritical CO_2, in RDRP methods, there is a wider range of possible green solvents to cover, and also room for improvements on existing systems.

Herein the use of cyclopentyl methylether (CPME), a green replacement for THF, as a cosolvent in SARA ATRP of methyl acrylate, styrene, glycidyl methacrylate and vinyl chloride was studied for the first time. The kinetic data obtained using CPME demonstrated a degree of control over the polymerization that is comparable to that in pure organic solvents/mixtures. This new CPME system proved to be very robust, as it presented excellent control features for different SARA agents (Cu(0), Fe(0) and $Na_2S_2O_4$) and different degrees of polymerization (100, 222 and 1000). Chain extension experiments, ^1H NMR and MALDI-TOF-MS spectra have confirmed the living character, high degree of end functionalization and well defined structure of the polymer chains prepared by this system.

In addition, CPME was used successfully (also for the first time) as a solvent in the nitroxide mediated polymerizations (NMP) of styrene and vinyl chloride and also in the reversible addition fragmentation chain transfer (RAFT) polymerizations of methyl acrylate, styrene, vinyl chloride and vinyl acetate. These polymerizations, in pure CPME, yielded polymers with polydispersity and k_p^{app} (apparent polymerization rate constant) values very close to those reported in the literature for similar systems using organic solvents, therefore establishing CPME as a transversal solvent/cosolvent for the 3 main RDRP techniques. The existence of chain end functionalities (derived from RAFT agents

or the nitroxide) was verified by ^{1}H NMR and ^{31}P NMR spectroscopy, and successful chain extension experiments with PVC macroinitiators (analyzed by GPC) confirmed the livingness of these systems.

Finally, a very fast and well controlled MA polymerization via SARA ATRP was observed for mixtures of DMSO, BMIM-PF_6 (1-butyl-3-methylimidazolium hexafluorophosphate) and glycols (ethylene glycol, diethylene glycol and triethylene glycol), using various SARA agents (Cu(0), Fe(0) and $Na_2S_2O_4$). One of the key reasons for this high polymerization rate is the existence of a polarity synergistic effect in the solvent mixture, which was observed with UV/Vis spectrophotometry measurements in the presence of the solvatochromic polarity probe Reichardt's Dye (30) (to determine the polarity parameter E_T (30)). Amazingly, the replacement of DMSO with water in the triethylene glycol mixtures allows the polymerization process to reach almost complete monomer conversion in just 15 min, while maintaining the polydispersity values close to 1.1 as in DMSO. This novel system, which has been termed "flash" SARA ATRP, is extremely attractive, from both the environmental and industrial implementation standpoints, and requires further investigation as to the reason behind its behavior.

Resumo

Os métodos de polimerização radicalar viva, LRP (em particular ATRP, NMP e RAFT), estão a ganhar rapidamente popularidade na área da química de polímeros, devido à sua capacidade única de sintetizar polímeros com estruturas e composições bem definidas (pesos moleculares predefinidos e baixos valores de polidispersividade) e com alto grau de funcionalização. Apesar da sua robustez e versatilidade, estes métodos são ainda fortemente baseados no uso de solventes orgânicos tóxicos (ex: THF, DMF, DMSO, DCM...), os quais não só são nocivos para o ambiente (o que levou à implementação de várias restrições legais ao seu uso na industria polimérica) mas também são extremamente prejudiciais à saúde humana. Isto dificulta a aplicação dos polímeros produzidos na área da biomedicina, a qual é uma das principais destinatárias dos métodos de LRP. Não obstante da recente introdução de solventes verdes neste campo, tais como água, álcoois, líquidos iónicos e CO_2 supercrítico, há ainda uma série de possíveis alternativas verdes por explorar e também oportunidades de melhoria em sistemas já existentes.

Neste trabalho o uso de ciclopentilmetiléter (CPME), um substituto verde de THF, como cosolvente em SARA ATRP de acrilato de metilo, estireno, metacrilato de glicidilo e cloreto de vinilo é apresentado pela primeira vez. Em todas estas polimerizações foram obtidos parâmetros cinéticos e de controlo do peso molecular cujos valores são comparáveis aos reportados para sistemas de solventes orgânicos puros. Este sistema de SARA ATRP em CPME apresentou baixos valores de polidispersividade mesmo para diferentes agentes SARA (Cu(0), Fe(0) e $Na_2S_2O_4$) e diferentes pesos moleculares (100, 222 e 1000), desta forma comprovando a sua robustez. O carácter vivo, alto grau de funcionalização e estrutura bem definida dos polímeros sintetizados foram confirmados por experiências de extensão de cadeia e análise de espectros de ^{1}H NMR e MALDI-TOF-MS, respetivamente.

Para além disso o CPME foi utilizado (também pela primeira vez) em sistemas de polimerização de estireno e cloreto de vinilo via NMP e de metil acrilato, estireno, acetato de vinilo e cloreto de vinilo via RAFT. Estes processos, em CPME puro, apresentaram valores de polidispersividade e de contante de velocidade de polimerização (k_p^{app}) muito próximos dos já registados para sistemas em solventes orgânicos. Estes resultados consagram o CPME como um solvente transversal às 3 principais técnicas de LRP. A existência

de grupos funcionais (derivados de agentes RAFT ou do nitróxido usado em NMP) foi atestada por ressonância magnética nuclear de ^{1}H e ^{31}P, e o sucesso de experiencias de extensão de cadeia, partindo de macroiniciadores de PVC, confirmou o carácter vivo das cadeias formadas por estes novos sistemas.

Por fim um novo sistema de polimerização rápida e controlada de MA por SARA ATRP foi desenvolvido em misturas compostas por DMSO, o liquido iónico BMIM-PF_6 (hexafluorofosfato de 1-butil-3-metilimidazólio) e glicóis (etilenoglicol, dietilenoglicol e trietilenoglicol), usando vários agentes SARA (Cu(0), Fe(0) e $Na_2S_2O_4$). Uma das principais razões para a rapidez deste processo é a existência de um efeito sinergístico de polaridade na mistura de solventes usada, observado através de testes solvatocrómicos recorrendo ao corante de Reichardt (30) e a espectrofotometria UV/Vis, os quais por sua vez permitiram a determinação do parâmetro de polaridade E_T (30). Espantosamente, a substituição de DMSO por água nas misturas DMSO/BMIM-PF_6/trietilenoglicol permitiu ao processo de polimerização atingir conversões de monómero de quase 100% em apenas 15 min, mantendo valores de polidispersividade próximos de 1.1 (tal como em DMSO), o que é um resultado inaudito em polimerizações de MA via ATRP. Este sistema original, que foi designado SARA ATRP "*flash*", é bastante promissor tanto em termos ambientais como de implementação na indústria, requerendo mais investigação para determinar exatamente os fenómenos por detrás do seu comportamento.

Thesis Outline

The first chapter of this thesis is an introductory (literature review) section in which reversible deactivation radical polymerization (RDRP) is first introduced and compared to the conventional free radical polymerization. The 3 main RDRP methods – NMP, ATRP and RAFT – are thoroughly described in terms of reaction mechanisms, kinetics, control and general components/conditions. In a further section the motivations and objectives of this work are presented.

In Chapter 2 the potential use of cyclopentyl methyl ether (a known greener replacement for tetrahydrofuran) in Supplemental Activator and Reducing Agent Atom Transfer Radical Polymerization (SARA-ATRP) is assessed for the first time. The results of kinetic experiments as well as chain livingness experiments (chain extensions and block copolymer synthesis) are presented, so as to draw conclusions about the feasibility of CPME as a co-solvent in this processes.

Chapter 3 continues the analysis initiated in Chapter 2, presenting the investigation conducted to evaluate the feasibility of CPME as a solvent for the RAFT and NMP processes. In a similar fashion this study comprises kinetic tests, chain extensions, block copolymerizations and structural analysis (H-NMR and MALDI-TOF-MS spectra).

Chapter 4 deals with the use of ionic liquid/glycol mixtures in SARA ATRP, specifically the mixtures of BMIM-PF_6 with EG, DEG and TEG (with either DMSO or water as co-solvents). Solvatochromic probe polarity tests complement the results of the main kinetic tests in order to evaluate the existence of synergistic effects (and possibly hyperpolarity effects), which are known in this kind of mixtures, and their role in the polymerization process.

Finally, in Chapter 5, the major conclusions of this work are summarized, along with open questions that should be answered in future works.

List of Publications

Published:

Maximiano, P., Mendes, J. P., Mendonça, P. V., Abreu, C. M. R., Guliashvili, T., Serra, A. C., et al., *Cyclopentyl methyl ether: A new green co-solvent for supplemental activator and reducing agent atom transfer radical polymerization*, Journal of Polymer Science Part A: Polymer Chemistry, **2015**. DOI: 10.1002/pola.27736.

Submitted:

Abreu, C. M. R., Maximiano, P., Guliashvili, T., Nicolas, J., Serra, A. C., Coelho, J. F. J., *Cyclopentyl Methyl Ether as A Green Solvent for Reversible-Addition Fragmentation Chain Transfer and Nitroxide-Mediated Polymerizations*, 2015.

Costa, J., Maximiano, P., Mendonça, P. V., Serra, A. C., Guliashvili, T., Coelho, J. F. J., *Ambient temperature "flash" SARA ATRP of methyl acrylate in water/ ionic liquid/glycols mixtures*, 2015

Contents

Acknowledgements V
Abstract VII
Resumo IX
Thesis Outline XI
List of Publications XIII
Contents XV
List of Tables XVII
List of Figures XIX
Nomenclature XXIII
List of acronyms XXV

Chapter 1 : Introduction 1

1.1 Free Radical Polymerization 1
1.2 Reversible Deactivation Radical Polymerization 3
1.2.1 Characteristics of RDRP methods 3
1.2.2 Nitroxide Mediated Polymerization 9
1.2.3 Atom Transfer Radical Polymerization 14
1.2.4 Reversible Addition Fragmentation Chain Transfer 26
1.3 The use of green solvents in RDRP 31
1.4 References 33

Chapter 2 : Cyclopentyl Methyl Ether: A New Green Co-Solvent for Supplemental Activator and Reducing Agent Atom Transfer Radical Polymerization 41

2.1 Abstract 41
2.2 Introduction 41
2.3 Experimental Section 43
2.4 Results and Discussion 43
2.4.1 Influence of the solvent mixture and composition 43
2.4.2 Influence of the catalytic system 45

2.4.3 Influence of the degree of polymerization 46
2.4.4 Polymerization of Styrene, Vinyl Chloride, and Glycidyl Methacrylate 47
2.5 Conclusions 50
2.6 References 50
Chapter 3 : Cyclopentyl Methyl Ether As A Green Solvent for Reversible-Addition Fragmentation Chain Transfer and Nitroxide-Mediated Polymerizations 57
3.1 Abstract 57
3.2 Introduction 57
3.3 Experimental Section 58
3.4 Results and discussion 58
3.4.1 RAFT Polymerization in CPME 59
3.4.2 NMP in CPME 64
3.5 Conclusions 68
3.6 References 68
Chapter 4 : Ambient temperature "flash" SARA ATRP of methyl acrylate in water/ ionic liquid/glycols mixtures 75
4.1 Abstract 75
4.2 Introduction 75
4.3 Experimental Section 76
4.4 Results and discussion 76
4.4.1 Influence of the glycol structure on the polymerization kinetics 76
4.4.2 Influence of the SARA agent nature 79
4.4.3 "Flash" SARA ATRP in water/BMIM-PF_6/TEG mixtures 80
4.4.4 "Livingness" of the PMA-Br chains 81
4.5 Conclusions 83
4.6 References 83
Chapter 5 : Conclusions and Future Work 89
Appendices 93

List of Tables

Table 1-1: Usual component proportions used in ATRP techniques. 25
Table 2-1: Molecular weight parameters of the PMA-Br prepared by SARA ATRP in CPME/EtOH/H_2O = 70/28/2 (v/v/v) at 30 °C, using different SARA agents 46
Table 2-2: Molecular Weight Parameters of the PS-Br, PGMA-Br, and Br-PVC-Br prepared by SARA ATRP in CPME-Based Mixtures. 49
Table 3-1: Kinetic and control parameters obtained for RAFT polymerizations in CPME with different monomers 62
Table 3-2: NMP of VC initiated by the BlocBuilder alkoxyamine at 42 °C, using CPME as a solvent under different experimental conditions. 66

List of Figures

Figure 1-1: Examples of monomers based on a vinyl functional group 1
Figure 1-2: FRP reaction mechanism. 2
Figure 1-3: Schematic representation of the main reversible deactivation equilibria in RDRP 4
Figure 1-4: Schematic representation of the detailed addition/fragmentation DT equilibria 5
Figure 1-5: Characteristic behavior of kinetic and DP vs fractional conversion plots exhibited by RDRP systems 6
Figure 1-6: Activation/Deactivation equilibrium in NMP 9
Figure 1-7: Ressonance structures of a nitroxide radical 12
Figure 1-8: Examples of nitroxides and an alkoxyamine used in NMP 13
Figure 1-9: Overall ATRP activation/deactivation equilibrium and the contributing subequilibria 14
Figure 1-10: Mechanisms of ISET and OSET processes 15
Figure 1-11: Representation of transition metals in the periodic table, highlighting those used successfully in ATRP so far 17
Figure 1-12: Examples of ligands for copper-based catalysts in ATRP and the respective values of k_{act} (in M^{-1} s^{-1}) for a system with a Cu(I)Br/L catalyst (L is one of these ligands) using the initiator EBiB, in MeCN at 35 °C 18
Figure 1-13: Examples of ATRP halogenated initiators and the respective values of k_{act} (in M^{-1} s^{-1}), in a system with a Cu(I)X/PMDETA catalytic complex (X = Br or Cl) in MeCN and at 35 °C 20
Figure 1-14: Experimental values of K_{eq} vs. values predicted using Kamlet-Taft polarity parameters of the solvents 22
Figure 1-15: Detailed mechanisms of SARA-ATRP and SET-LRP 24
Figure 1-16: Schematic representation of the thiocarbonylthio moiety and compounds based on it. 26
Figure 1-17: Complete RAFT mechanism 27
Figure 1-18: Proposed mechanism of termination responsible for rate retardation, for an intermediate species stabilized by resonance 28

Figure 1-19: Guidelines for the choice of the Z group in RAFT agents 29
Figure 1-20: Guidelines for the choice of the R group in RAFT agents 30
Figure 1-21: Solvent classification based on the LCA and EHS methods 32
Figure 2-1: General mechanism of the Cu(0)/CuX_2/L-catalyzed SARA ATRP (L: ligand and X: halide) 42
Figure 2-2: Chemical structure of cyclopentyl methyl ether and some of its "green" aspects 43
Figure 2-3: (a) Kinetic plots of conversion and $\ln[M]_0/[M]$ vs. time and (b) plot of number-average molecular weights and $Đ$ vs. monomer conversion for the SARA ATRP of MA in CPME/EtOH/H_2O = 70/28/2 (v/v/v) at 30 °C 44
Figure 2-4: ^1H NMR spectrum of a PMA sample obtained by SARA ATRP in CPME/EtOH/H_2O = 70/28/2 (v/v/v) at 30 °C. 45
Figure 2-5: (a) Kinetic plots of conversion and $\ln[M]_0/[M]$ *vs.* time and (b) plot of number-average molecular weights and $Đ$ *vs*. monomer conversion for the SARA ATRP of MA in CPME/EtOH/H_2O = 70/28/2 (v/v/v) at 30 °C, using different SARA agents. 46
Figure 2-6: (a) Kinetic plots of conversion and $\ln[M]_0/[M]$ *vs.* time and (b) plot of number-average molecular weights and $Đ$ *vs*. monomer conversion for the SARA ATRP of MA in CPME/EtOH/H_2O = 70/28/2 (v/v/v) at 30 °C, for different targeted DP values. 47
Figure 2-7: (a) Kinetic plots of conversion and $\ln[M]_0/[M]$ versus time and (b) plot of number-average molecular weights and $Đ$ versus monomer conversion for the SARA ATRP of Sty in CPME/DMF = 70/30 (v/v) at 60 °C 48
Figure 2-8: GPC chromatograms of a α,ω-di(bromo)PVC macroinitiator and PMA-*b*-PVC-*b*-PMA triblock copolymer, after "one-pot" chain extension by SARA ATRP in CPME/DMSO = 70/30 (v/v). 49
Figure 2-9: ^1H NMR of a purified PMA-*b*-PVC-*b*-PMA triblock copolymer obtained by "one-pot" SARA ATRP in CPME/DMSO = 70/30 (v/v) 50
Figure 3-1: RAFT polymerization of MA in CPME at 60 °C mediated by DDMAT using AIBN as conventional initiator 59
Figure 3-2: RAFT polymerization of Sty in CPME at 60 °C mediated by DDMAT using AIBN as conventional initiator 60
Figure 3-3: RAFT polymerization of VC in CPME at 42 °C mediated by CMPCD using Trigonox as conventional initiator 61

Figure 3-4: The ^{1}H NMR spectrum in d_8 -THF of PVAc-CTA (M_n^{SEC} = 9000; $Đ$ = 1.18) obtained in Table 1, entry 3 63
Figure 3-5: SEC traces of the PVC-CTA macro-CTA, and the "one-pot" extended PVC 63
Figure 3-6: SEC traces of the PVAc-CTA macro-CTA, and the PVAc-*b*-PVC block copolymer 64
Figure 3-7: NMP of Sty in CPME at 80 °C initiated by SG1-based BlocBuilder® alkoxyamine..... 65
Figure 3-8: NMP of VC in CPME at 42 °C initiated by SG1-based BlocBuilder® alkoxyamine. 65
Figure 3-9: ^{31}P NMR spectra in d_8 -THF of the purified PVC obtained in Table 3-2, entry 4. 67
Figure 3-10: SEC chromatograms of the PVC-SG1 macroinitiato and the PVC-*b*-PVC diblock copolymer after "one-pot" chain extension in CPME. 67
Figure 4-1: Chemical structure of the different glycols investigated. 77
Figure 4-2: Experimental E_T (30) values as a function of the glycol molar fraction in BMIM-PF_6/DMSO/glycol mixtures with Reichardt's dye 30..... 78
Figure 4-3: (a) Kinetic plots of conversion and $\ln[M]_0/[M]$ vs. time and (b) plot of number-average molecular weights and $Đ$ vs. monomer conversion for the SARA ATRP of MA in DMSO/BMIM-PF_6/TEG = 45/45/10 (v/v/v), DMSO/BMIM-PF_6/EG = 48/48/4 (v/v/v) and DMSO/BMIM-PF_6/DEG = 46/46/8 (v/v/v) at 30 °C 79
Figure 4-4: (a) Kinetic plots of conversion and $\ln[M]_0/[M]$ vs. time and (b) plot of number-average molecular weights and $Đ$ vs. monomer conversion for the SARA ATRP of MA in DMSO/BMIM-PF_6/TEG = 45/45/10 (v/v/v) at 30 °C, using different SARA agents 79
Figure 4-5: (a) Kinetic plots of conversion and $\ln[M]_0/[M]$ vs. time and (b) plot of number-average molecular weights and $Đ$ vs. monomer conversion for the SARA ATRP of MA in water/BMIM-PF_6/ TEG = 10/45/45 (v/v/v) at 30 °C..... 80
Figure 4-6: Experimental E_T (30) values of water/BMIM-PF_6/TEG mixtures with Reichardt's dye 30 81
Figure 4-7: SEC traces of the PMA-Br macroinitiator before and after the chain extension experiment..... 82
Figure 4-8: ^{1}H NMR spectrum ($CDCl_3$) of a PMA-Br obtained by "flash" SARA ATRP in water/BMIM-PF_6/TEG = 10/45/45 (v/v). 82

Nomenclature

$[M]$: Monomer concentration at any given time (mol/L or M)

$[M]_0$: Monomer concentration at the beginning of the reaction (M)

$[I]_0$: Initiator concentration at the beginning of the reaction (M)

$[P\bullet]$: Concentration of growing/active radicals at any given time (M)

$[R\text{-}Y]_0$: Initial alkoxyamine concentration (M)

$[X\text{-}Mt^{m+1}/L]$: Concentration of deactivator metal complex at any given time (M)

$[Mt^m/L]$: Concentration of activator metal complex at any given time (M)

$[CTA]_0$: Initial concentration of chain transfer agent (M)

k_x: Reaction rate constant (the index *x* indicates the type of reaction: *d* – dissociation; *i* – addition of first monomer unit to primary radicals; *p* – propagation; *tc* – termination by coupling; *td* – termination by disproportionation; *t* – termination (global); *tr* – chain transfer; *act* – activation; *deact* – deactivation; *a* – addition; -*a* – inverse addition; f – fragmentation; -f – inverse fragmentation; *c* – combination; *disp* – disproportionation; *comp* – comproportionation; *iR* – addition of first monomer unit to R leaving groups in reinitiation) (s^{-1} or $M^{-1}s^{-1}$, whichever is specified)

r_p: Overall rate of polymerization ($M\ s^{-1}$)

K_{eq}: Equilibrium constant of activation/deactivation processes in PRE systems

K_{ex}: Equilibrium constant for exchange process in DT systems

f: Initiation efficiency

$Đ$: Polydispersity Index ($= M_w/M_n$)

DP_n: Average degree of polymerization

DP_T: Targeted degree of polymerization

M_n^{th}: Theoretical number average polymer molecular weight (g/mol)

M_n^{GPC}: Number average polymer molecular weight determined by gel permeation chromatography (g/mol)

M_n^{SEC}: Number average polymer molecular weight determined by size exclusion chromatography (g/mol)

p: Fractional monomer conversion

M_A: Molecular weight of compound A (indicated in the index) (g/mol)

t: Time (s)

$E_{1/2}$: Redox potential (V)

$E_{1/2}^{0}$: Standard redox potential (V)

β^{m}: Stability constant of a Mt^{m}/L complex

R: Ideal gas constant (8.314 J mol^{-1} K^{-1})

F: Faraday's constant (96485.340 C mol^{-1})

T: Absolute temperature (K)

C_{tr}: Chain transfer constant

ϕ: Partition coefficient for reversible chain transfer

E_T (30): Reichardt's Dye (30) Polarity Parameter (kcal mol^{-1})

h: Planck's constant (6.626×10^{-34} J s)

c: Speed of light in vacuum (3×10^{8} m s^{-1})

N_A: Avogadro's constant (6.022×10^{23} mol^{-1})

ν: Frequency (s^{-1})

λ: Wavelength (nm)

λ_{max}: Wavelength (nm) corresponding to the maximum in the absorption spectra

List of acronyms

^{1}H NMR: Proton Nuclear Magnetic Ressonance
^{31}P NMR: Phosphorus-31 Nuclear Magnetic Ressonance
A(R)GET: Activators (Re)generated by Electron Transfer
AIBN: Azobisisobutyronitrile
ATRP: Atom Transfer Radical Polymerization
BMIM-PF_6: 1-butyl-3-methylimidazolium hexafluorophosphate
BPO: Benzoil Peroxide
Bpy: 2,2'-bipyridine
BrPN: 2-Bromopropionitrile
CCT: Catalytic Chain Transfer
$CDCl_3$: Deuterated Chloroform
$CHBr_3$: Bromoform
CLRP: Controlled/Living Radical Polymerization
CMPCD: Cyanomethyl methyl(phenyl)-carbamodithioate
CMRP: Cobalt Mediated Radical Polymerization
CPME: Cyclopentyl methyl ether
CTA: Chain Transfer Agent
$CuBr_2$: Copper (II) Bromide
d_8-THF: Deuterated Tetrahydrofuran
DCM: Dichloromethane
DDMAT: 2-(Dodecylthiocarbonothioylthio)-2-methyl propionic acid
DEBrPA: N,N-Diethyl-α-bromopropionamide
DEG: Diethylene Glycol
DEP: Diethyl phosphite
DEPN (or SG1): N-tert-butyl-N-[1-diethylphosphono-(2,2-dimethylpropyl)]nitroxide
DHB: 2,5-dihydroxybenzoic acid
DMF: Dimethylformamide
DMSO: Dimethyl Sulfoxide
DP: Degree of Polymerization
DPAIO: 2,2-diphenyl-3-phenylimino-2,3-dihydroindol-1-yloxyl
DT: Degenerative Transfer
e-ATRP: Electrochemical ATRP
EBiB: Ethyl α-bromoisobutyrate
EBPA: Ethyl α-bromophenylacetate
EG: Ethylene Glycol
EHS: Environmental, Health and Safety
ELINCS: European List of Notified Chemical Substances
Et_6TREN: Tris[2-(diethylamino)ethyl]amine
EtOH: Ethanol

FDA: Food and Drug Administration
FRP: Free Radical Polymerization
GMA: Glycidyl Methacrylate
GPC: Gel Permeation Chromatography
HABA: 2-(4-hydroxyphenylazo)benzoic acid
ICAR: Initiators for Continuous Activator Regeneration
ISET: Inner-sphere Electron Transfer
ITP: Iodine Transfer Polymerization
LCA: Life Cycle Assessment
LF: Living Chain Fraction
MA: Methyl acrylate
MADIX: Macromolecular Design by Interchange of Xanthate
MALDI-TOF MS: Matrix-Assisted Laser Desorption/Ionization Time of Flight Mass Spectroscopy
MAMA-SG1 (or BlocBuilder®): 2-((tert-butyl(1-(diethoxyphosphoryl)-2,2-dimethylpropyl)amino)oxy)-2-methylpropanoic acid
MBrAc: Methyl bromoacetate
MBriB: Methyl α-bromoisobutyrate
MBrP: Methyl 2-bromopropionate
MClP: Methyl 2-cloropropionate
Me_4 Cyclam: 1,4,8,11-Tetramethyl(1,4,8,11-tetraazacyclotetradecane)
Me_6TREN: Tris[2-(dimethylamino)ethyl]amine
MeCN: Acetonitrile
MIP: Methyl 2-iodopropionate
MMA: Methyl Methacrylate
MW: Molecular Weight
N[2,2,2]: 1,1,4,7,10,10-Hexamethyltriethylenetetramine
N[2,3,2]: N,N'-bis[2-(dimethylamino)ethyl]-N,N'-dimethylpropane-1,3-diamine
$Na_2S_2O_4$: Sodium dithionite
$NaHSO_3$: Sodium bisulfite
NMP: Nitroxide-Mediated Polymerization
NMR: Nuclear Magnetic Ressonance
NPPMI: *N*-propyl-pyridylmethanimine
NVP: N-vinyl pirrolidone
OSET: Outer-sphere Electron Transfer
PE: Polyethylene
PEBr: 1-Phenyl ethylbromide
PGMA: Polyglycidyl methacrylate
PMA: Polymethyl acrylate
PMDETA: N,N,N′,N′′,N′′-Pentamethyldiethylenetriamine
PMMA: Polymethyl methacrylate
PRE: Persistent Radical Effect
PS: Polystyrene

PTFE: Polytetrafluroethylene
PVAc: Polyvinyl acetate
PVC: Polyvinyl chloride
RAFT: Reversible Activation Fragmentation Chain Transfer
RDRP: Reversible Deactivation Radical Polymerization
SARA: Supplemental Activator and Reducing Agent
SBRP: Stibine mediated Radical Polymerization
SEC: Size Exclusion Chromatography
SET-LRP: Single Electron Transfer Living Radical Polymerization
SFRP: Stable Free Radical Polymerization
SR&NI: Simultaneous Reverse & Normal Initiation
Sty: Styrene
TEISO: 1,1,3,3-tetraethyl-1,3-dihydroisoindol-2-yloxyl
TEG: Triethylene Glycol
TEMPO: 2,2,6,6-tetramethyl-1-piperidynyl-N-oxy
TERP: Tellurium mediated Radical Polymerization
THF: Tetrahydrofuran
TIPNO: N-tert-butyl-N-[1-phenyl-2-(methylpropyl)]nitroxide
TMEDA: Tetramethylethylenediamine
TMS: Tetramethylsilane
TPMA: Tris(2-pyridylmethyl)amine
TSCA: Toxic Substances Control Act
VAc: Vinyl Acetate
VC: Vinyl Chloride

CHAPTER 1

Introduction

Chapter 1: Introduction

1.1 Free Radical Polymerization

Since the first decades of the 20th century free radical polymerization (FRP) has played a major role in polymer industry, accounting (today) for the production of nearly 50% of all commercially available polymers. [1-3] Polystyrene (PS), polyethylene (PE), polyvinyl chloride (PVC), poly(meth)acrylates, poly(meth)acrylamides, polyvinyl acetate (PVAc) and polytetrafluoroethylene (PTFE) are examples of such polymers, which form the basis of everyday materials like plastics, rubbers, paints, glues and so on. Vinyl-based monomers (with the appropriate functionalities), like those illustrated in Figure 1-1 are the repeating units to afford polymers prepared by radical based methods.

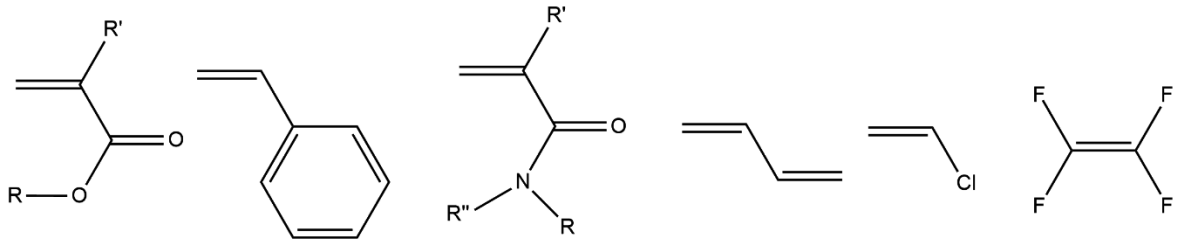

Figure 1-1: Examples of monomers based on a vinyl functional group. From left to right: acrylates (if R'= H) or methacrylates (if R' = CH_3), styrene, acrylamides (if R' = H) or methacrylamides (if R' = CH_3), butadiene, vinyl chloride and tetrafluoroethylene

The FRP reaction mechanism, depicted in Figure 1-2, is composed of a series of elementary steps, starting from the generation of radicals via homolitic cleavage of initiator species (initiation), followed by successive addition of monomer units to the radicals (propagation) and finally bimolecular reactions between two radicals that end chain growth (termination), either by disproportionation or coupling. [2, 4] Chains also terminate due to chain transfer reactions [2], in which the reactive radical is transferred to another species (e.g. solvent), monomer unit, polymer chain or to another position along the same chain (backbiting), and continues to grow on the basis of these species (i.e. there is no radical loss as in termination reactions) [1]. However, in the absence of chain transfer agents, this process is only important at high temperatures, which indicates that termination is the predominant chain breaking process in FRP. [2]

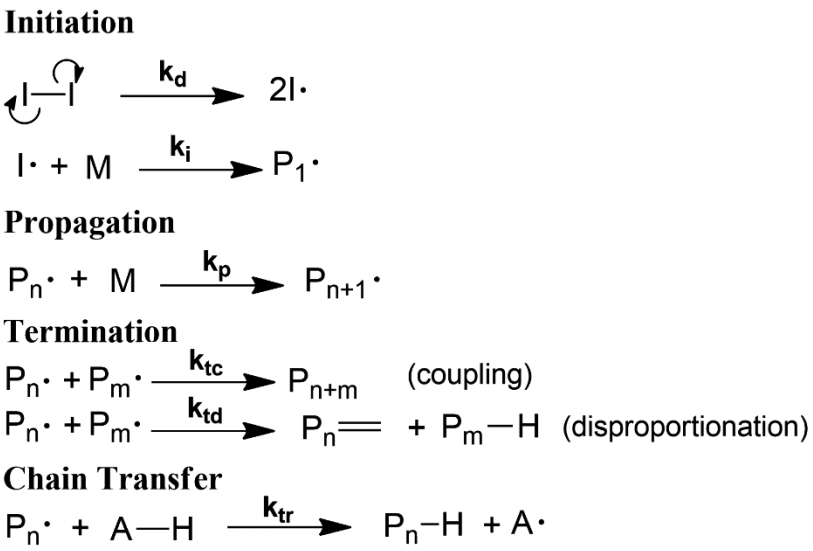

Figure 1-2: FRP reaction mechanism. I represents an initiator fragment, M a monomer unit, P_n a polymer chain of n repeating units and A a chain transfer agent. Adapted from ref. 4.

Initiation reactions in FRP are generally slow [2, 4] (in order to achieve high molecular weights) and dominated by the rate of dissociation [4]. The generation of primary radicals by homolitic bond cleavage is triggered either by heat (in the case of peroxides or diazenes, for example BPO and AIBN), light (e.g. for benzoin and benzophenone) or redox (electron transfer) reactions (typically involving metals and organic substrates). [1] Propagation proceeds with high regioselectivity, as chains tend to grow in a linear fashion (head-to-tail) [2, 4], and chemoselectivity, attaining high molecular weights. Stereoselectivity is typically low [2], yielding mostly atatic polymers. Termination is diffusion controlled and it is so fast (k_t is in the order of 10^7-10^8 M^{-1} s^{-1}, vs. 10^2-10^4 M^{-1} s^{-1} for k_p values) that the growing radicals in the system have a very short lifetime (in the order of 1 second), thus preventing manipulation/functionalization of the chains and construction of well-defined architectures. [2, 5] Once a polymer chain terminates it cannot grow any further (it is said to be "dead"). New polymer chains start to grow at a fast rate from primary radicals being generated slowly. [1] This results in a very wide distribution of molecular weights (high $Đ$ values) and the impossibility of conducting block copolymerization or reinitiation. [2]

The overall rate of polymerization in steady-state conditions (radical concentration constant over time), and neglecting chain transfer reactions, can be computed from the rates of initiation, propagation and termination, yielding the following expression [2]:

$$r_p = k_p[M][P\bullet] = k_p[M]\sqrt{fk_d[I]_0/k_t} \quad (1)$$

where f, the initiator efficiency, is a factor accounting for recombination and other side reactions that result in a loss of primary radicals generated. [1]

The biggest advantage of FRP is the fact that it can be conducted in bulk monomer, in a solvent, in suspension or in emulsions, for almost all vinyl monomer functionalities in a broad range of reaction conditions (even tolerant to water or impurities), therefore making it a very versatile and robust polymerization process to be applied at industrial scale. [1, 2, 6, 7]

1.2 Reversible Deactivation Radical Polymerization

Despite its undeniable industrial success, the fast radical termination in FRP hampers its application in specific areas where tailor-made polymer structures (e.g. stars, networks, graft and block copolymers [1, 5, 8]) and responsive chain functionalities are required. To achieve that purpose, techniques such as anionic polymerization were developed, in which termination reactions are prevented (due to electrostatic repulsion between chains), thereby allowing the control over chain length, composition and architecture. [2, 4] The polymers synthetized by this method are said to be "living", as they retain enough end functionalities to allow further reinitiation whenever fresh monomer is added to the reaction mixture. [3] However anionic polymerization is not nearly as robust as FRP, since only a limited number of monomers can be polymerized, and only under very strict conditions. [1, 3, 4, 6]

In an effort to merge the living character of anionic polymerization with the versatility of radical chemistry, reversible deactivation radical polymerization (RDRP) methods (also called controlled/living radical polymerization, CLRP) have been devised and are currently gaining much attention from both the industrial and academic domains. [3, 5, 6, 8]

1.2.1 Characteristics of RDRP methods

The main feature of all RDRP methods is the presence of a fast dynamic equilibrium between active macroradicals (that can propagate and terminate as in FRP) and dormant (deactivated) chains. [1-9] In this equilibrium a "capping" molecular group (X) binds re-

versibly to the active chains, yielding the dormant species, either in an activation/deactivation process, which may be spontaneous (thermally driven) or catalyzed (presented in Figure 1-3 a) and Figure 1-3 b), respectively), or via degenerative (reversible) transfer reactions between chains (Figure 1-3 c)). [1-3, 5-7, 9] While termination reactions are not avoided, the constant shift between dormant and active species minimizes their occurrence [9], providing that the chains are dormant most of the time (because termination only takes place when they are active) [6]. This effect ensures that the majority of chains (> 90%) [2, 5, 8], despite being deactivated, remain "alive", because the terminal functional groups that they possess (the moieties derived from the "capping" group) allow for further activation and subsequent propagation (as in anionic polymerization), as long as there are monomer units in the system and the functional groups remain attached. It should be noted that, even when radical concentration in FRP and RDRP systems is equal, termination per chain is much slower for the latter [3], thus resulting in radicals with an extended average lifetime (approximately 1 h) [1, 2].

For the equilibria based on the activation/deactivation cycles (Figure 1-3 a) and b)), the predominance of the dormant state is a consequence of the persistent radical effect (PRE). [2] As activation proceeds, the active chains (P_n•) and the deactivator species (X or X-Y) are formed but, unlike the growing radicals, these species are generally stable as they are unable to react (couple) with themselves. [1-3] However the growing radicals not only react with the stable radicals but they also terminate with each other and, as a result of

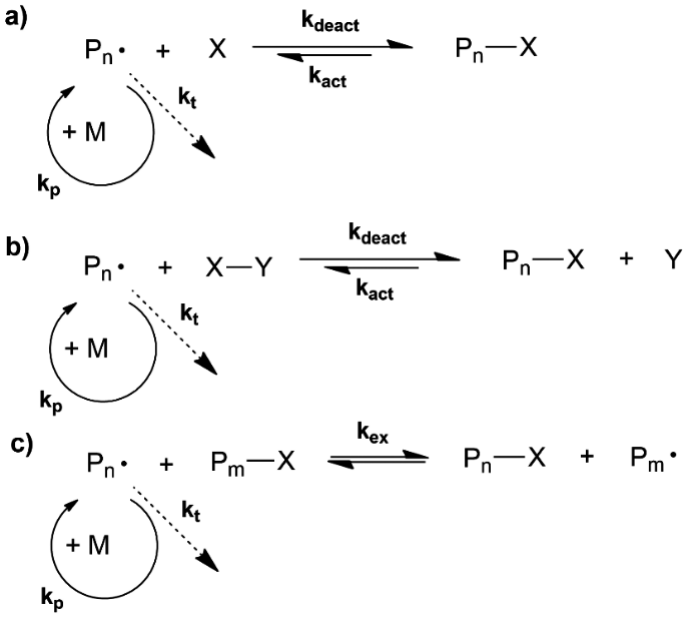

Figure 1-3: Schematic representation of the main reversible deactivation equilibria in RDRP. a) – Mechanism based on the PRE; b) – Mechanism based on the PRE mediated by a catalyst Y; c) – Mechanism based on a degenerative chain transfer process. Adapted from ref. 9.

their gradual disappearance, the stable deactivator species begins to accumulate in the system. [1-4, 6] The increase in stable radical concentration with time (following a 1/3 power law [2]), which is named PRE, drives the equilibria of Figure 1-3 a) and b) to the right, hence increasing the rate of chain deactivation and decreasing the probability of irreversible chain breaking reactions. [2, 6, 8] Nevertheless, the near absence of termination does not alone guarantee a controlled polymerization. In order for chains to grow simultaneously they also have to be generated (ideally) at the same time, which means that initiation in this kind of RDRP systems needs to be very fast. [2, 6, 7] Furthermore, the rate of activation/deactivation should be compatible with that of propagation[7] (only a few monomer units should be incorporated in each cycle, in a time window of milliseconds [2]), and a high degree of chemoselectivity should be obtained [4]. If all of these criteria are fulfilled the chains will grow equally and at a concerted pace, resulting in $Đ$ values close to 1 ($1.0 < Đ < 1.5$). [1, 5, 9] Different methods of RDRP based on PRE exist today, depending on the type of deactivator species employed, like nitroxide mediated polymerization (NMP), organometallic mediated processes like cobalt mediated radical polymerization (CMRP), polymerization using *iniferters* and catalytic techniques like atom transfer radical polymerization (ATRP). [2, 3, 7] However the most successful of these are NMP and ATRP [3, 6, 8], and for that reason they will be discussed in detail on the next sections.

On the other hand, in degenerative transfer (DT) processes, like those of Figure 1-3 c), chains exchange active radicals with one another through a chain transfer agent. The exchange process may occur via atom/group transfer (e.g. for alkyl iodides in ITP, for cobalt porphyrins in CCT or for Te and Sb based organometallic species in TERP an SBRP, respectively) or via addition/fragmentation reactions (e.g. with thiocarbonylthio compounds in RAFT) like those displayed in Figure 1-4. [1-3, 10] In DT a conventional initiator is typically required, since in the exchange equilibrium there is no loss or gain of radicals during deactivation/activation (they simply change positions). [2-4] By using a large amount of chain transfer agent in comparison to initiator[2] it is possible to keep the majority of chains in the dormant state, therefore reducing the amount of reactive radicals in every instant to a minimum (with a concentration at least a thousand times smaller than

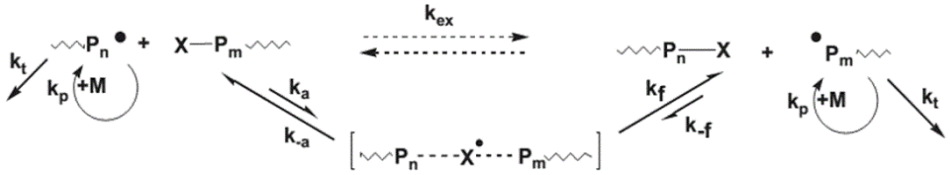

Figure 1-4: Schematic representation of the detailed addition/fragmentation DT equilibria. Reproduced from ref. 2.

that of dormant species [1]). Furthermore, unlike PRE-based systems, the DT equilibrium in Figure 1-3 c) is thermodynamically neutral (the equilibrium constant, K_{ex}, equals 1) [1, 2, 4, 7], instead of being preferentially shifted to one direction, because deactivation occurs in both ways and needs to be balanced so that chains grow uniformly. This is due to the nature of the intermediate species formed during exchange, when a dormant chain (P_n–X) is added to an active chain (P_m•). Upon fragmentation the intermediate radical formed may either release the active chain again or it may yield the previously dormant chain (now active). [2] Both processes are fast (ideally occurring at the same rate), resulting in a short lifetime of intermediate species and a good control over polymerization (but only if $k_{tr} > k_p$). [2, 4, 7] Within the scope of DT processes, RAFT has received more attention from the scientific community [3, 6, 8] and will be discussed later on.

The control over the molecular weight and structure of the polymer achieved by RDRP systems is evidenced by the following observations [6, 7]:

i. First order kinetics of polymerization with respect to monomer concentration (plot of ln ($[M]_0/[M]$) vs. t is a straight line passing through the origin of the axis), according to equation 2:

$$r_p = -\frac{d[M]}{dt} = k_p[M][P\bullet] \Leftrightarrow \ln\left(\frac{[M]_0}{[M]}\right) = \ln(1-p) = k_p{}^{app}t \qquad (2)$$

This suggests that the number of growing radicals is constant (in equation 2 a constant [P•] is included in the apparent polymerization rate constant, $k_p{}^{app}$), in the steady-state conditions that develop as a consequence of a balance between activation and deactivation rates (rather than initiation and termination like FRP) [1, 2].

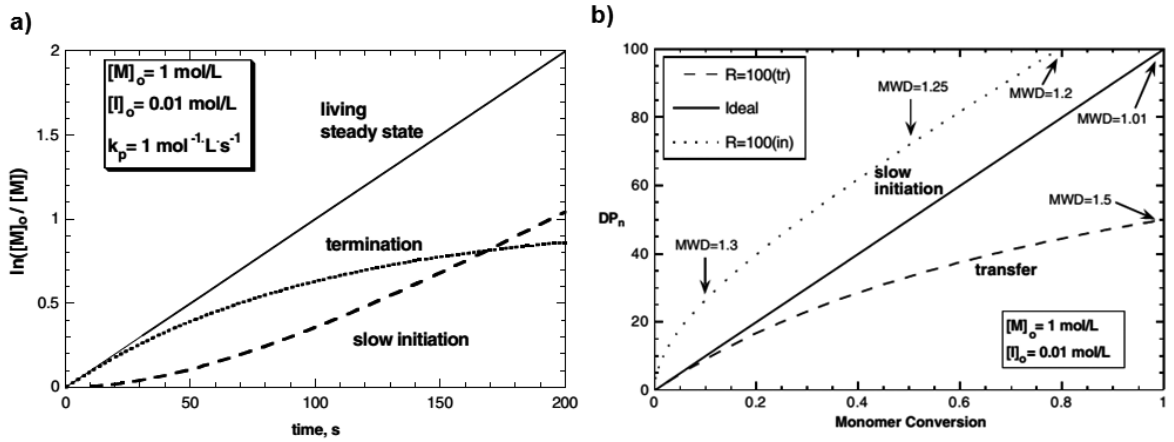

Figure 1-5: Characteristic behavior of kinetic a) and DP vs fractional conversion b) plots exhibited by RDRP systems. The effect of termination and slow initiation is represented by the dotted and dashed lines (respectively) in a), whereas in b) the dotted and dashed lines recreate systems with a rate of initiation and chain transfer to monomer (respectively) 100 times slower than propagation. Adapted from ref. 1.

A direct consequence of this equation is that by increasing the target degree of polymerization ($DP_T = [M]_0/[I]_0$) less radicals will be present in the system (because $[I]_0$ is smaller for the same $[M]_0$) and thus the polymerization will be slower (and vice-versa). Some deceleration may take place [7], especially at high conversions, due to inevitable termination reactions [4]. The possible behaviors of the kinetic plots are shown in Figure 1-5 a). It should be noted that a linear kinetic plot is not a sufficient condition to state that the polymerization was controlled. [3]

ii. Measured values of molecular weight (M_n^{GPC}) grow linearly with conversion and are in good agreement with theoretically predicted values (M_n^{th}), which are calculated by the following equation:

$$M_n^{th} = DP_T \times p \times M_{monomer} + M_{initiator} = \frac{[M]_0}{[I]_0} \times p \times M_{monomer} + M_{initiator} \quad (3)$$

This is also indicative of an efficient initiation ($f \approx 1$) as less radicals generate longer (higher MW) chains, and near absence of irreversible chain transfer (because this would prevent chains from reaching the targeted DP) [7], as is exemplified in Figure 1-5 b).

iii. Polydispersity values ($Đ$) decrease with conversion (approximately following a Poisson distribution), except at high conversions (where deviations may take place as a result of functionality losses, mainly due to chain transfer reactions [1]). This evolution of $Đ$ with conversion for PRE-based systems and DT-based systems is described by equations 4 and 5, respectively [1]:

$$\frac{M_w}{M_n} = 1 + \frac{1}{DP_n} + \frac{[I]_0 k_p}{[X] k_{deact}} \left(\frac{2}{p} - 1 \right) \quad (4)$$

$$\frac{M_w}{M_n} = 1 + \frac{1}{DP_n} + \frac{k_p}{k_{tr}} \left(\frac{2}{p} - 1 \right) \quad (5)$$

where [X] represents the concentration of deactivator species (in the case of catalyzed systems it will be [X-Y] as indicated in Figure 1-3).

iv. Chains exhibit a high degree of end functionalization (identifiable, for example, by NMR spectroscopy) that is neither affected by a slower initiation nor by the exchange process. Therefore chain breaking reactions are the main causes for the loss of terminal functional groups, especially at high conversions, as bigger chains are more susceptible to this processes [4].

Chain livingness, i.e. the ability to further react in the presence of monomer, can be verified by conducting chain extension experiments, in which more monomer is added to the reaction mixture (one-pot experiment) or to a solution of an already isolated polymer macroinitiator (essentially composed of dormant chains). Analysis of the initial and extended polymer samples by GPC or SEC should reveal a shift of the curve towards higher molecular weights after the chain extension experiment. Alternatively polymer livingness can be assessed by quantifying the percentage of chain-end functionality or by determining the amount of free deactivator at the end of the polymerization. [1, 3]

The control that RDRP methods exert over the polymerization is extremely advantageous, as it allows the synthesis of polymers with predetermined MW's, low $Đ$ values and with a wide range of compositions and architectures, all of which were unattainable via traditional FRP. [2, 3] These include block, gradient and graft copolymers, star-shaped polymers, networks formed by crosslinking, cyclic polymers, hyperbranched polymers (all having reactive/responsive end functional groups), and molecular composites. [2, 8, 9] Here are listed a few examples of such materials and their potential applications [2, 3, 8, 9]:

- Replacements for commercial polymers with enhanced mechanical, thermal and chemical properties/stabilities. One good example is thermoplastic elastomers, used in adhesives, sealants, lubricants, coatings, flexographic printing, chromatographic packing, etc.;
- Supersoft elastomers (consisting of lightly crosslinked graft copolymers);
- Additives for paints, coatings, inks and cosmetics, to control rheology and pigment dispersion, for instance (some are already produced at commercial scale by DuPont® [8]);
- Surfactants (amphiphilic block copolymers) [11]
- Capsules (typically block copolymers) for controlled delivery of drugs, genes, enzymes, proteins and other bioactive agents; [11-13]
- Bioresponsive materials (e.g. pH and temperature sensors); [13]
- Nanostructured materials that serve as electronic components (such as transistors);
- Organic/Inorganic and Organic/Biopolymer hybrids with unique properties (for example to separate peptides with very high resolution);
- Surface modifications;
- Recyclable and/or biodegradable polymers.

In addition, a large variety of monomers can now be polymerized via RDRP and the main methods in this category (ATRP, NMP and RAFT) have been successfully extended to dispersed systems as well. [1, 3] Despite the vast range of possibilities, RDRP still has certain limitations. Since the probability of occurrence of chain breaking reactions is bigger for longer chains (as they are active for longer times the probability of termination/transfer per chain is higher), it is difficult to produce higher target DP polymers with good control. [1, 3] The rate of polymerization in RDRP is also generally smaller than in FRP [2, 4] and for these reasons the production of well-defined high MW chains (MW > 100 000) by this techniques is rarely possible.

In the following sections the 3 main RDRP techniques – NMP, ATRP and RAFT – will be discussed thoroughly.

1.2.2 Nitroxide Mediated Polymerization

NMP is one of the methods that can be classified as stable free radical polymerizations (SFRP), which rely on a reversible deactivation reaction between the growing macroradicals and a stable radical, in this case a nitroxide (species with a >N-O• moiety), as illustrated in Figure 1-6 [1, 2, 6]. The control over the polymerization in this system is governed by the PRE, as the stable radicals should be unable to terminate with themselves, transfer to the monomer or participate in other side reactions, therefore accumulating in the system over time as the transient radicals terminate with themselves. [2, 6] In reality, side reactions such as nitroxide degradation and disproportionation between active chains and the nitroxide (possibly via β-H elimination) may take place, resulting in deviations from this ideal behavior. [1, 6] The activation of dormant species (alkoxyamines) occurs spontaneously by thermal (or photo induced) homolitic dissociation of the C-O bond between the chain and the nitroxide. [6]

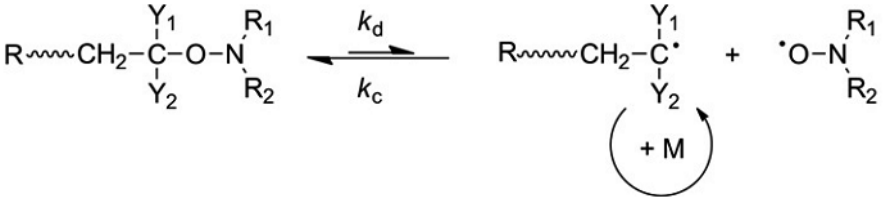

Figure 1-6: Activation/Deactivation equilibrium in NMP. Adapted from ref. 6.

Kinetic considerations

As discussed previously, NMP, like other RDRP systems, has first-order kinetics with respect to monomer concentration in steady-state conditions (and absence of chain transfer reactions). It should be noted however that, for systems obeying the PRE, the process actually has different stages regarding its kinetics. Just after the start of the reaction a pre-equilibrium stage takes place, during which the concentration of both the initiating and nitroxide radicals increases with time, as decomposition of the initiating species is effected. [6] In this stage the polymerization exhibits a 2/3 power law kinetics, which is corroborated by equations derived from PRE theory. [1, 6] When the concentration of both radicals reaches a level high enough to allow their bimolecular coupling, a state of quasi-equilibrium is reached (that is represented in Figure 1-6), in the so called intermediate regime, which is governed by the already enunciated first order kinetics of equation 2. [1, 6] Eventually, as termination drains away the concentration of growing radicals and they stop being replenished by initiator decomposition, the quasi-equilibrium disappears and another kinetic stage is established until the concentration of active radicals reaches 0 (corresponding to the maximum concentration of nitroxide species).[6]

As the ideal RDRP conditions exist during the intermediate stage, it is desirable that it lasts throughout most of the polymerization process, which means that the pre-equilibrium stage must be extremely short lived and termination reactions should be relatively slow ([P•] should be low). [1] In most practical cases this first condition holds true, as the pre-equilibrium lasts only a few milliseconds. [6, 8] However one thermodynamic parameter is crucial to determine if the quasi-equilibrium is reached: the activation/deactivation equilibrium constant, K_{eq} (= k_d/k_c). For this to happen the following condition must be verified [6]:

$$K_{eq} < \frac{[R-Y]_0 k_c}{4k_t} \tag{6}$$

A high K_{eq} is desirable to attain a good control (it would mean that k_{deact} in equation 4 is high and thus $Đ$ is closer to 1) but if K_{eq} is very high (disrespecting equation 6) the cross coupling of radicals is no longer thermodynamically favored and, as a consequence, the equilibrium of Figure 1-6 never develops and the nitroxide acts only as an inert species (with concentration increasing linearly with time as a result of the alkoxyamine decomposition). [6] On the other hand if K_{eq} is very small, the equilibrium is so shifted to-

wards dormant species that the concentration of growing radicals is extremely low, resulting in poor propagation rates and impractically long reaction times [2, 6]. This is one of the major limitations of NMP, as many nitroxides have low values of K_{eq}, particularly TEMPO derivatives, requiring high temperatures (above 100 °C for TEMPO) to conduct most polymerizations at a reasonable rate [6]. The value of K_{eq} for a dormant alkoxyamine chain depends mostly on the dissociation rate constant (k_d) which, in turn, is a function of both the alkyl fragment and the nitroxide fragment stabilities. [6] k_d values typically follow an order similar to that of the stability of the nitroxide radicals for ring sizes (*vide infra*) and there are correlations linking radical stabilizing effects (resonance, steric strain and polarity) to an increase in k_d. [6] Whenever the use of other nitroxides is restricted, additives may be employed to enhance the overall kinetics, such as strong organic acids (e.g. camphorsulfonic acid) that react with the nitroxide, lowering its concentration; reducing agents for the nitroxide (e.g. ascorbic acid); acyl compounds (to weaken the C-ON bond) and initiators with long half-times [1, 6].

Radical sources

NMP is the simplest RDRP method to execute, as only a source of primary radicals and of nitroxide radicals is needed. In the so called bimolecular initiation this species are generated independently, as the primary radicals are produced from any conventional FRP initiators, while the nitroxide comes from dissociation of some molecule bearing the desired radical structure. [1, 2, 6] Although this method takes advantage of commercially available initiators, the unpredictable efficiency of their dissociation imposes some limitations regarding the control over the MW and may also change the polymerization kinetics significantly, rendering them irreproducible (the nitroxide and initiator should be present in a 1:1 proportion, since an excess of nitroxide pushes the equilibrium of Figure 1-6 towards dormant species, lowering the overall rate of polymerization). [1, 6]

This very important limitation was suppressed by the development of unimolecular initiators, i.e. molecules that, upon dissociation via homolitic cleavage of a bond, yield both the primary radicals and the nitroxides on the desired 1:1 proportion. [1, 6] Alkoxyamines (species with generic formula R_3-O-N-R_1R_2, where R_3 is an alkyl substituent) are widely used for this purpose, as they possess a thermally unstable C–O bond that easily cleaves homolitically, sometimes even at moderate temperatures. [1, 2] These molecules provide a better control over the polymerization (when compared to bimolecular systems) and can also be fine-tuned to allow subsequent chemical modifications of the polymer chains

from both end functional groups.[1, 2, 6] One of the most versatile alkoxyamines used is MAMA-SG1 (commercialized under the name BlocBuilder®), which is represented in Figure 1-8. [6]

Figure 1-7: Ressonance structures of a nitroxide radical. Reproduced from ref. 6.

Nitroxides

Nitroxide radicals are remarkably stable due to the existence of a delocalized unpaired electron in the p orbitals along the N-O π bond, creating a stabilizing resonance effect (between the two mesomeric forms of the radical, shown in Figure 1-7). [6] However, the stability of a radical is also strongly dependent on the nature of the substituent groups attached to the nitrogen atom, which may generate further stabilizing effects due to resonance or steric strain. [6] On the other hand, they may also destabilize the structure due to side reactions. [6]

Historically, the first nitroxide employed in NMP was TEMPO, but such a system could only polymerize styrene, at a high temperature (120 °C) and slow rate (due to a relatively slow decomposition rate of the alkoxyamine chain). [2, 6] This prompted the creation of a wide array of nitroxides, either having cyclic (typically between 5 to 8 atoms in the ring) or acyclic (open chain) structures, with or without heteroatoms. [6] The order of stability for these types of structures (and therefore the order of increasing k_d values) is as follows: 5-membered rings < 6-membered rings < open chains < 7-membered rings. [14] Some examples of nitroxides are shown in Figure 1-8. Structures with tertiary sp^3 carbons directly bonded to the nitrogen are the most stable (providing that steric strain does not favor the homolitic cleavage of these bonds instead of the C-O bonds), since a hydrogen atom on the vicinal carbons has a destabilizing effect. [2, 6] However some nitroxides having H atoms in vicinal carbons (e.g. TIPNO and DEPN) are actually stable enough to mediate polymerizations, not only of styrene but other monomers. [2, 6]

Monomers

Years of research in different methods to synthesize nitroxides and alkoxyamines led to the creation of a vast library of these species, which currently covers many of the existing vinyl monomer families. From the initial TEMPO systems intended for styrene, NMP can now be used to polymerize styrene derivatives, vinylpyridines, acrylates, acrylonitrile (AN), acrylic acid (AA), acrylamides, dienes, VC and some cyclic monomers, for

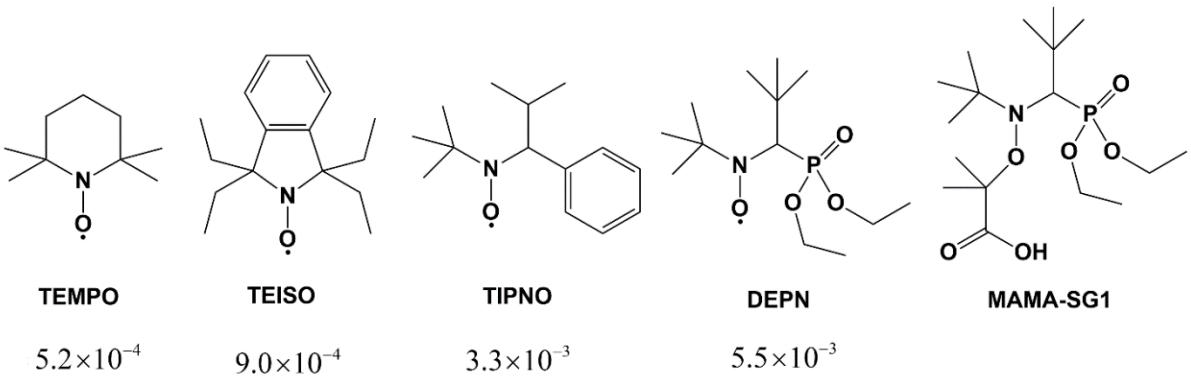

Figure 1-8: Examples of nitroxides and an alkoxyamine used in NMP. Numbers underneath the nitroxides are the values of k_d (in s^{-1}) for the respective alkoxyamines based on the styryl alkyl fragment, at 120 °C. Adapted from ref. 6.

instance. [6] However no control can be achieved during homopolymerization of monomers that are classified as "less activated monomers" (i.e. vinyl monomers whose resulting radicals have low stability) such as VAc and N-vinylpirrolidone (NVP) but, in the case of NVP, copolymerization via NMP seems to be controlled. [6] This method also shows major limitations for methacrylates, as so far only one nitroxide (DPAIO) was able to homopolymerize MMA successfully. [2, 6] All other nitroxides failed at this task due to β-H abstraction side reactions, and only copolymerization with small amounts of Sty (1-9 % mol) or other well controlled monomers yielded well-defined polymethacrylates. [6]

Solvent

Bulk polymerization is a common method in NMP (especially for TEMPO systems) but several reports are available dealing with solution and dispersion polymerizations. [15] Organic solvents, like 1,4-dioxane [16], chlorobenzene [15], DMF [17] and DMSO [18], are the most used, but polymerizations in water (using water soluble SG1-based alkoxyamines in dispersed media) [19], water/alcohol solutions [20] and ionic liquids [6] have also been reported. With respect to solvent effects, the rate and control of NMP seem to be dependent primarily on the viscosity of the solvent (since the nitroxide radicals diffuse freely across the system) and the ability of the solvent molecules to solvate and stabilize the nitroxide radicals or the polymer chains. [15, 21] The latter effect has a strong influence on the values of k_d for the alkoxyamine chains, since it may weaken the C-NO bond. [15, 16, 21] It is also crucial to select a solvent that does not promote side reactions (like chain transfer). [22]

1.2.3 Atom Transfer Radical Polymerization

ATRP is perhaps the most versatile and efficient of the RDRP techniques and, because of this, it is the target of intense investigation from the scientific community that is growing exponentially (with the number of published ATRP-related papers doubling each year and largely surpassing RAFT and NMP methods). [5, 9]

Mechanism

Besides the conventional initiation, propagation and termination reactions, typical of a radical polymerization, the ATRP mechanism also includes a reversible deactivation equilibrium, where active chains are deactivated by coupling with a (pseudo)halogen atom (X) radical, and dormant chains are activated by homolitic cleavage of the dormant alkyl halide chain C-X bond, as shown below in Figure 1-9. [2, 5, 9] These processes are mediated by a catalyst (consisting of a transition metal/ligand complex with a counterion) which, during activation, abstracts the halogen atom and undergoes oxidation, whereas in deactivation the inverse process takes place as the metal is reduced to a lower oxidation state. [2, 9, 10] The main equilibrium is actually a combination of electron transfer processes, comprising four subequilibria that are depicted in Figure 1-9. [2, 9]

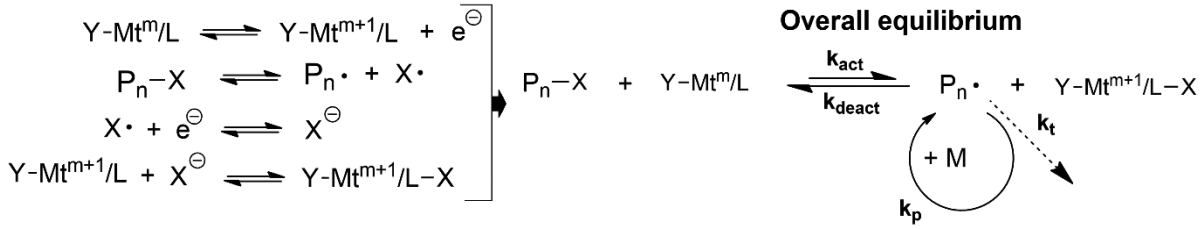

Figure 1-9: Overall ATRP activation/deactivation equilibrium and the contributing subequilibria. X is a halogen atom (X = Cl, Br, I), Mt^m is a transition metal in the oxidation state m, L is a ligand and Y is a counterion. Adapted from ref. 9.

Two different electron transfer processes can describe this reaction: inner-sphere (ISET) and outer-sphere (OSET), whose mechanisms differ only in the nature of the transition state. In ISET, the process forms one intermediate species that is composed of both the metal center and the dormant alkyl halide (C-X-Mt). [5, 10, 23] This intermediary is formed when the halogen atom binds to the metal center, and it is subsequently decomposed as the C-X bond of the alkyl halide is cleaved homolytically (all of this in one step). [23] On the other hand, in the OSET process, the alkyl halide chains and the metal center are not bonded in the same species and so the electrons are transferred in such a way that

the alkyl halide turns into an anion and the positive charge of the metal is increased. [5, 9, 23] After the transfer, the halogen atom decouples from the chain by heterolytic cleavage of the C-X bond and binds to the metal cation. [23] This events may either happen in a concerted manner like ISET or in different steps. [5] Figure 1-10 summarizes the mechanism of both ISET and OSET. It has been shown that, even though both processes take place, OSET is energetically less favored than ISET (the intermediate has a bigger activation energy), and consequently it is $\sim 10^{10}$ times slower than ISET under normal ATRP conditions, which is indicative that ISET is the dominant redox mechanism in ATRP. [5, 10] Still, OSET remains an undesirable side reaction, especially for very active catalysts (with high reducing potential), and has been credited with being responsible for the limited conversions observed during polymerization of acrylonitrile and electrophilic acrylates. [2]

In certain conditions other side reactions should be considered in ATRP that result in catalyst consumption/loss of activity and limited conversion, namely: monomer π-coordination, activator disproportionation, halide dissociation (in aqueous media), radical coupling (formation of organometallic species), ligand degradation by acids and β-H elimination. [2, 10] These can be avoided by careful choice of ligand, monomer, solvent or other reaction conditions. [2, 10] On the other hand, this fine-tuning may also be used inversely, to take advantage of some of these side reactions (for instance β-H elimination reactions may be enhanced via a CCT process mediated by Fe when low MW polymers are desired). [2]

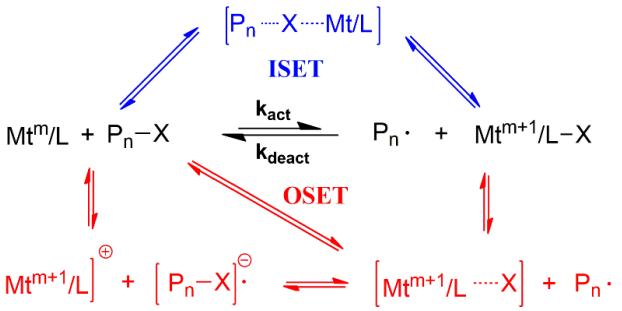

Figure 1-10: Mechanisms of ISET and OSET processes. Adapted from ref. 5.

Kinetic and control aspects

Like NMP, ATRP is governed by the PRE (with the same stages of kinetics previously discussed in Section 1.2.2) but there is a fundamental difference between the linear steady-state kinetics of these two processes. In the case of ATRP the rate of polymerization depends not only on the concentration of deactivator species but also on the concentration of activator ([X-Mt^{m+1}/L] and [Mt^{m}/L] respectively), according to the following expression [2, 5, 9]:

$$r_p = k_p[M][P\bullet] = k_p K_{eq}[M][I]_0 \times \frac{[Mt^m/L]}{[X - Mt^{m+1}/L]} \quad (7)$$

where K_{eq} is the ATRP equilibrium constant (= k_{act}/k_{deact}). This equation suggests that a low deactivator concentration would favor kinetics, but this would lead to a loss of control, according to equation 4, unless the catalyst can provide a high value of k_{deact} in compensation. [2, 5, 9] Regardless of this consideration, the concentration of deactivator species always increases with time, due to the PRE, and deviations from linearity may take place at high conversions. [2, 5, 10] Is worth mentioning that the amount of deactivator in the mixture may also be lowered by certain phenomena inherent to the system, such as solubility issues of the metal complex in the solvent or occurrence of side reactions. [9]

Similarly, the value of K_{eq} should be low so that a good control over the MW can be achieved (i.e $k_{act} << k_{deact}$), but k_{act} should still be high enough to enable the polymerization to take place at a reasonable rate. [10] The nature of the catalytic complex (both the metal and the ligand), the initiator and the monomer, and also the reaction conditions (particularly the solvent polarity, the temperature and pressure) have a strong influence on k_{act} (and to a less extent on k_{deact}) and therefore on K_{eq}. [2, 5, 9, 10] As a result, this tradeoff between polymerization rate and control can be regulated by choosing the appropriate reaction components and conditions.

Catalytic complex

The centerpiece of an ATRP polymerization is the catalyst, composed of a transition metal atom coordinated by a ligand and in the presence of a counterion. A suitable ATRP catalyst should have the following characteristics: (1) the transition metal should have interchangeable oxidation states that differ only by one electron; (2) the metal should have a good capability to abstract and accommodate (through expansion of the coordination sphere) the halogen atom; (3) the ligand should form a relatively strong dative bond with the metal center. [9, 10] This factors greatly determine the extent of the ATRP equilibrium (i.e. the value of K_{eq}), which in turn contributes to both the control and kinetics of the polymerization.

Many transition metals have been used successfully in ATRP, which are represented in Figure 1-11, but catalysts based on copper (Cu(I) and Cu(II)) have proven to the most versatile and cost-effective (despite not being the most active in some cases). [9] The ligands can also be of various natures, either being nitrogen, phosphorous, sulfur, oxygen or

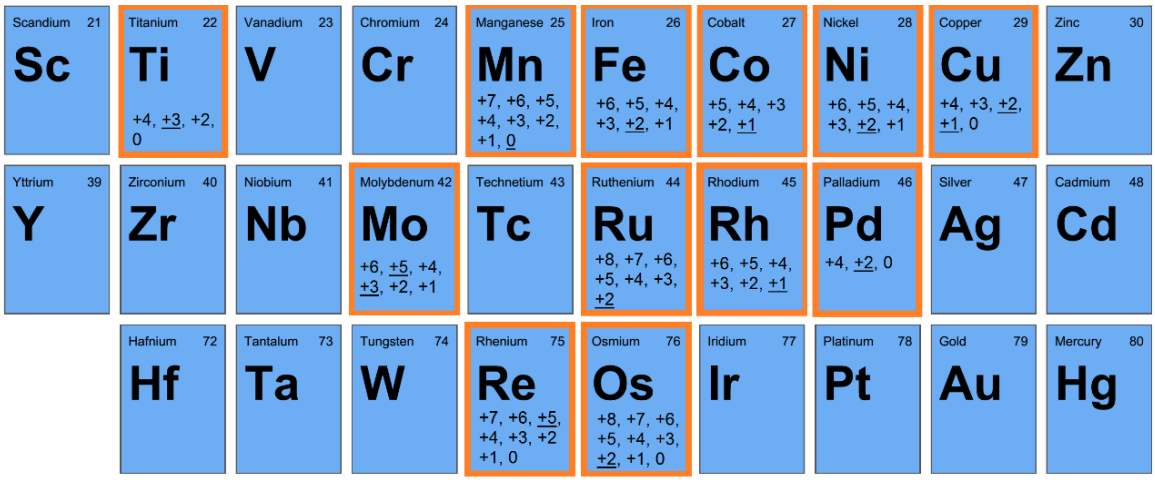

Figure 1-11: Representation of transition metals in the periodic table, highlighting those used successfully in ATRP so far [1,2] (with an orange box). The numbers below the chemical element symbols are possible positive oxidation states of these elements. The underlined oxidation states are those typically used as catalysts in ATRP.

carbon based (depending on the atoms that form the dative covalent link with the metal), with different molecular geometries (linear, branched or cyclic) and denticities (most commonly bi, tri and tetradentate). [9] Nitrogen ligands seem the most suitable to use in conjunction with Cu metal centers, while other type of ligands prove more adequate to other metals. [9, 10] Counterions are usually Br^- or Cl^-, but carboxylates, thiocyanates and hexafluorophosphate are also reported. [2, 10]

Perhaps the most important consideration to take when designing an appropriate catalyst for ATRP is the ligand composition and structure, because the ligand can be engineered to achieve the desired catalytic activity. [9] In fact, a linear correlation between the values of log K_{eq} and the catalyst's redox potential ($E_{1/2}$) exists for many ligands (on Cu(I) and Cu(II) complexes). [2, 5, 9, 10] $E_{1/2}$ is a measure of the reducing power of a species, as more negative values of $E_{1/2}$ mean more reducing power, and so it becomes clear the reason for this relationship (since in the activation process the metal complex acts as a reducing species). In turn, the values of $E_{1/2}$ depend both on the relative concentrations of the metal's oxidation states, [Cu(II)]/[Cu(I)], and their relative stabilities, β^{II}/β^{I} (the latter being a function of the ligand nature and coordination geometry), according to the Nernst equation (assuming 1:1 coordination) [2, 10]:

$$E_{1/2} = E_{1/2}{}^{0} + \frac{RT}{F}\ln\left(\frac{[Cu(II)]}{[Cu(I)]}\right) - \frac{RT}{F}\ln\left(\frac{\beta^{II}}{\beta^{I}}\right) \quad (8)$$

Equation 8 indicates that a ligand yielding a very stable Cu(II) complex enhances the reducing power of the catalyst ($E_{1/2}$ decreases as β^{II}/β^{I} increases) thus increasing the value of K_{eq}. [2, 10] The values of k_{act} and K_{eq} depend primarily on [2, 5, 9, 10]:

i. The number of nitrogen atoms (bidentate < tridentate < tetradentate);
ii. The size of the chain linking those atoms (C4 < C3 << C2);
iii. The type of structure (linear ~ cyclic < branched);
iv. The nature of the nitrogen compound (imides < alkyl amines ~ pyridines);
v. The existence of steric effects around the metal center (decreases k_{act});
vi. The presence of charge on the ligand (anionic < neutral).

Figure 1-12 shows some examples of common nitrogen-based ligands used for Cu catalyzed ATRP, and illustrates the rules mentioned above. It is important to note that K_{eq} does not only depend on the catalyst's reduction potential, but also on the halogenophilicity of the metal, i.e. its capacity to abstract a halogen atom. [2, 9, 10]

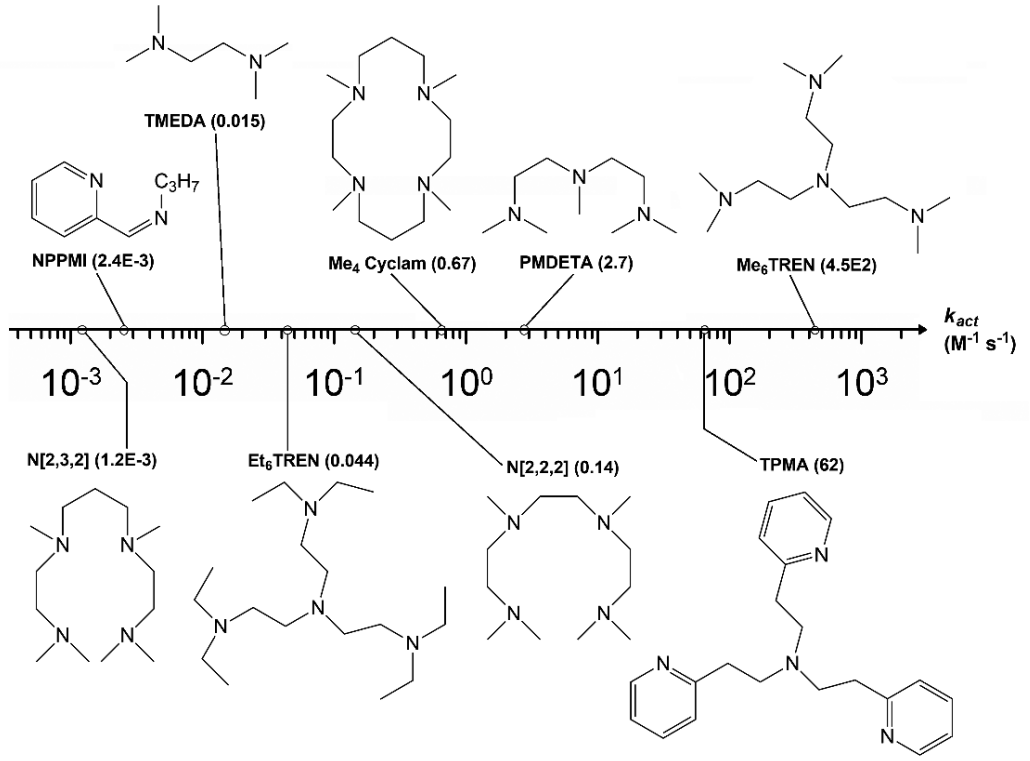

Figure 1-12: Examples of ligands for copper-based catalysts in ATRP and the respective values of k_{act} (in M^{-1} s^{-1}) for a system with a Cu(I)Br/L catalyst (L is one of these ligands) using the initiator EBiB, in MeCN at 35 °C. Adapted from ref. 5.

Initiators

With respect to initiation systems, two possibilities arise in ATRP: normal initiation and reverse initiation. In the normal ATRP, the initiator is typically an alkyl halide, R-X (or other similar/derivate halogenated compounds, like halogenated alkanes, benzyl halides, haloesters, haloketones, halonitriles and sulfonyl halides) that is fed into the mixture along with the metal catalyst (in a 1:1 ratio) in its lower oxidation state (Cu(I) in the case

of copper). [2, 5, 9] Because using the lower oxidation state of the metal may lead to the irreversible oxidation of the catalyst in the presence of air [2, 10] (particularly in industrial scale reactors, where deoxygenation may be incomplete) a reverse initiation mode was developed, which uses the metal in its oxidized form in conjugation with a conventional FRP initiator (such as azo compounds and peroxides) [2, 9, 10]. Still, in this technique, a large amount of catalyst is needed that cannot be lowered independently (since the catalyst is the only source of transferable halogen atoms), and no block copolymers can be produced. [2, 10] As a result several ATRP variations have been developed that allow simultaneously to employ alkyl halides as initiators and oxidized metal complexes as catalysts, and they are now the mainstream of ATRP (*vide infra*).

The concentration and structure of the alkyl halide initiator are important "design" parameters in any ATRP experiment. The former directly determines the target degree of polymerization thus giving chains of different lengths and also different polymerization rates, while the latter is a key parameter influencing the catalytic activity, k_{act}. [2, 5, 9, 10] Indeed it has been found that the value of K_{eq} correlates very well with bond dissociation energies of the alkyl halides, which is a measure of the stability of the growing radical chains/initiator fragments (varying inversely with their values). [2, 5, 9, 10] Therefore it is with no surprise that k_{act} values increase with the same effects that stabilize this radicals, namely [2, 5, 9, 10]:

i. The degree of substitution of the carbon atom adjacent to the halogen atom: primary < secondary < tertiary
ii. The leaving halogen atom: Cl < Br < I (Note: F is not used because the C-F bond does not undergo homolitic cleavage and I is rarely used in ATRP).
iii. Polarity or resonance effects induced by adjacent groups (e.g.: -Ph ~ -C(O)OR << -CN).

Examples of common ATRP initiators are presented in Figure 1-13, which also demonstrates the previous rules.

Monomers

One of the reasons for the success of ATRP techniques is their ability to polymerize a vast array of monomer families (larger than NMP), that includes acrylates, methacrylates, styrenes, (meth)acrylamides, acrylonitrile, vinylpyridines, dienes and also some cyclic monomers. [9, 10] Nevertheless, the polymerization of acidic monomers (e.g. acrylic

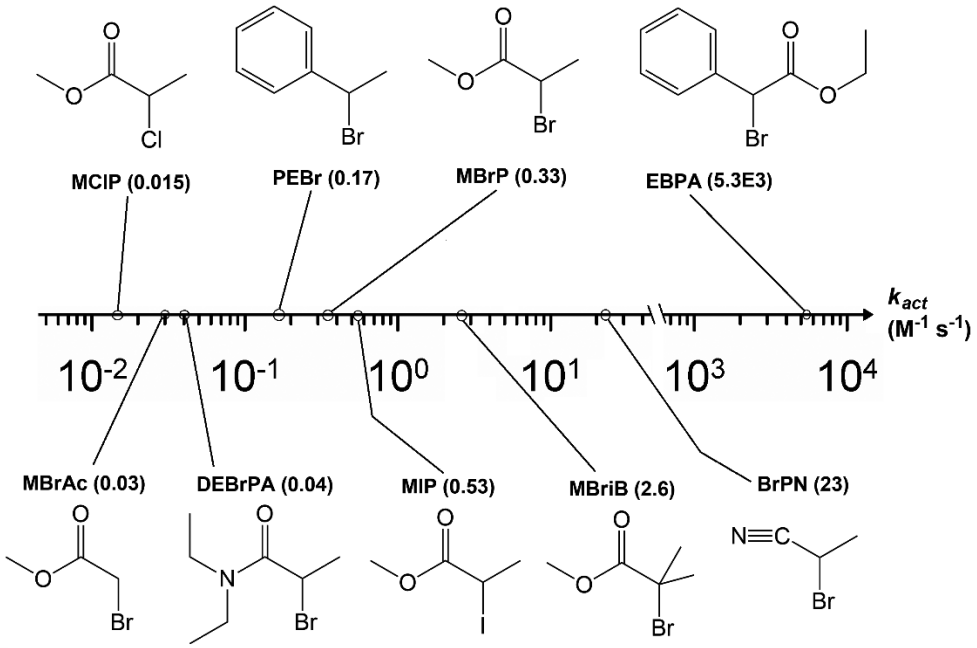

Figure 1-13: Examples of ATRP halogenated initiators and the respective values of k_{act} (in M^{-1} s^{-1}), in a system with a Cu(I)X/PMDETA catalytic complex (X = Br or Cl) in MeCN and at 35 °C. Adapted from ref. 5.

acid) via ATRP is problematic, as this monomers tend to protonate the ligands (which are basic), forming salts. [9] One solution to this problem was devised, which consists in using the neutral sodium salt of the monomer, and various acidic monomers have since been polymerized successfully. [9] The class of less activated monomers, that includes VAc, alkyl-substituted olefins (e.g. propylene) and some halogenated alkenes still present great challenges for ATRP, due to the very low stability of growing radicals and resulting low values of k_{act} and K_{eq}. [9]

The structure of the monomer is also an important parameter as it generally dictates the choices for the remaining reactants. This is due to the fact that each monomer has its own value of k_p (for the same temperature), which means that the polymerization of each one will have a unique behavior in terms of both control and kinetics, according to equations 4 and 7 respectively [9, 10], thus requiring proper catalysts, initiators and reaction conditions. In particular, the monomer structure is pivotal in the choice of initiator structure [10], since one of the requirements for a good control, as stated previously, is a fast initiation, at least in comparison to propagation. [9] To achieve this goal, the initiator must have a reactivity close to that of the monomer and so, as a general rule of thumb, the chemical structure of the dormant chain and the initiator should be identical. [9]

The different reactivities of the monomers also result in different values of k_{act} and K_{eq} (since the dissociation of the alkyl halide chains yield a radical based upon the terminal

monomer unit), generally following this order: acrylonitrile > methacrylates > styrene ~ acrylates > acrylamides >> vinyl chloride > vinyl acetate. [2, 5] This aspect is of extreme importance when preparing block copolymers, as it defines the order in which the monomers must be added: more reactive monomers should be reinitiated with less reactive ones. [2, 5] The reason behind this rule is concerned with the fact that the rate of reinitiaton (proportional to k_{act} of the first monomer) should be greater or equal to the rate of propagation of the second monomer [9], otherwise the chains will not reinitiate at the same time which results in an ill-controlled polymerization (e.g. methacrylates can be reinitiated with styrene but not with acrylonitrile). However there is a technique, named halogen exchange, which may mitigate this limitation and effectively make copolymers in any order. [2, 5, 9] The basic principle is to perform the polymerization of the first block with an alkyl bromide and then use a CuCl catalyst for the synthesis of the second block (instead of a CuBr catalyst). [2, 5] Because the C-Cl bond is stronger than the C-Br bond, the dormant chains will preferentially have Cl terminals and therefore a lower k_{act} can be achieved for the more reactive second monomer. [2, 5, 9] The result is a more controlled polymerization as the rate of monomer propagation decreases in comparison to the rate of reinitiation. [2, 9]

Solvent

ATRP has been successfully performed in bulk, solution and dispersed media (suspension, emulsion and miniemulsion) [5, 9], and common solvents used for solutions include DMF [9, 10], DMSO [24-26], acetone [9, 10], benzene [9, 10], toluene [9, 10], THF [27], MeCN [25, 28], ethyl acetate [9, 10], ethylene carbonate [9, 10] and also water [9, 28] or water/alcohol mixtures[10, 24]. Some non-conventional solvents such as supercritical CO_2 [9] and ionic liquids[29-31] have also been employed in ATRP successfully. A capable solvent for ATRP should fulfil the following requirements: (1) it must not act as a chain transfer agent [9, 10]; (2) it must not poison the catalyst [9, 10]; (3) it must not promote or participate in side reactions [9, 10]; (4) it should be compatible with the reaction conditions, when they are restricted (e.g. the boiling point of a solvent should be high when high temperatures are to be used); (5) it should solubilize the polymer and the catalytic complex effectively (and additives, if present), when homogeneous systems are desired. The latter condition can influence control quite significantly [32], because premature precipitation of polymer chains or low concentration of catalytic complexes leads to high values of $Đ$ [9].

Although the introduction of a solvent should theoretically lower the polymerization rate (due to a lower monomer concentration), it is actually possible to increase it using polar solvents. [5] In fact a strong correlation was found between values of K_{eq} and the polarity of various solvents (described by Kamler-Taft polarity parameters), as can be seen in Figure 1-14. [5] Three phenomena may be responsible for this observations [28]:

a) Changes in the structure of the catalytic complex: Cu(I) complexes in more polar solvents (like acetonitrile) assume a monomeric form, which is more active that the dimeric form generated in less polar solvents (like acetone). [9]
b) Increased catalyst solubility [9]
c) Stabilization of the intermediate species formed during the ISET process and the Cu(II) complex [5], which results in higher activation rates (k_{act}).

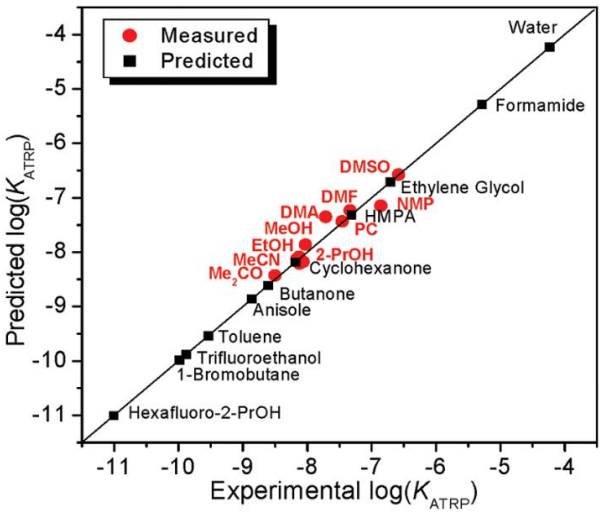

Figure 1-14: Experimental values of K_{eq} vs. values predicted using Kamlet-Taft polarity parameters of the solvents. Taken from ref. 5.

Temperature and pressure

The kinetics and control over the polymerization can also be controlled by adjusting the temperature of the system. Because propagation has a higher activation energy than termination it is possible to increase the ratio k_p/k_t with temperature, which leads to smaller dead chain fractions and thus better control. [5, 9, 10] An increase in temperature leads to higher K_{eq}, improving the reaction kinetics as well. [9, 10] One should be careful when increasing temperature though, as it favors side reactions such as chain transfer, monomer self-initiation and catalyst decomposition. [5, 9, 10] Increasing pressure favors propagation and decreases termination rates (due to different activation volumes) therefore enhancing MW control [5].

Variants of ATRP

As previously mentioned, the PRE results from the accumulation of deactivator complex (Y-Mt^{m+1}/L-X) over time due to some unavoidable termination reactions. [2, 9, 10] This feature is of extreme importance, as it drives the equilibrium of Figure 1-4 towards dormant species, resulting in reduced termination rates and subsequent good control over the polymerization (see equation 4). [2, 10]

Notwithstanding, this accumulation of deactivator species also creates some difficulties. Since this transition metal complexes are often present in large concentrations (>1000 ppm [33, 34]) and induce color on the polymer, certain troublesome techniques are required to purify the product (e.g. adsorption and precipitation), which tend to be expensive. [5, 26] In addition, most of the metals used in ATRP (including Cu) are toxic, thus creating environmental issues and preventing any applications of the polymer in the field of biomedicine. [5, 13, 35] To reduce the amount of metal complex used in the system to less than 100 ppm [33, 34], and therefore solve this issues (without compromising control and kinetics), several ATRP variations have been developed, namely:

a) *Simultaneous Reverse and Normal Initiation (SR&NI) ATRP* [2, 10]: this technique is meant to solve the issues involving reverse ATRP, by using both the alkyl halide and conventional initiators, in conjunction with the oxidized metal complex. Because the alkyl halides are now the sources of transferable halogen atoms, the catalyst can be used in much smaller quantities than in reverse ATRP. However using a conventional initiator has a severe drawback since the radicals can generate new chains which contaminate the final product.
b) *Initiators for Continuous Activator Regeneration (ICAR) ATRP* [2, 5]: as with SR&NI ATRP, in this method a conventional initiator is used together with the main alkyl halide initiator, but the main difference is the large excess of conventional initiator compared to the catalyst (see Table 1-1 below). Under this conditions, the initiator acts as a reducing agent, transforming the accumulating Cu (II) species into Cu (I) activators. Since the activator is regenerated, its initial concentration can be lower (< 50 ppm).
c) *Activators (Re)Generated by Electron Transfer (A(R)GET) ATRP*: relies on the use of alkyl halides and the oxidized metal catalyst (Cu(II)) along with reducing agents (e.g. ascorbic acid, tin(II) 2-ethylhexanoate, hydrazine,…) to reduce Cu(II) to Cu(I) *in situ*, which presents an enormous advantage over the previous two methods because the

reducing agents are not able of generating new chains. [2, 5, 10] In the initial version of this method (AGET) the reducing agents were used in concentrations close to the initial concentration of catalyst, but it was later realized that, no matter how low the catalyst concentration was, this formulation always led to further accumulation of metal complex due to the PRE. [10] Therefore, in a later version (ARGET), a large excess of reducing agent is used to regenerate the activators during the course of the reaction and it was verified that this could diminish the initial concentration of catalyst quite significantly (to less than 50 ppm and even 10 ppm). [2, 10]

d) *Supplemental Activator and Reducing Agent (SARA) ATRP*: a special case of ARGET ATRP is when the reducing agent is also capable of activating dormant chains, therefore acting as a secondary activator (the main activator being the Cu(I) complex). This is the case of zero-valent metals (in the form of wire or powder), such as Cu(0), Fe(0), Zn(0) and Mg(0) [5] and also inorganic sulfites, such as $NaHSO_3$ and $Na_2S_2O_4$ [33]. In the first case, the ligand must be added to the system in an amount equivalent to the total amount of metallic species present to ensure complete solubilization.

Historically the Cu(0)/Cu(II)X_2 system has given rise to a debate in the scientific community over the actual mechanism taking place during the reaction because another alternative, named SET-LRP, has also been proposed. The advocates of SET-LRP claim that Cu(0) is the main activator and that all Cu(I)X species formed instantaneously disproportionate into Cu(0) and Cu(II)X_2. [5, 23, 36] Furthermore, it is proposed that the main electron transfer pathway during activation is OSET instead of ISET. [10, 23, 36] Both alternatives are depicted in Figure 1-15. There are, however, clear evidences against the proposed SET-LRP mechanism, which are backed by experimental data [5, 10, 23, 36]: (1) as indicated before, the OSET process is much slower than ISET; (2) it has been found that the disproportionation of Cu(I) under normal

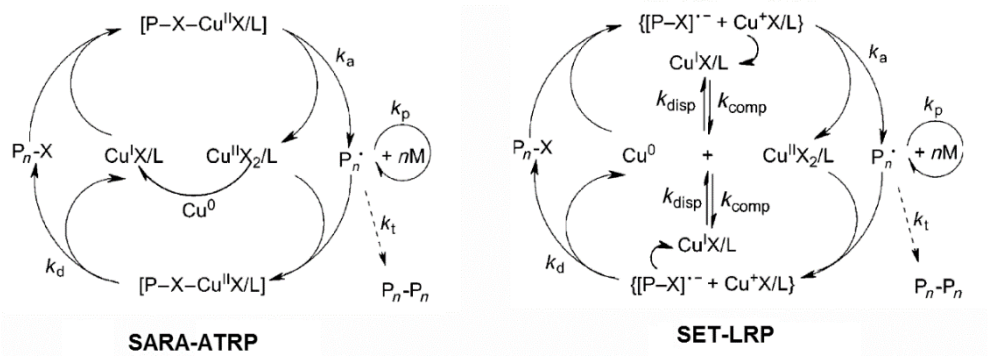

Figure 1-15: Detailed mechanisms of SARA-ATRP and SET-LRP. Adapted from ref. 23.

ATRP conditions is almost negligible; (3) alkyl halides tend to react more with the Cu(I) complex than with Cu(0); (4) the mechanism violates the principle of microscopic reversibility. The mechanism of SARA-ATRP, where Cu(0) comproportionates with Cu(II) to yield the activator, is thereby the most likely to take place.

e) *Electrochemical ATRP (e-ATRP)* [5]: in this method the Cu(II) reduction is performed by passing an electric current through the system (via an anode and a cathode). The advantage of this setup over the previous ones is that no side products are formed as a result of the oxidation of reducing agents. In addition, the applied electric potential can easily be modified to allow fine tuning of the [Cu(I)X/L]/[Cu(II)X_2/L] ratio, which governs the kinetics and control of the polymerization, and also to deactivate the catalyst at any desired instant. This technique can also be used to remove the catalyst at the end by electrodeposition achieving concentrations as low as 1 ppm, which is useful for electronic and biomedical applications. The most relevant disadvantage of this method deals with the difficulties to control the polymerization for high conversions.

Table 1-1 summarizes the ratios of the various species used in practice for all of these methods. Notice the clear advantage of ICAR, ARGET and SARA ATRP over the other methods in terms of initial amount of catalyst used. In addition, the use of oxidized species as catalysts means that ATRP, unlike NMP and RAFT, is somewhat tolerant to O_2.

Table 1-1: Usual component proportions used in ATRP techniques. Adapted from refs. 2 and 33.

ATRP Method	Alkyl halide (R-X)	Activator (Cu(I)X)	Deactivator (Cu(II)X_2)	Ligand (L)	Reducing Agent (RA)	Conventional initiator (I-I)
Normal	1	1	–	1	–	–
Reverse	–	–	1	1	–	0.5
SR&NI	1	–	0.2	0.2	–	0.1
ICAR	1	–	< 0.01	0.01	–	< 0.1
AGET	1	–	0.2	0.2	0.18	–
ARGET	1	–	< 0.1	0.1	< 0.1	–
SARA	1	–	< 0.1	1.1[a]	1	–

[a] Assuming RA is a zero-valent metal (otherwise this value is equal to 0.1).

1.2.4 Reversible Addition Fragmentation Chain Transfer

As stated in section 1.2.1 RAFT, unlike the previous two methods, does not rely on the PRE to exert control over the MW, but instead on a degenerative chain transfer process (based on a reversible addition/fragmentation scheme), already presented in Figure 1-4. The basic principle behind RAFT is the usage of a chain transfer agent (CTA) that provides an interchangeable capping group, i.e. a moiety that is able to exchange its position from one dormant chain to one active chain. [37] Although many compounds are capable of performing addition/fragmentation chemistry (such as unsaturated methacrylate oligomers, vinyl ethers, allylic compounds and thionoesters)[10, 38], the original chain transfer agents used in RAFT (and so far the most successful) are those based on the thiocarbonylthio group, represented in Figure 1-16, like dithioesters, dithiocarbamates, trithiocarbonates and xanthates (in the latter case RAFT is often called MADIX) or other classes, depending on the nature of the Z and R groups [37, 38].

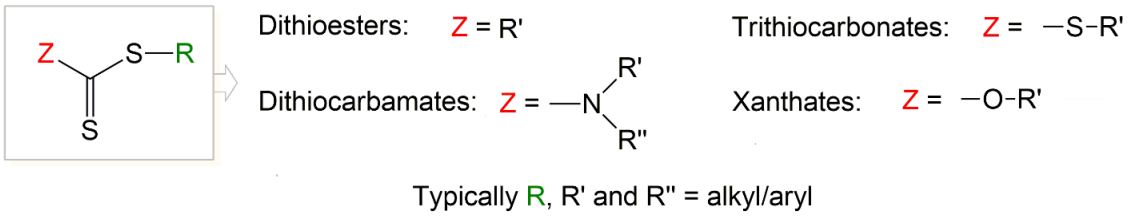

Figure 1-16: Schematic representation of the thiocarbonylthio moiety and compounds based on it. [1]

Of the 3 main RDRP techniques RAFT is the one that resembles FRP the most, both mechanistically and kinetically. RAFT polymerizations require a conventional FRP initiator to start the polymerization [37], because in the DT equilibria of Figure 1-4 the radicals are neither being consumed nor generated in the overall process (i.e. the number of radicals is the same on both sides of the equilibria), and consequently an external source of radicals needs to exist [39]. Upon dissociation of this initiator the first chains (P_n•) are formed by monomer addition and they are rapidly trapped in a reversible equilibrium (pre-equilibrium) with the RAFT agent. In this process the chains become dormant and the radical is transferred to the R group on the RAFT agent moiety, which leaves the intermediary species. [38] The radical R• is able to start other new chains (P_m•) that are themselves trapped in the main equilibria, where they are reversibly deactivated by the addition of the RAFT capping group, as seen in Figure 1-17. [38] During this equilibria an intermediate species is formed, which may either undergo fragmentation (activating the

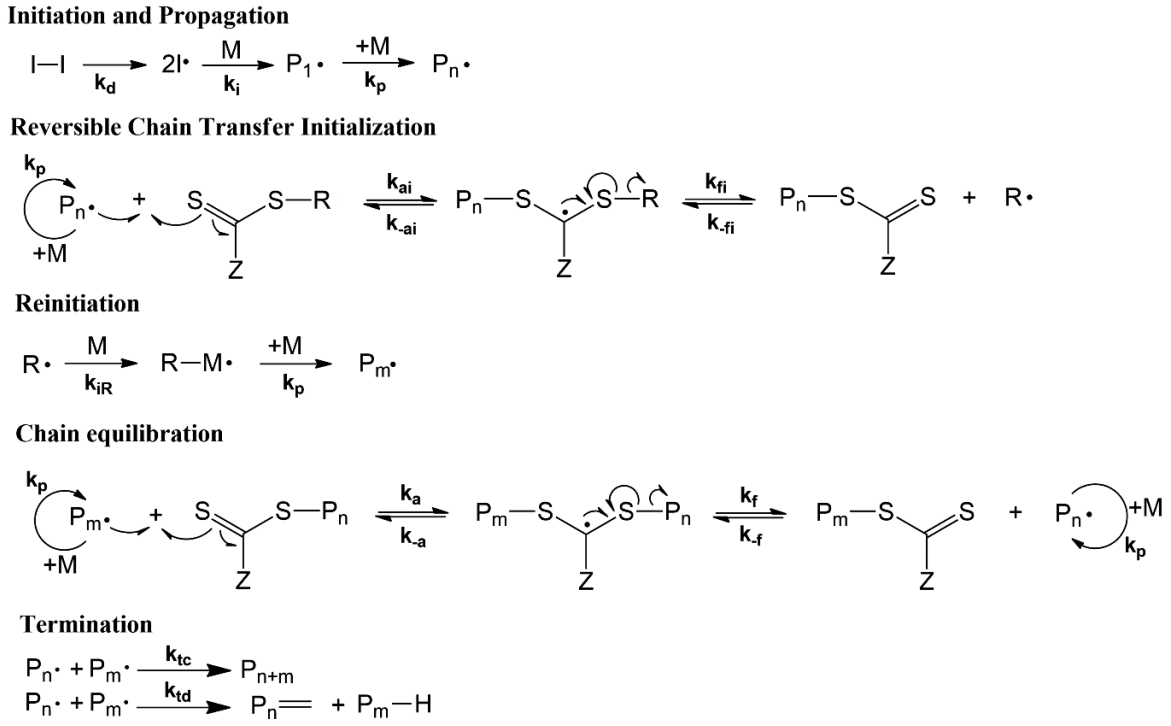

Figure 1-17: Complete RAFT mechanism. Adapted from refs. 38 and 39.

previously dormant chain) or revert back to the original reactants (in inverse addition). [2, 38] Since, ideally, both alternatives occur with equal speed (i.e. K_{ex} = 1), both chains have an equal opportunity to grow and as a result their MW's are well controlled. [2, 38]

In contrast to the other RDRP methods (and similarly to FRP), termination is not suppressed in RAFT [38, 39], since due to the nature of the equilibria there are always active chains that may couple or disproportionate. Therefore the key aspect for achieving a good control in RAFT is to ensure that the exchange process is fast when compared to propagation ($k_{tr} > k_p$), as can be seen on equation 5, so that the majority chains retain their end functionalities. [2, 38] To evaluate this, a chain transfer constant, C_{tr}, is defined as follows [38]:

$$C_{tr} = \frac{k_{tr}}{k_p} = \frac{k_a \phi}{k_p} = \frac{k_a}{k_p} \frac{k_f}{k_{-a} + k_f} \tag{9}$$

where ϕ is a partition coefficient, which is the fraction of intermediate species that undergoes fragmentation to yield the products in the equilibria. For the main equilibrium ϕ = 0.5 (because $k_{-a} = k_f$) but for the pre-equilibrium it is desired that $\phi > 0.5$, so that most of the R• groups can be released, to begin reinitiation (typically K_{ex} in here is > 10^6). [2, 39]

It has been determined that, in order for a RAFT polymerization to be living and controlled, C_{tr} must be greater than 10. [38, 39] The most efficient thiocarbonylthio RAFT agents can have C_{tr} values greater than 100. [38, 39]

Because, during chain equilibration, the number of radicals remains unchanged, RAFT kinetics does not depend on this equilibrium (unlike the PRE-based systems) and as a result the steady state is reached solely by a balance between initiation and termination. [2, 10, 38, 39] Therefore the steady-state kinetic law of RAFT matches that of FRP (equation 1). [1, 2, 10] However, kinetics on the early stages of the polymerization may be dependent on the rates of addition and fragmentation of the asymmetrical pre-equilibrium, which are different from those of the symmetrical main equilibrium (as stated previously ϕ should be greater than 0.5, and so a high rate of fragmentation is desired). [2] Furthermore, it is important that both the rate of addition and fragmentation are high, so that the main equilibria is established rapidly. [38] If the rate of fragmentation is low then the intermediate species formed upon addition may participate in side reactions, thus reducing the overall rate of polymerization [38, 39]. This phenomena, called retardation, can be observed in some systems where the intermediate radicals are relatively stable and terminate with active chains present in the system (especially when $[CTA]_0$ is high). [2, 38, 39]

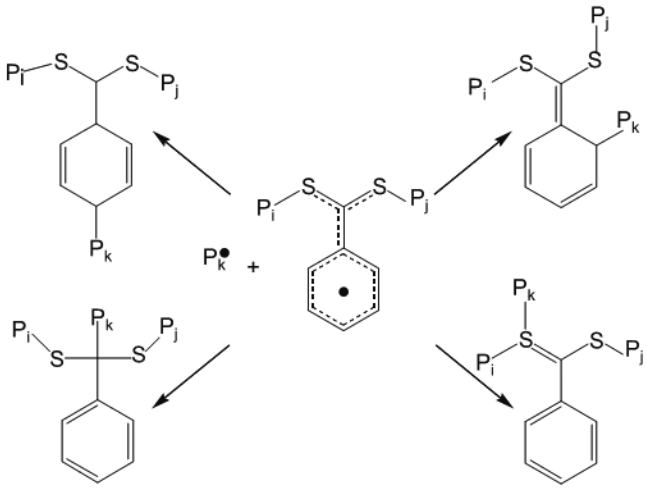

Figure 1-18: Proposed mechanism of termination responsible for rate retardation, for an intermediate species stabilized by resonance. Taken from ref. 2.

Monomers and RAFT agents

The points discussed previously tell us that an efficient RAFT agent should have the following characteristics [38]: (1) it should possess a reactive double bond (in this case C=S) in order to achieve a high k_a and C_{tr}; (2) the intermediate species should fragment quickly (high k_f) and should not participate in side reactions; (3) the intermediate of the pre-equilibrium should preferentially fragment to yield the products instead of the reactants ($k_{fi} \geq k_{-ai}$); (4) the leaving groups R• should be capable to efficiently generate new chains ($k_{iR} \geq k_p$). It is possible to fulfill these requirements by using a RAFT agent that

possesses the appropriate R and Z groups for a given monomer. Because of this, RAFT has the unique advantage of being able to cover almost all vinyl monomers. [1]

The Z group modifies both the addition and fragmentation rates, as it determines the stability of the intermediate radical. [2, 39] Therefore if Z induces radical stabilizing effects (like resonance or polarity) the rate of addition will increase and the rate of fragmentation decrease, and the more stabilizing groups lead to higher C_{tr} values (e.g. phenyl groups are more stabilizing than lone pair donor groups). [2, 37, 39] These effects are exemplified in Figure 1-19. The groups are chosen according to the monomers intended for polymerization, to ensure that the stability of the intermediate radicals is close to the stability of the macroradical chains (to balance the main equilibrium). More stabilizing groups are intended for more activated monomers, like styrenes, (meth)acrylates, acrylamides and acrylonitrile, and the less stabilizing Z groups are more suitable for less activated monomers, like VAc and NVP. [2] However it should be noted that if the intermediate radicals are too stable (e.g. Z = phenyl) retardation or other side reactions (like hydrolysis, and cycloadditions) might occur. [2, 39] Also the Z group must be chosen so that the RAFT agent is compatible with the reaction conditions (in terms of solvent solubility and temperature stability for instance) and to provide specific functionalities if needed (although R is more suitable for that purpose). [38, 39]

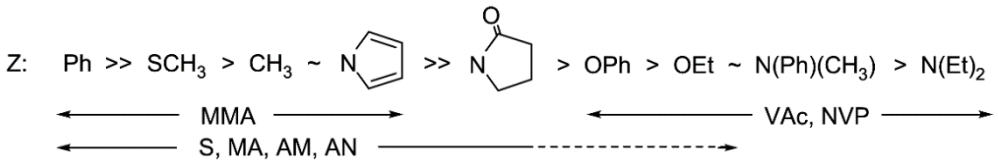

Figure 1-19: Guidelines for the choice of the Z group in RAFT agents. Fragmentation rates increase and addition rates (and C_{tr} values) decrease from left to right. Dashed lines indicate a partial control (controlled MW but with retardation). Adapted from refs. 38 and 39.

On the other hand, the choice of R has a great impact on the rate of fragmentation during the pre-equilibrium, and therefore on its partition coefficient. [39] For this values to be sufficiently high, the R• radicals should be more stable than the active chains (P_n•), which have a structure derived from the monomer. [2] As can be seen in Figure 1-20, charge delocalization effects (resonance and polarity) enhance the stability of R• and increase the values of C_{tr} but steric effects also play a key role in determining the leaving ability of R (e.g. the 4th group from the left in Figure 1-20 has similar stability to the MMA units in the chain but has a very low C_{tr} due to steric strain). [39, 40] It is also important that R• has the ability to add to monomer units, rather than react again with the RAFT

agent, and for that it must provide a high rate of reinitiation compared to inverse fragmentation. [40] This rate must also be higher than the rate of propagation and while for monomers with low k_p (e.g. Sty, MA) this is not an issue, for monomers with high k_p (e.g. MMA, VAc) R should be chosen carefully. [39, 40]

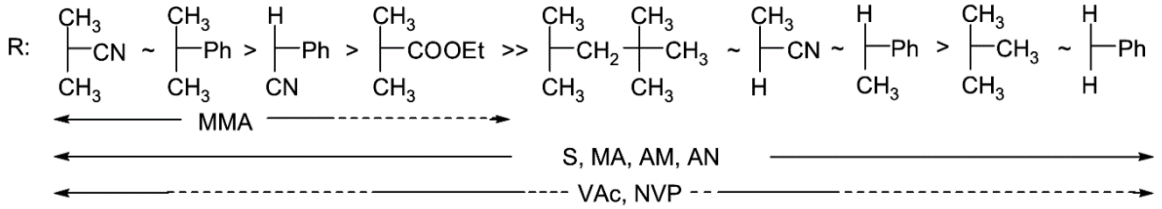

Figure 1-20: Guidelines for the choice of the R group in RAFT agents. Fragmentation rates and C_{tr} values decrease from left to right. Dashed lines indicate a partial control (controlled MW but with retardation). Adapted from refs. 38 and 39.

Although the thiocarbonylthio class of compounds provides this unique control features in RAFT, the moieties derived from them that remain attached to the chains may induce undesired color and odor in the final products. [2] A wide array of methods can be used to functionalize these groups into more suitable ones (such as cycloadditions, thermolysis, radical reactions and reactions with nucleophiles and ionic reducing agents). [39] The applicability of these methods depends on the nature of the group Z, and so this is an additional criteria for its choice. [39]

Initiator

In RAFT polymerization any source of radicals can be used, such as thermal initiators and also photoinitiators, but attention should be paid to the concentration used. [38] A high concentration of initiator leads to a faster polymerization (see equation 1) but the bigger concentration of radicals also increases the rate of termination (much more than in NMP or ATRP) and the occurrence of side reactions involving the initiator (including possible RAFT agent oxidation). [38] This concentration also determines the degree of polymerization, according to equation 10 [2, 38]:

$$DP_n = p\frac{[M]_0}{[CTA]_0 + f[I]_0} \quad (10)$$

Because of all this, a RAFT polymerization typically has an excess of chain transfer agent with respect to initiator. [38] The common practice is to employ an amount of CTA and initiator such that the target DP is 10% of the target DP without the CTA (i.e. with all radicals being derived from the initiator). [38]

Solvents

RAFT polymerizations, like NMP and ATRP, are versatile enough to be carried out in bulk, solution, emulsion and suspension. [37] Organic solvents are still the most widely used, examples being THF [41], MeCN [42], DMSO [43], DMF, benzene, ethyl acetate and butan-2-one, but water and aqueous alcohol solutions, ionic liquids and supercritical CO_2 are used as well [37, 38].

The first and foremost condition that the solvent has to ensure is the solubilization of the CTA, and solvents should be chosen accordingly. [38, 42] If there are no restrictions in terms of temperature and CTA nature, these two factors can be varied to enhance solubility of the CTA in the solvent. [38, 42] If this condition is verified, then the choice of solvent seems to have only minor effects on polymerization rates and MW control (some reports exist of a small loss of polymerization rate and gain of MW control in RAFT polymerizations of MMA using more polar solvents, due to a lower k_p). [42] It should be noted that RAFT agents (especially the more active) undergo hydrolysis in the presence of polar solvents and Lewis bases. [38]

Reaction conditions [38]

The usage of high temperatures is beneficial to RAFT processes, as it increases the rate of polymerization (and mitigates retardation and termination), while favoring an increase in C_{tr} (thus enhancing the control over the MW). Similar effects have been reported for increased pressures. However the temperature should not be risen to very high levels (the highest reported was 180 °C), as RAFT agent degradation and side reactions start to become important.

1.3 The use of green solvents in RDRP

The literature review on the 3 main RDRP techniques presented in the previous sections has revealed that organic solvents still have a dominant presence in this field. Although their wide use throughout the industry makes them preferential choices for a potential scale-up of RDRP methods, their toxicity (and sometimes carcinogenicity) is a crippling issue when the polymers are intended for biomedical applications. In addition, this toxicity and the volatility of the typical organic solvents used in polymer industry (associated with the large volumes employed) gave rise to major environmental concerns,

which ultimately led to several regulations limiting their use (e.g. in paint industry). [44-47] With all these unfavorable circumstances associated with organic solvents, the demand for safer and greener alternatives is now higher than ever.

The emerging field of green chemistry deals with the environmental and health issues which are typically associated with the chemical industry, aiming at safer and more sustainable processes. [44, 48] One of its 12 principles clearly states that "the use of auxiliary substances (e.g. solvents, separation agents, etc.) should be made unnecessary, wherever possible, and innocuous, when used". [44, 49] A green solvent is therefore any solvent which is neither harmful to the environment nor to human health, and they must: (1) have low toxicity; (2) be recyclable; (3) be chemically inert; (4) not be able to contaminate the final product. [45, 49] One way to describe these aspects quantitatively is to classify the solvent in terms of its scores in both the EHS and LCA methods, which describe health/safety and environmental performances, respectively. [45] Green solvents have low values on both these methods' indicators, as seen in Figure 1-21.

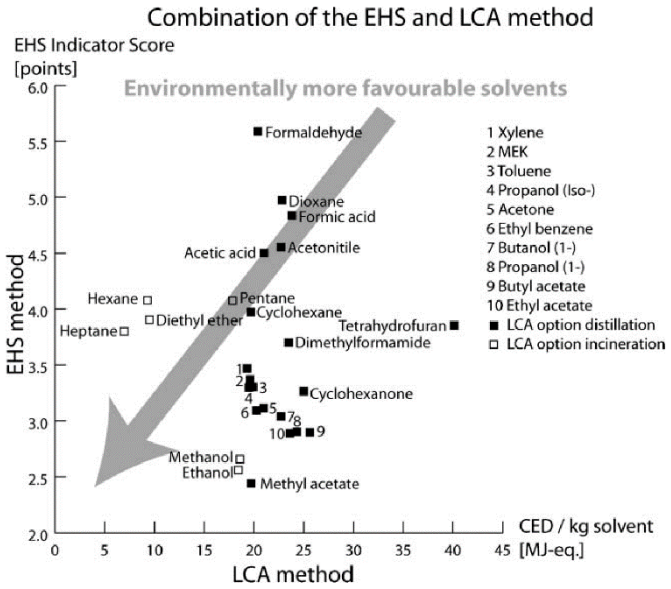

Figure 1-21: Solvent classification based on the LCA and EHS methods. The LCA method deals with the environmental impacts associated with pollutant emissions and resource consumption throughout the life cycle of a product. Two options for solvent treatment were considered: incineration and distillation. The EHS method relates to potential health and safety hazards of a substance. Adapted from ref. 45.

Only recently have green solvents began to be used in RDRP systems: water [19, 37, 50-52], water-alcohol [13, 34, 53-56], ionic liquids [6, 29, 30, 37, 38, 57, 58] and supercritical CO_2 [59-63] are now reported for ATRP, NMP and RAFT, but there are still many other possibilities to consider. One of the objectives of this work is to extend the scope of green solvents used in RDRP systems by testing, for the first time, cyclopentyl methyl

ether, a green replacement for THF, in ATRP, NMP and RAFT polymerizations. There is also room for improvement on existing green solvent RDRP systems and so, in another part of this work, a reported synergistic effect between the ionic liquid BMIM-PF_6 and ethylene glycols (EG, DEG and TEG) [64] will be exploited for the first time, in order to replace DMSO as a co-solvent for the ionic liquid and, possibly, to improve the system kinetics [31].

1.4 References

[1] Matyjaszewski, K., Davis, T. P., *Handbook of Radical Polymerization*. John Wiley & Sons, New York, 2003.

[2] Braunecker, W., Matyjaszewski, K., *Controlled/living radical polymerization: Features, developments, and perspectives*, Progress in Polymer Science, **2007**, 32, 93-146.

[3] Zetterlund, P. B., Kagawa, Y., Okubo, M., *Controlled/living radical polymerization in dispersed systems*, Chemical Reviews, **2008**, 108, 3747-3794.

[4] Greszta, D., Mardare, D., Matyjaszewski, K., *"Living" Radical Polymerization. 1. Possibilities and Limitations*, Macromolecules, **1994**, 27, 638-644.

[5] Matyjaszewski, K., *Atom Transfer Radical Polymerization (ATRP): Current status and future perspectives*, Macromolecules, **2012**, 45, 4015-4039.

[6] Nicolas, J., Guillaneuf, Y., Lefay, C., Bertin, D., Gigmes, D., Charleux, B., *Nitroxide-mediated polymerization*, Progress in Polymer Science, **2013**, 38, 63-235.

[7] Matyjaszewski, K., *Overview : Fundamentals of Controlled / Living Radical Polymerization*, ACS Symposium Series, **1998**, 2-30.

[8] Matyjaszewski, K., Spanswick, J., *Controlled/living radical polymerization*, Materials Today, **2005**, 8, 26-33.

[9] Matyjaszewski, K., Xia, J., *Atom transfer radical polymerization*, Chemical reviews, **2001**, 101, 2921-2990.

[10] di Lena, F., Matyjaszewski, K., *Transition metal catalysts for controlled radical polymerization*, Progress in Polymer Science, **2010**, 35, 959-1021.

[11] Cordeiro, R., Rocha, N., Mendes, J. P., Matyjaszewski, K., Guliashvili, T., Serra, A. C., et al., *Synthesis of well-defined poly(2-(dimethylamino)ethyl methacrylate) under mild conditions and its co-polymers with cholesterol and PEG using Fe(0)/Cu(ii) based SARA ATRP*, Polymer Chemistry, **2013**, 4, 3088-3088.

[12] Góis, J. R., Rocha, N., Popov, A. V., Guliashvili, T., Matyjaszewski, K., Serra, A. C., et al., *Synthesis of well-defined functionalized poly(2-(diisopropylamino)ethyl methacrylate) using ATRP with sodium dithionite as a SARA agent*, Polymer Chemistry, **2014**, 5, 3919-3919.

[13] Mendonça, P. V., Konkolewicz, D., Averick, S. E., Serra, A. C., Popov, A. V., Guliashvili, T., et al., *Synthesis of cationic poly ((3-acrylamidopropyl) trimethylammonium chloride) by SARA ATRP in ecofriendly solvent mixtures*, Polymer Chemistry, **2014**, 5, 5829-5836.

[14] Moad, G., Rizzardo, E., *Alkoxyamine-Initiated Living Radical Polymerization: Factors Affecting Alkoxyamine Homolysis Rates*, Macromolecules, **1995**, 28, 8722-8728.

[15] Ding, X. Z., Fischer, A., Yang, S., Wu, P., Brembilla, A., Lochon, P., *Solvent effects on TEMPO-mediated radical polymerizations: Behaviour of 3-vinylpyridine in a protic solvent*, European Polymer Journal, **2001**, 37, 1561-1569.

[16] Harrisson, S., Couvreur, P., Nicolas, J., *Use of Solvent Effects to Improve Control Over Nitroxide-Mediated Polymerization of Isoprene*, Macromolecular Rapid Communications, **2012**, 33, 805-810.

[17] Kuo, K.-H., Chiu, W.-Y., Cheng, K.-C., *Influence of DMF on the polymerization of tert-butyl acrylate initiated by 4-oxo-TEMPO-capped polystyrene macroinitiator*, Polymer International, **2008**, 57, 730-737.

[18] Hlalele, L., Klumperman, B., *In Situ NMR and Modeling Studies of Nitroxide Mediated Copolymerization of Styrene and n-Butyl Acrylate*, Macromolecules, **2011**, 44, 6683-6690.

[19] Charleux, B., Nicolas, J., *Water-soluble SG1-based alkoxyamines: A breakthrough in controlled/living free-radical polymerization in aqueous dispersed media*, Polymer, **2007**, 48, 5813-5833.

[20] Chenal, M., Mura, S., Marchal, C., Gigmes, D., Charleux, B., Fattal, E., et al., *Facile Synthesis of Innocuous Comb-Shaped Polymethacrylates with PEG Side Chains by Nitroxide-Mediated Radical Polymerization in Hydroalcoholic Solutions*, Macromolecules, **2010**, 43, 9291-9303.

[21] Beckwith, A. L. J., Bowry, V. W., Ingold, K. U., *Kinetics of nitroxide radical trapping. 1. Solvent effects*, Journal of the American Chemical Society, **1992**, 114, 4983-4992.

[22] Lessard, B., Tervo, C., Marić, M., *High-Molecular-Weight Poly(tert-butyl acrylate) by Nitroxide-Mediated Polymerization: Effect of Chain Transfer to Solvent*, Macromolecular Reaction Engineering, **2009**, 3, 245-256.

[23] Guliashvili, T., Mendonça, P. V., Serra, A. C., Popov, A. V., Coelho, J. F. J., *Copper-Mediated Controlled/"Living" Radical Polymerization in Polar Solvents: Insights into Some Relevant Mechanistic Aspects*, Chemistry - A European Journal, **2012**, 18, 4607-4612.

[24] Abreu, C. M. R., Mendonça, P. V., Serra, A. C., Coelho, J. F. J., Popov, A. V., Guliashvili, T., *Accelerated Ambient-Temperature ATRP of Methyl Acrylate in Alcohol–Water Solutions with a Mixed Transition-Metal Catalyst System*, Macromolecular Chemistry and Physics, **2012**, 213, 1677-1687.

[25] Braunecker, W., Tsarevsky, N. V., Gennaro, A., Matyjaszewski, K., *Thermodynamic components of the atom transfer radical polymerization equilibrium: Quantifying solvent effects*, Macromolecules, **2009**, 42, 6348-6360.

[26] Mendonça, P. V., Serra, A. C., Coelho, J. F. J., Popov, A. V., Guliashvili, T., *Ambient temperature rapid ATRP of methyl acrylate, methyl methacrylate and styrene in*

polar solvents with mixed transition metal catalyst system, European Polymer Journal, **2011**, 47, 1460-1466.

[27] Ye, J., Narain, R., *Water-Assisted Atom Transfer Radical Polymerization of N-Isopropylacrylamide: Nature of Solvent and Temperature*, The Journal of Physical Chemistry B, **2009**, 113, 676-681.

[28] Nanda, A. K., Matyjaszewski, K., *Effect of [bpy]/[Cu(I)] ratio, solvent, counterion, and alkyl bromides on the activation rate constants in atom transfer radical polymerization*, Macromolecules, **2003**, 36, 599-604.

[29] Biedroń, T., Kubisa, P., *Atom-Transfer Radical Polymerization of Acrylates in an Ionic Liquid*, Macromolecular Rapid Communications, **2001**, 22, 1237-1242.

[30] Carmichael, A. J., Haddleton, D. M., Bon, S. A. F., Seddon, K. R., *Copper(I) mediated living radical polymerisation in an ionic liquid*, Chemical Communications, **2000**, 1237-1238.

[31] Mendes, J. P., Branco, F., Abreu, C. M. R., Mendonça, P. V., Popov, A. V., Guliashvili, T., et al., *Synergistic Effect of 1-Butyl-3-methylimidazolium Hexafluorophosphate and DMSO in the SARA ATRP at Room Temperature Affording Very Fast Reactions and Polymers with Very Low Dispersity*, ACS Macro Letters, **2014**, 3, 544-547.

[32] Fuente, L. D. L., Ferna, M., *Synthesis of Poly(methyl methacrylate) in a Pyridine Solution by Atom Transfer Radical Polymerization*, Journal of Polymer Science, Part A: Polymer Chemistry, **2001**, 39, 3443-3450.

[33] Abreu, C. M. R., Mendonça, P. V., Serra, A. C., Popov, A. V., Matyjaszewski, K., Guliashvili, T., et al., *Inorganic sulfites: Efficient reducing agents and supplemental activators for atom transfer radical polymerization*, ACS Macro Letters, **2012**, 1, 1308-1311.

[34] Abreu, C. M. R., Serra, A. C., Popov, A. V., Matyjaszewski, K., Guliashvili, T., Coelho, J. F. J., *Ambient temperature rapid SARA ATRP of acrylates and methacrylates in alcohol-water solutions mediated by a mixed sulfite/Cu(ii)Br2 catalytic system*, Polymer Chemistry, **2013**, 4, 5629-5636.

[35] Góis, J. R., Konkolewicz, D., Popov, A. V., Guliashvili, T., Matyjaszewski, K., Serra, A. C., et al., *Improvement of the control over SARA ATRP of 2-(diisopropylamino)ethyl methacrylate by slow and continuous addition of sodium dithionite*, Polymer Chemistry, **2014**, 5, 4617-4626.

[36] Konkolewicz, D., Wang, Y., Krys, P., Zhong, M., Isse, A. A., Gennaro, A., et al., *SARA ATRP or SET-LRP. End of controversy?*, Polymer Chemistry, **2014**, 5, 4409-4409.

[37] Chiefari, J., Chong, B. Y. K., Ercole, F., Krstina, J., Jeffery, J., Le, T. P. T., et al., *Living Free-Radical Polymerization by Reversible Addition–Fragmentation Chain Transfer: The RAFT Process*, Macromolecules, **1998**, 31, 5559-5562.

[38] Moad, G., Rizzardo, E., Thang, S. H., *Radical addition-fragmentation chemistry in polymer synthesis*, Polymer, **2008**, 49, 1079-1131.

[39] Keddie, D. J., Moad, G., Rizzardo, E., Thang, S. H., *RAFT agent design and synthesis*, Macromolecules, **2012**, 45, 5321-5342.

[40] Chong, B. Y. K., Krstina, J., Le, T. P. T., Moad, G., Postma, A., Rizzardo, E., et al., *Thiocarbonylthio Compounds [S=C(Ph)S-R] in Free Radical Polymerization with Reversible Addition-Fragmentation Chain Transfer (RAFT Polymerization). Role of the Free-Radical Leaving Group (R)*, Macromolecules, **2003**, 60, 2256-2272.

[41] Abreu, C. M. R., Mendonça, P. V., Serra, A. C., Coelho, J. F. J., Popov, A. V., Gryn'ova, G., et al., *Reversible addition-fragmentation chain transfer polymerization of vinyl chloride*, Macromolecules, **2012**, 45, 2200-2208.

[42] Benaglia, M., Rizzardo, E., Alberti, A., Guerra, M., *Searching for more effective agents and conditions for the RAFT polymerization of MMA: Influence of dithioester substituents, solvent, and temperature*, Macromolecules, **2005**, 38, 3129-3140.

[43] Thomas, D. B., Convertine, A. J., Myrick, L. J., Scales, C. W., Smith, A. E., Lowe, A. B., et al., *Kinetics and Molecular Weight Control of the Polymerization of Acrylamide via RAFT*, Macromolecules, **2004**, 37, 8941-8950.

[44] Anastas, P. T., Kirchhoff, M. M., *Origins, Current Status, and Future Challenges of Green Chemistry*, Accounts of Chemical Research, **2002**, 35, 686-694.

[45] Capello, C., Fischer, U., Hungerbühler, K., *What is a green solvent? A comprehensive framework for the environmental assessment of solvents*, Green Chemistry, **2007**, 9, 927.

[46] EU VOC-directive, *Council Directive 1999/13/EC of 11 March 1999 on the limitation of emissions of volatile organic compounds due to the use of organic solvents in certain activities and installations*, Official Journal of the European Communities: Brussels, **1999**.

[47] United States Environmental Protection Agency, *National Volatile Organic Compound Emission Standards for Consumer Products*, Final Rule. Federal Register, Vol. 63, 176, **1998**, pp. 48819-48847.

[48] Doble, M., Rollins, K., Kumar, A., *Green Chemistry and Engineering*. Elsevier Science, 2010.

[49] Kerton, F. M., *Alternative Solvents for Green Chemistry*. The Royal Society of Chemistry, Cambridge, 2009.

[50] Lobb, E. J., Ma, I., Billingham, N. C., Armes, S. P., Lewis, A. L., *Facile Synthesis of Well-Defined, Biocompatible Phosphorylcholine-Based Methacrylate Copolymers via Atom Transfer Radical Polymerization at 20 °C*, Journal of the American Chemical Society, **2001**, 123, 7913-7914.

[51] McCormick, C. L., Lowe, A. B., *Aqueous RAFT Polymerization: Recent Developments in Synthesis of Functional Water-Soluble (Co)polymers with Controlled Structures*, Accounts of Chemical Research, **2004**, 37, 312-325.

[52] Nguyen, N. H., Rosen, B. M., Jiang, X., Fleischmann, S., Percec, V., *New efficient reaction media for SET-LRP produced from binary mixtures of organic solvents and H2O*, Journal of Polymer Science Part A: Polymer Chemistry, **2009**, 47, 5577-5590.

[53] Kimani, S. M., Moratti, S. C., *Ambient-temperature copper-catalyzed atom transfer radical polymerization of methacrylates in ethylene glycol solvents*, Journal of Polymer Science Part A: Polymer Chemistry, **2005**, 43, 1588-1598.

[54] Lligadas, G., Percec, V., *Ultrafast SET-LRP of methyl acrylate at 25 °C in alcohols*, Journal of Polymer Science Part A: Polymer Chemistry, **2008**, 46, 2745-2754.

[55] McDonald, S., Rannard, S. P., *Room Temperature Waterborne ATRP of n-Butyl Methacrylate in Homogeneous Alcoholic Media*, Macromolecules, **2001**, 34, 8600-8602.

[56] Xiao, X., He, S., Dan, M., Su, Y., Huo, F., Zhang, W., *Brush macro-RAFT agent mediated dispersion polymerization of styrene in the alcohol/water mixture*, Journal of Polymer Science Part A: Polymer Chemistry, **2013**, 51, 3177-3190.

[57] Biedroń, T., Kubisa, P., *Ionic liquids as reaction media for polymerization processes: atom transfer radical polymerization (ATRP) of acrylates in ionic liquids*, Polymer International, **2003**, 52, 1584-1588.

[58] Sarbu, T., Matyjaszewski, K., *ATRP of methyl methacrylate in the presence of ionic liquids with ferrous and cuprous anions*, Macromolecular Chemistry and Physics, **2001**, 202, 3379-3391.

[59] Grignard, B., Calberg, C., Jerome, C., Wang, W., Howdle, S., Detrembleur, C., *Supported ATRP of fluorinated methacrylates in supercritical carbon dioxide: preparation of scCO2 soluble polymers with low catalytic residues*, Chemical Communications, **2008**, 5803-5805.

[60] Hawkins, G., Zetterlund, P. B., Aldabbagh, F., *RAFT polymerization in supercritical carbon dioxide based on an induced precipitation approach: Synthesis of 2-ethoxyethyl methacrylate/acrylamide block copolymers*, Journal of Polymer Science Part A: Polymer Chemistry, **2015**, n/a-n/a.

[61] McHale, R., Aldabbagh, F., Zetterlund, P. B., Okubo, M., *Nitroxide-Mediated Radical Precipitation Polymerization of Styrene in Supercritical Carbon Dioxide*, Macromolecular Chemistry and Physics, **2007**, 208, 1813-1822.

[62] Xia, J., Johnson, T., Gaynor, S. G., Matyjaszewski, K., DeSimone, J., *Atom Transfer Radical Polymerization in Supercritical Carbon Dioxide*, Macromolecules, **1999**, 32, 4802-4805.

[63] Zong, M., Thurecht, K. J., Howdle, S. M., *Dispersion polymerisation in supercritical CO2 using macro-RAFT agents*, Chemical Communications, **2008**, 5942-5944.

[64] Sarkar, A., Trivedi, S., Baker, G. A., Pandey, S., *Multiprobe Spectroscopic Evidence for "Hyperpolarity" within 1-Butyl-3-methylimidazolium Hexafluorophosphate Mixtures with Tetraethylene Glycol*, The Journal of Physical Chemistry B, **2008**, 112, 14927-14936.

CHAPTER 2

Cyclopentyl Methyl Ether: A New Green Co-Solvent for Supplemental Activator and Reducing Agent Atom Transfer Radical Polymerization

The contents of this chapter are published in: ***Maximiano, P.****, Mendes, J. P., Mendonça, P. V., Abreu, C. M. R., Guliashvili, T., Serra, A. C., et al., "Cyclopentyl methyl ether: A new green co-solvent for supplemental activator and reducing agent atom transfer radical polymerization", Journal of Polymer Science Part A: Polymer Chemistry, 2015, DOI: 10.1002/pola.27736.*

Chapter 2: Cyclopentyl Methyl Ether: A New Green Co-Solvent for Supplemental Activator and Reducing Agent Atom Transfer Radical Polymerization

2.1 Abstract

A new green solvent, cyclopentyl methyl ether (CPME), is used for the first time in solvent mixtures for the successful supplemental activator and reducing agent atom transfer radical polymerization (SARA ATRP) of both activated and non-activated monomers. The SARA ATRP of methyl acrylate (MA), glycidyl methacrylate (GMA), styrene (Sty), and vinyl chloride (VC) in CPME-based mixtures is studied and presents similar features to those reported in the literature using other SARA ATRP systems. Moreover, CPME-based mixtures are suitable solvents for the controlled SARA ATRP of MA using different SARA agents, such as Fe(0), Cu(0), or $Na_2S_2O_4$. The chemical structure and the retention of the chain-end functionality of the polymers are confirmed by ^{1}H NMR and MALDI-TOF analyses and the preparation of a well-defined PMA-*b*-PVC-*b*-PMA triblock copolymer. The method reported here presents an additional improvement in the search for new ecofriendly ATRP systems.

2.2 Introduction

Reversible deactivation radical polymerization (RDRP) methods are very effective techniques that allow the preparation of tailor-made polymers with targeted molecular weight, architecture, chain-end functionality and importantly with low dispersity (*Đ*). [1] Atom transfer radical polymerization (ATRP) is one of the most robust and versatile RDRP techniques, which has been used for the polymerization of a wide range of monomers. [2, 3] In ATRP, the fine control over the molecular weight of the polymers is provided by a metal-catalyzed (transition metal complexes with appropriate ligands) dynamic equilibrium between growing radicals ($P_n^{\bullet}$) and alkyl halide dormant species (P_n–X). [4] However, the main issue associated with the original ATRP technique is the use of a high concentration of metal catalyst required to guarantee the equilibrium, typically higher than

1000 parts per million (ppm), which can be problematic from both contamination of polymer and environmental standpoints. Therefore, new ATRP variation techniques [5-8] have been developed aiming to reduce the total amount of metal used to successfully mediate the polymerizations without losing their main features. [9, 10] Supplemental activator and reducing agent (SARA) ATRP is one of the most recent developed ATRP variations and it is considered to be a very attractive technique since it allows the use of a low concentration of soluble catalyst (e.g. 100 ppm [8]). With this approach, zero valent metals [8, 11-15] or Food and Drug Administration (FDA)-approved inorganic sulphites [16-20] have been successfully used as SARA agents. The role of these species is to continuously regenerate the activator (e.g., CuX; X: halide) by deactivator reduction (e.g., CuX_2) and to slowly generate growing radicals by supplemental activation (Figure 2-1). [4]

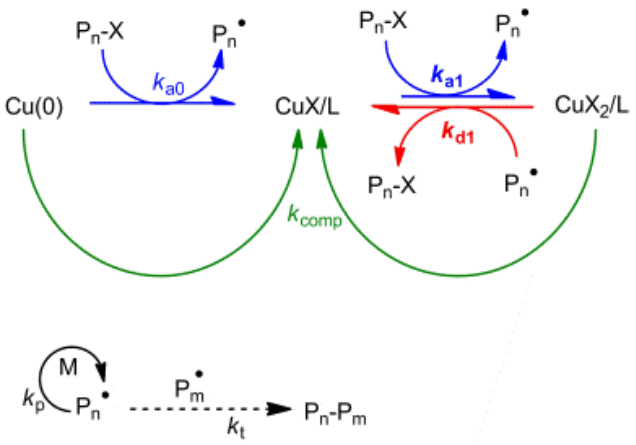

Figure 2-1: General mechanism of the Cu(0)/CuX_2/L-catalyzed SARA ATRP (L: ligand and X: halide).

Besides the concerns about the amount of metal catalyst used in the polymerization, current research efforts on ATRP are also focused on the use of alternative ecofriendly solvents to the traditional organic ones used, such as dimethylformamide (DMF) [15], dimethyl sulfoxide (DMSO) [21] or tetrahydrofuran (THF), [22] which present high concern when considering pharmaceutical usages. [23] Recently, our research group has demonstrated the possibility of using the industrial solvent sulfolane, which is a more acceptable solvent, as a universal solvent for the preparation of a wide range of polymers by SARA ATRP. [20] This strategy aims to potentiate the implementation of ATRP at an industrial scale, as well as to provide harmless reaction conditions for the preparation of polymers for the biomedical field. On this matter, it is worth to notice that the SARA ATRP of acrylates, methacrylates and acrylamides has also been successfully performed in alcohol/water mixtures [11-13, 18, 19] or even aqueous medium. [13, 24]

In the search of new ecofriendly solvents, the attention was turned to cyclopentyl methyl ether (CPME) (Figure 2-2), an ethereal solvent which has emerged as a green alternative to similar solvents (e.g., THF). This feature is a direct consequence of unique properties, such as high hydrophobicity, relative stability under both acidic and basic conditions and low formation of peroxides as by products. [25] In addition, CPME reveals negative skin sensitization,[26] presents no genotoxicity and no mutagenicity, [27] and it is approved by the Toxic Substances Control Act (TSCA) and the European List of Notified Chemical Substances (ELINCS). Due to the above mentioned advantages, CPME has been employed as a green process solvent for organic synthesis. [28] Despite of being already used as solvent for radical reactions, [29] CPME has never been reported in ATRP reactions (or ATRP variations). Particularly, the use of CPME in place of DMSO and/or THF in controlled radical polymerization (including ATRP) of VC is very challenging. This is because DMSO and THF are only known best solvents for homogeneous and heterogeneous living polymerizations of vinyl chloride (VC) and the replacement of above solvents with less toxic and recyclable CPME is very attractive.

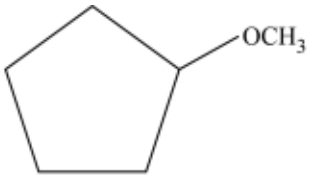

Ecofriendly, high hydrophobicity, negative skin sensitization, no mutagenicity and no genotoxicity

Figure 2-2: Chemical structure of cyclopentyl methyl ether and some of its "green" aspects

In this work, CPME-based mixtures were used for the first time as solvents for the SARA ATRP of different monomer families: (meth)acrylates, styrene (Sty) and vinyl chloride (VC). The three most studied SARA agents (Cu(0), Fe(0) and $Na_2S_2O_4$) were tested and allowed the preparation of well-defined poly(methyl acrylate) (PMA). In addition, an unique PMA-*b*-PVC-*b*-PMA block copolymer (PVC: poly(vinyl chloride)) was prepared using the SARA ATRP developed system.

2.3 Experimental Section

The materials, analytical techniques and experimental procedures used in this chapter are described in detail on Appendix A.

2.4 Results and Discussion

2.4.1 Influence of the solvent mixture and composition

There are several reports on the controlled polymerization of MA (used as model monomer). [4, 11, 16, 17, 21, 30] In this study, the SARA ATRP of MA was firstly investigated using the catalytic system of Cu(0)/$CuBr_2$/Me_6TREN. [4, 20, 24, 30] Preliminary experiments using just CPME as the polymerization solvent were not successful due the insolubility of several catalytic complexes in this solvent ($CuBr_2$/ligand; ligand: Me_6TREN, TPMA, Bpy, PMDETA or TREN). Alternatively, CPME was mixed with DMSO, which is a common solvent used in the controlled polymerization of MA. [21] Several CPME/DMSO ratios were tested and the minimum amount of DMSO required for the complete dissolution of the $CuBr_2$/Me_6TREN complex was found to be 30% (v/v). The kinetic results showed that the SARA ATRP of MA in CPME/DMSO = 70/30 (v/v) was extremely well-controlled ($Đ \leq 1.1$) at a reasonable polymerization rate (see Appendix A, Figure A1), proving the usefulness of the CPME as a green solvent for the SARA ATRP of MA. Aiming to achieve a complete harmless reaction solvent mixture, DMSO was replaced by EtOH, which has been also used for the SARA ATRP of different monomers. [11, 13, 17] In this case, the addition of a small amount of water was also required to allow a complete dissolution of the catalytic complex. The optimum value of the water content was found to be 2% (v/v), based on a compromise between the solubility of the catalytic system and the miscibility of the solvents, since CPME and water are not miscible. Figure 2-3 (b) shows that this ecofriendly SARA ATRP system provided a stringent control over the $Đ$ throughout the entire reaction, and the theoretical molecular weights were in close agreement with the experimental ones.

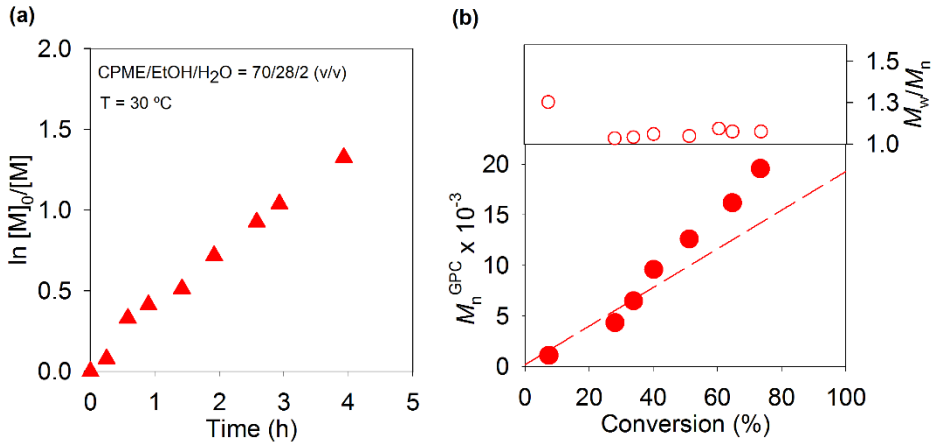

Figure 2-3: (a) Kinetic plots of conversion and $\ln[M]_0/[M]$ vs. time and (b) plot of number-average molecular weights (M_n^{GPC}) and $Đ$ (M_w/M_n) vs. monomer conversion for the SARA ATRP of MA in CPME/EtOH/H_2O = 70/28/2 (v/v/v) at 30 °C. Reaction conditions: $[MA]_0$/[solvent] = 2/1 (v/v); $[MA]_0/[EBiB]_0/Cu(0)/[CuBr_2]_0/[Me_6TREN]_0$ = 222/1/Cu(0) wire/0.1/1.1.

Results also suggested that the amount of water used in the solvent mixture (2%) was not enough to afford an increase in the polymerization rate (compare Figure 2-3 (b) with Figure A1 (b)), as it was observed for other water-containing solvent mixtures used in SARA ATRP. The structure of the well-defined Br-terminated PMA was confirmed by ^{1}H NMR spectroscopy (Figure 2-4) and it was in agreement with other results reported in the literature for Cu(0)-catalyzed RDRP of MA. [21, 31]

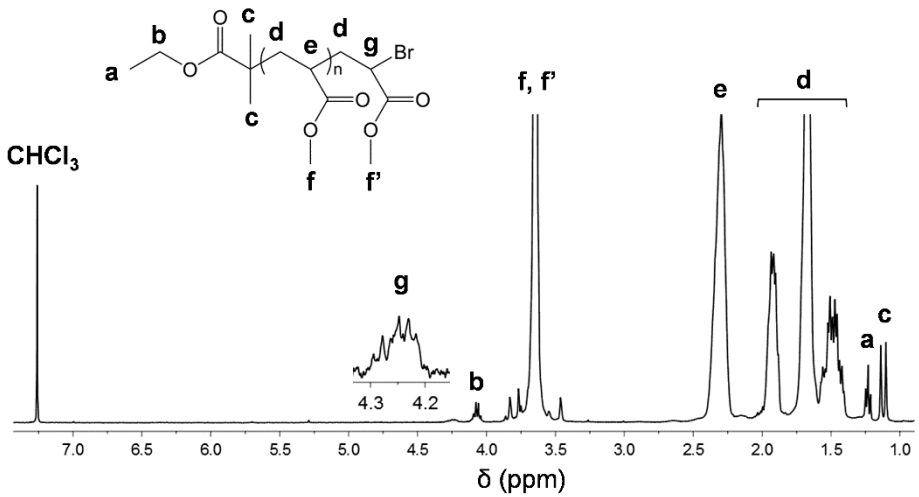

Figure 2-4: ^{1}H NMR spectrum of a PMA sample (M_{n}^{GPC} = 10 600 ; $Đ$ = 1.28) obtained by SARA ATRP in CPME/EtOH/H_2O = 70/28/2 (v/v/v) at 30 °C.

2.4.2 Influence of the catalytic system

The viability of the new reaction solvent mixture (CPME/EtOH/H_2O) was investigated using the most common SARA agents: Cu(0), [4, 13, 24] Fe(0) [8, 11, 12, 14] and $Na_2S_2O_4$. [16-19] Besides the use of an ecofriendly solvent mixture, the use of these SARA agents is very attractive considering the preparation of polymers for biomedical applications. On this matter, it is worth noting that zero valent metals can be easily removed from the reaction medium after the polymerization (iron is also a very biocompatible metal), while $Na_2S_2O_4$ is a FDA-approved compound. The polymerization rate was in the same order when either Cu(0) or Fe(0) were used as SARA agents (Figure 2-5 (a)).

In the case of $Na_2S_2O_4$, the polymerization was considerably slower (Table 2-1), most probably due to the very low solubility of $Na_2S_2O_4$ in the reaction solvent mixture. A similar behavior has been observed when DMSO was used as the polymerization solvent. [16] Nevertheless, the results also show that regardless the SARA agent used, the polymerization system allowed an excellent control over the molecular weight of PMA

(Figure 2-5 (b) and Table 2-1). This observation suggests that the SARA ATRP is a very robust and versatile technique for the preparation of well-defined polymers under different experimental conditions near room temperature.

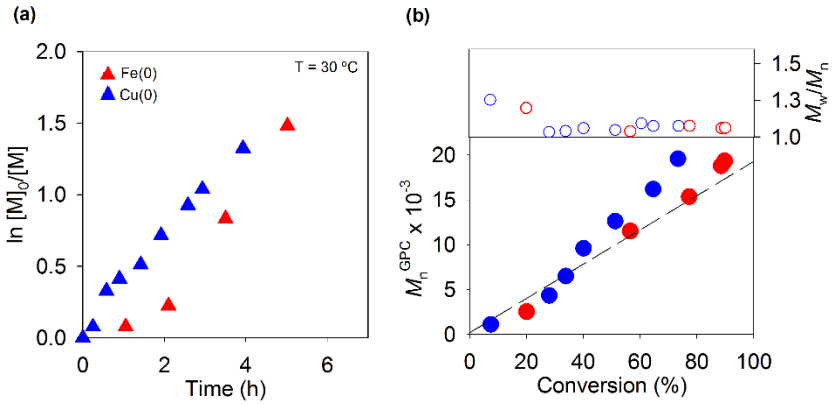

Figure 2-5: (a) Kinetic plots of conversion and ln[M]$_0$/[M] *vs.* time and (b) plot of number-average molecular weights (M_n^{GPC}) and $Đ$ (M_w/M_n) *vs.* monomer conversion for the SARA ATRP of MA in CPME/EtOH/H_2O = 70/28/2 (v/v/v) at 30 °C, using different SARA agents. Reaction conditions: [MA]$_0$/[solvent] = 2/1 (v/v); [MA]$_0$/[EBiB]$_0$/[SARA agent]$_0$/[$CuBr_2$]$_0$/[Me_6TREN]$_0$= 222/1/Cu(0) wire or Fe(0) powder/0.1/1.1.

Table 2-1: Molecular weight parameters of the PMA-Br prepared by SARA ATRP in CPME/EtOH/H_2O = 70/28/2 (v/v/v) at 30 °C, using different SARA agents. Reaction conditions: [MA]$_0$/[EBiB]$_0$ = 222; [MA]$_0$/[solvent] = 2/1 (v/v); [Fe(0) or Cu(0)]/[$CuBr_2$]$_0$/[Me_6TREN]$_0$ = Cu(0) wire or Fe(0) powder/0.1/1.1; [$Na_2S_2O_4$]/[$CuBr_2$]$_0$/[Me_6TREN]$_0$ = 1/0.1/0.5.

Entry	SARA agent	k_p^{app} (h-1)	Time (h)	Conv. (%)	M_n^{GPC} x 10^{-3}	$Đ$
1	Cu(0)	0.332	3.9	73	19.6	1.08
2	Fe(0)	0.344	5.0	77	15.4	1.08
3	$Na_2S_2O_4$	0.194	7.9	42	4.7	1.01

2.4.3 Influence of the degree of polymerization

The targeted degree of polymerization (DP) has a major role in the rate of reaction due to different concentration of radicals during the polymerization. In addition, the control over the polymerization and the maximum monomer conversion that can be achieved could be compromised for high targeted DP values. In this work, the targeted DP of MA was investigated in the range of 100 – 1000 in order to evaluate the robustness of the SARA ATRP using a CPME-based mixture. As expected, the rate of polymerization decreased with the increase of the targeted DP (Figure 2-6 (a)). The solvent mixture used (CPME/EtOH/H_2O = 70/28/2 (v/v/v)) allowed the preparation of very well-defined PMA

($Đ \approx 1.1$) and high monomer conversion was achieved, suggesting that the SARA ATRP system developed is quite robust.

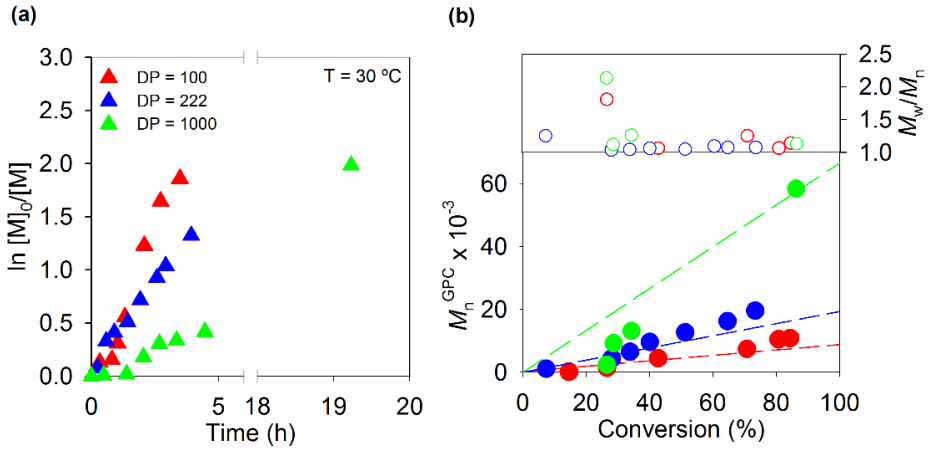

Figure 2-6: (a) Kinetic plots of conversion and $\ln[M]_0/[M]$ *vs.* time and (b) plot of number-average molecular weights (M_n^{GPC}) and $Đ$ (M_w/M_n) *vs.* monomer conversion for the SARA ATRP of MA in CPME/EtOH/H_2O = 70/28/2 (v/v/v) at 30 °C, for different targeted DP values. Reaction conditions: $[MA]_0/[solvent]$ = 2/1 (v/v); $[MA]_0/[EBiB]_0/Cu(0)/[CuBr_2]_0/[Me_6TREN]_0$= DP/1/Cu(0) wire/0.1/1.1.

2.4.4 Polymerization of Styrene, Vinyl Chloride, and Glycidyl Methacrylate

The application of the new solvent mixture developed for the SARA ATRP technique was extended to the polymerization of three relevant monomers: Sty, GMA, and VC. The CPME-based mixtures, as well as the catalytic complexes and initiators, were adjusted according to the structure of the monomers, to provide well-controlled polymerizations. [20, 32]

Figure 2-7 shows the kinetic data obtained for the polymerization of Sty in a CPME/DMF = 70/30 (v/v) mixture. The polymerization was first-order with respect to monomer conversion and both the reaction rate and the control over the molecular weight were in the same range of previous results reported by our group on the Fe(0)-catalyzed SARA ATRP of Sty in DMF. [15] Additionally, this work allowed the polymerization of Sty at a lower temperature (60 °C) than the usual value (>70 °C) reported in the literature. [15, 33-36] This fact could potentially contribute to the decrease of the well-known side reactions occurring for the Sty polymerization at high temperatures, such as the loss of the chain-end functionality or monomer self-initiation. [3] The chemical structure of the PS prepared by SARA ATRP was confirmed by ^{1}H NMR analysis (Appendix A,

Fig. A3) and the "living" character of the polymer was evaluated by a self-extension experiment (Appendix A, Fig. A2).

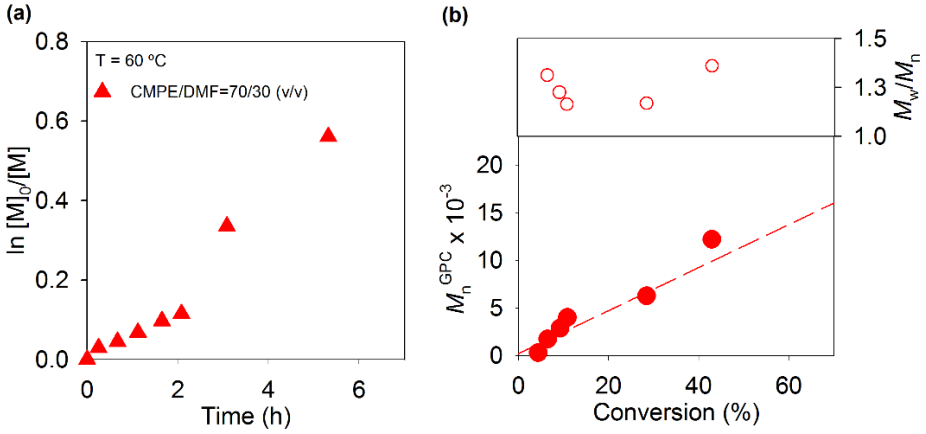

Figure 2-7: (a) Kinetic plots of conversion and ln[M]$_0$/[M] versus time and (b) plot of number-average molecular weights (M_n^{GPC}) and $Đ$ (M_w/M_n) versus monomer conversion for the SARA ATRP of Sty in CPME/DMF = 70/30 (v/v) at 60 °C. Reaction conditions: [Sty]$_0$/[solvent] = 2/1 (v/v); [Sty]$_0$/[EBiB]$_0$/Cu(0)/[$CuBr_2$]$_0$/[PMDETA]$_0$ = 222/1/Cu(0) wire/0.1/1.1.

The presence of the epoxide ring in the structure of GMA makes this monomer very attractive for the preparation of complex polymeric structures, through post-polymerization ring-opening reactions. GMA-based polymers have been used in several areas, such as adhesives, drug-delivery, or coatings, among others, proving the versatility and economical value of this monomer. [37-39] The polymerization of GMA by SARA ATRP was recently reported by our research group using a mixed-metal catalytic system in toluene/DMF mixtures. [32] In this work, it was possible to replace the harmful toluene by the ecofriendly CPME, with very promising results in terms of $Đ$ (Table 2-2, entry 2). In addition, the polymerization was considerably faster than the previously reported, [32] with monomer reaching relatively high conversion (70%) after 1.2 h of reaction.

The use of a CPME/DMSO = 70/30 (v/v) mixture for the SARA ATRP of VC (non-activated monomer) allowed the preparation of well-defined structures (Table 2-2, entries 3–4). Similar results were obtained using a previously reported SARA ATRP system in sulfolane. [20] This observation corroborates the versatility and robustness of the SARA ATRP technique for both activated and non-activated monomers. In addition, a α,ω-di(bromo)PVC (p(VC) = 61.8%, M_n^{th} = 5000, M_n^{GPC} = 6100, $Đ$ = 1.57, see Appendix A, Fig. A5) obtained by bromoform-initiated SARA ATRP was used as a macroinitiator for the preparation of a PMA-*b*-PVC-*b*-PMA (p(MA) = 77.3%, M_n^{th} = 39400, M_n^{GPC} = 40700, $Đ$ =

1.49) triblock copolymer by "one-pot" SARA ATRP in CPME/DMSO = 70/30 (v/v). The chromatograms shown in Figure 2-8 demonstrate a shift of the macroinitiator molecular weight distribution towards high molecular weight values (lower retention volume), with no increase of the dispersity of the block copolymer.

Table 2-2: Molecular Weight Parameters of the PS-Br, PGMA-Br, and Br-PVC-Br prepared by SARA ATRP in CPME-Based Mixtures.

Entry	Monomer	Solvent (v/v)	$[M]_0/[I]_0$[d]	Time (h)	Conv. (%)	M_n^{GPC} x 10^{-3}	$Đ$
1	Sty[a]	CPME/DMF = 70/30	222	3	28	6.2	1.17
2	GMA[b]	CPME/DMF = 70/30	222	1.2	70	17.5	1.27
3	VC[c]	CPME/DMSO = 70/30	222	7.5	37	6.7	1.58
4	VC[c]	CPME/DMSO = 70/30	100	10	62	6.1	1.57

[a] Reaction conditions: $[Sty]_0/[solvent]$ = 2/1 (v/v); $[Sty]_0/[EBiB]_0/[Cu(0)]_0/[CuBr_2]_0/[PMDETA]_0$ = 222/1/Cu(0) wire/0.1/1.1; T = 60 °C.

[b] Reaction conditions: $[GMA]_0/[solvent]$ = 2/1 (v/v); $[GMA]_0/[EBiB]_0/[Fe(0)]_0/[CuBr2]_0/[TPMA]_0$ = 222/1/1/0.1/1.1; T = 30 °C

[c] Reaction conditions: $[VC]_0/[solvent]$ = 1/1 (v/v); $[VC]_0/[CHBr_3]_0/[Cu(0)]0/[CuBr_2]_0/[TREN]_0$ = DP/1/Cu(0) wire/0.1/1.1; T = 42 °C.

[d] M: monomer; I: initiator (EBiB for Sty and GMA and $CHBr_3$ for VC)

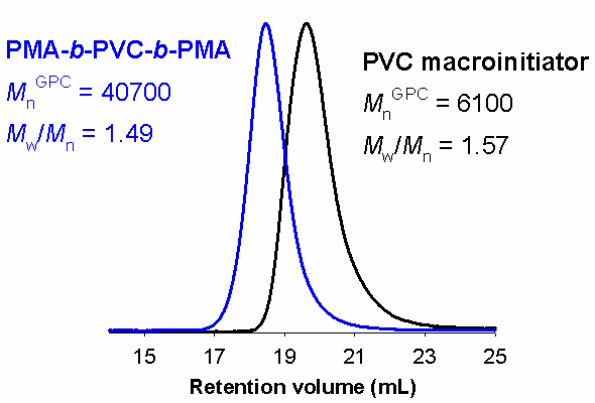

Figure 2-8: GPC chromatograms of a α,ω-di(bromo)PVC (p(VC) = 61.8%, M_n^{th} = 5000, M_n^{GPC} = 6100, $Đ$ = 1.57) macroinitiator (black line) and PMA-*b*-PVC-*b*-PMA (p(MA) = 77.3%, M_n^{th} = 39400, M_n^{GPC} = 40700, $Đ$ = 1.49) triblock copolymer (blue line), after "one-pot" chain extension by SARA ATRP in CPME/DMSO = 70/30 (v/v).

These results suggest that the PVC prepared by SARA ATRP, using this system, is able to retain enough chain-end functionality to allow the preparation of copolymeric structures, which is of extreme importance for the macromolecular engineering field. The structure of the block copolymer was confirmed by ^{1}H NMR analysis (Figure 2-9).

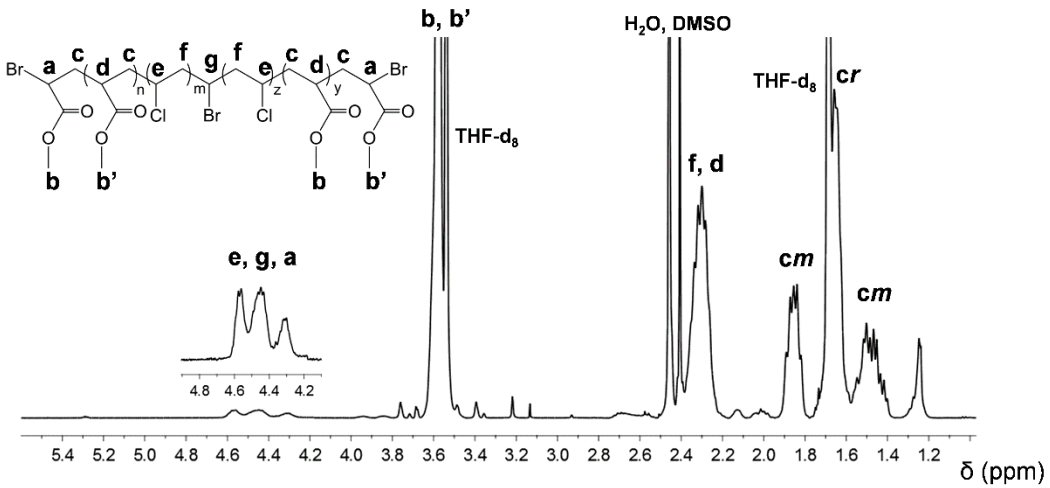

Figure 2-9: ^{1}H NMR of a purified PMA-*b*-PVC-*b*-PMA (M_n^{GPC} = 40700, $Đ$ = 1.49) triblock copolymer obtained by "one-pot" SARA ATRP in CPME/DMSO = 70/30 (v/v); solvent: d_8-THF.

2.5 Conclusions

The use of environmentally attractive CPME in solvent mixtures for the Cu(0)-catalyzed SARA ATRP of several monomer families was demonstrated. Well-defined PMA, PGMA, PS, and PVC were obtained using several experimental conditions. In addition, the biocompatible Fe(0) and $Na_2S_2O_4$ were successfully used as SARA agents to mediate the MA polymerization. As a proof-of-concept, the SARA ATRP system developed was also used for the preparation of a PMA-*b*-PVC-*b*-PMA triblock copolymer. Besides the eco-friendly nature of both CPME and SARA agents used, the SARA ATRP technique can be of particular interest due to the low concentration of soluble metal catalyst employed. Therefore, the strategy presented here could be useful for the preparation of well-defined materials for biomedical applications.

2.6 References

[1] Braunecker, W., Matyjaszewski, K., *Controlled/living radical polymerization: Features, developments, and perspectives*, Progress in Polymer Science, **2007**, 32, 93-146.

[2] Kamigaito, M., Ando, T., Sawamoto, M., *Metal-Catalyzed Living Radical Polymerization*, Chemical Reviews, **2001**, 101, 3689-3746.

[3] Matyjaszewski, K., Xia, J., *Atom transfer radical polymerization*, Chemical reviews, **2001**, 101, 2921-2990.

[4] Guliashvili, T., Mendonça, P. V., Serra, A. C., Popov, A. V., Coelho, J. F. J., *Copper-Mediated Controlled/"Living" Radical Polymerization in Polar Solvents: Insights into Some Relevant Mechanistic Aspects*, Chemistry - A European Journal, **2012**, 18, 4607-4612.

[5] Jakubowski, W., Matyjaszewski, K., *Activators Regenerated by Electron Transfer for Atom-Transfer Radical Polymerization of (Meth)acrylates and Related Block Copolymers*, Angewandte Chemie, **2006**, 118, 4594-4598.

[6] Magenau, A. J. D., Strandwitz, N. C., Gennaro, A., Matyjaszewski, K., *Electrochemically Mediated Atom Transfer Radical Polymerization*, Science, **2011**, 332, 81-84.

[7] Matyjaszewski, K., Jakubowski, W., Min, K., Tang, W., Huang, J., Braunecker, W. A., et al., *Diminishing catalyst concentration in atom transfer radical polymerization with reducing agents*, Proceedings of the National Academy of Sciences of the United States of America, **2006**, 103, 15309-15314.

[8] Zhang, Y., Wang, Y., Matyjaszewski, K., *ATRP of methyl acrylate with metallic zinc, magnesium, and iron as reducing agents and supplemental activators*, Macromolecules, **2011**, 44, 683-685.

[9] Pintauer, T., Matyjaszewski, K., *Atom transfer radical addition and polymerization reactions catalyzed by ppm amounts of copper complexes*, Chemical Society Reviews, **2008**, 37, 1087-1097.

[10] Tsarevsky, N. V., Matyjaszewski, K., *"Green" atom transfer radical polymerization: from process design to preparation of well-defined environmentally friendly polymeric materials*, Chemical reviews, **2007**, 107, 2270-2299.

[11] Abreu, C. M. R., Mendonça, P. V., Serra, A. C., Coelho, J. F. J., Popov, A. V., Guliashvili, T., *Accelerated Ambient-Temperature ATRP of Methyl Acrylate in Alcohol–Water Solutions with a Mixed Transition-Metal Catalyst System*, Macromolecular Chemistry and Physics, **2012**, 213, 1677-1687.

[12] Cordeiro, R., Rocha, N., Mendes, J. P., Matyjaszewski, K., Guliashvili, T., Serra, A. C., et al., *Synthesis of well-defined poly(2-(dimethylamino)ethyl methacrylate) under mild conditions and its co-polymers with cholesterol and PEG using Fe(0)/Cu(ii) based SARA ATRP*, Polymer Chemistry, **2013**, 4, 3088-3088.

[13] Mendonça, P. V., Konkolewicz, D., Averick, S. E., Serra, A. C., Popov, A. V., Guliashvili, T., et al., *Synthesis of cationic poly ((3-acrylamidopropyl) trimethylammonium chloride) by SARA ATRP in ecofriendly solvent mixtures*, Polymer Chemistry, **2014**, 5, 5829-5836.

[14] Mendonça, P. V., Serra, A. C., Coelho, J. F. J., Popov, A. V., Guliashvili, T., *Ambient temperature rapid ATRP of methyl acrylate, methyl methacrylate and styrene in polar solvents with mixed transition metal catalyst system*, European Polymer Journal, **2011**, 47, 1460-1466.

[15] Rocha, N., Mendonça, P. V., Mendes, J. P., Simões, P. N., Popov, A. V., Guliashvili, T., et al., *Facile Synthesis of Well-Defined Telechelic Alkyne-Terminated Polystyrene in Polar Media Using ATRP With Mixed Fe/Cu Transition Metal Catalyst*, Macromolecular Chemistry and Physics, **2013**, 214, 76-84.

[16] Abreu, C. M. R., Mendonça, P. V., Serra, A. C., Popov, A. V., Matyjaszewski, K., Guliashvili, T., et al., *Inorganic sulfites: Efficient reducing agents and supplemental activators for atom transfer radical polymerization*, ACS Macro Letters, **2012**, 1, 1308-1311.

[17] Abreu, C. M. R., Serra, A. C., Popov, A. V., Matyjaszewski, K., Guliashvili, T., Coelho, J. F. J., *Ambient temperature rapid SARA ATRP of acrylates and methacrylates in alcohol-water solutions mediated by a mixed sulfite/Cu(ii)Br2 catalytic system*, Polymer Chemistry, **2013**, 4, 5629-5636.

[18] Góis, J. R., Konkolewicz, D., Popov, A. V., Guliashvili, T., Matyjaszewski, K., Serra, A. C., et al., *Improvement of the control over SARA ATRP of 2-(diisopropylamino)ethyl methacrylate by slow and continuous addition of sodium dithionite*, Polymer Chemistry, **2014**, 5, 4617-4626.

[19] Góis, J. R., Rocha, N., Popov, A. V., Guliashvili, T., Matyjaszewski, K., Serra, A. C., et al., *Synthesis of well-defined functionalized poly(2-(diisopropylamino)ethyl methacrylate) using ATRP with sodium dithionite as a SARA agent*, Polymer Chemistry, **2014**, 5, 3919-3919.

[20] Mendes, J. P., Branco, F., Abreu, C. M. R., Mendonça, P. V., Serra, A. C., Popov, A. V., et al., *Sulfolane: an Efficient and Universal Solvent for Copper-Mediated Atom Transfer Radical (co)Polymerization of Acrylates, Methacrylates, Styrene, and Vinyl Chloride*, ACS Macro Letters, **2014**, 3, 858-861.

[21] Percec, V., Guliashvili, T., Ladislaw, J. S., Wistrand, A., Stjerndahl, A., Sienkowska, M. J., et al., *Ultrafast Synthesis of Ultrahigh Molar Mass Polymers by Metal-Catalyzed Living Radical Polymerization of Acrylates, Methacrylates, and Vinyl Chloride Mediated by SET at 25 °C*, Journal of the American Chemical Society, **2006**, 128, 14156-14165.

[22] Ye, J., Narain, R., *Water-Assisted Atom Transfer Radical Polymerization of N-Isopropylacrylamide: Nature of Solvent and Temperature*, The Journal of Physical Chemistry B, **2009**, 113, 676-681.

[23] Prat, D., Hayler, J., Wells, A., *A survey of solvent selection guides*, Green Chemistry, **2014**, 16, 4546-4551.

[24] Konkolewicz, D., Krys, P., Góis, J. R., Mendonça, P. V., Zhong, M., Wang, Y., et al., *Aqueous RDRP in the Presence of Cu0: The Exceptional Activity of CuI Confirms the SARA ATRP Mechanism*, Macromolecules, **2014**, 47, 560-570.

[25] Watanabe, K., Yamagiwa, N., Torisawa, Y., *Cyclopentyl methyl ether as a new and alternative process solvent*, Organic Process Research and Development, **2007**, 11, 251-258.

[26] Watanabe, K., *The Toxicological Assessment of Cyclopentyl Methyl Ether (CPME) as a Green Solvent*, Molecules, **2013**, 18, 3183-3194.

[27] Antonucci, V., Coleman, J., Ferry, J. B., Johnson, N., Mathe, M., Scott, J. P., et al., *Toxicological Assessment of 2-Methyltetrahydrofuran and Cyclopentyl Methyl Ether in Support of Their Use in Pharmaceutical Chemical Process Development*, Organic Process Research & Development, **2011**, 15, 939-941.

[28] Sakamoto, S., *Contribution of Cyclopentyl Methyl Ether (CPME) to Green Chemistry*, Chim. Oggi-Chem. Today, **2013**, 31, 24-27.

[29] Kobayashi, S., Kuroda, H., Ohtsuka, Y., Kashihara, T., Masuyama, A., Watanabe, K., *Evaluation of cyclopentyl methyl ether (CPME) as a solvent for radical reactions*, Tetrahedron, **2013**, 69, 2251-2259.

[30] Zhang, Y., Wang, Y., Peng, C.-h., Zhong, M., Zhu, W., Konkolewicz, D., et al., *Copper-Mediated CRP of Methyl Acrylate in the Presence of Metallic Copper: Effect of Ligand Structure on Reaction Kinetics*, Macromolecules, **2012**, 45, 78-86.

[31] Nyström, F., Soeriyadi, A. H., Boyer, C., Zetterlund, P. B., Whittaker, M. R., *End-group fidelity of copper(0)-meditated radical polymerization at high monomer conversion: an ESI-MS investigation*, Journal of Polymer Science Part A: Polymer Chemistry, **2011**, 49, 5313-5321.

[32] Catalao, F., Gois, J. R., Trino, A. S. M., Serra, A. C., Coelho, J. F. J., *Facile synthesis of well-controlled poly(glycidyl methacrylate) and its block copolymers via SARA ATRP at room temperature*, Polymer Chemistry, **2015**, 6, 1875-1882.

[33] Jakubowski, W., Kirci-Denizli, B., Gil, R. R., Matyjaszewski, K., *Polystyrene with Improved Chain-End Functionality and Higher Molecular Weight by ARGET ATRP*, Macromolecular Chemistry and Physics, **2008**, 209, 32-39.

[34] Jakubowski, W., Min, K., Matyjaszewski, K., *Activators Regenerated by Electron Transfer for Atom Transfer Radical Polymerization of Styrene*, Macromolecules, **2006**, 39, 39-45.

[35] Lutz, J. F., Matyjaszewski, K., *Nuclear magnetic resonance monitoring of chain-end functionality in the atom transfer radical polymerization of styrene*, Journal of Polymer Science Part A: Polymer Chemistry, **2005**, 43, 897-910.

[36] Tom, J., Hornby, B., West, A., Harrisson, S., Perrier, S., *Copper(0)-mediated living radical polymerization of styrene*, Polymer Chemistry, **2010**, 1, 420-422.

[37] Hagit, A., Soenke, B., Johannes, B., Shlomo, M., *Synthesis and Characterization of Dual Modality (CT/MRI) Core–Shell Microparticles for Embolization Purposes*, Biomacromolecules, **2010**, 11, 1600-1607.

[38] Han, T. L., Kumar, R. N., Rozman, H. D., Noor, M. A. M., *GMA grafted sago starch as a reactive component in ultra violet radiation curable coatings*, Carbohydrate Polymers, **2003**, 54, 509-516.

[39] Papakonstantinou, A. E., Eliades, T., Cellesi, F., Watts, D. C., Silikas, N., *Evaluation of UDMA's potential as a substitute for Bis-GMA in orthodontic adhesives*, Dental Materials, **2013**, 29, 898-905.

CHAPTER 3

Cyclopentyl Methyl Ether As A Green Solvent for Reversible-Addition Fragmentation Chain Transfer and Nitroxide-Mediated Polymerizations

The contents of this chapter were submitted as part of the following paper: Abreu, C. M. R., ***Maximiano, P.****, Guliashvili, T., Nicolas, J., Serra, A. C., Coelho, J. F. J., "Cyclopentyl Methyl Ether as A Green Solvent for Reversible-Addition Fragmentation Chain Transfer and Nitroxide-Mediated Polymerizations", 2015.*

Chapter 3: Cyclopentyl Methyl Ether As A Green Solvent for Reversible-Addition Fragmentation Chain Transfer and Nitroxide-Mediated Polymerizations

3.1 Abstract

Cyclopentyl methyl ether (CPME) was successfully used as an environmentally friendly alternative to regularly employed organic solvents (e.g., tetrahydrofuran (THF), dimethyl sulfoxide (DMSO), dichloromethane (DCM) and dimethylformamide (DMF)) for the reversible-addition fragmentation chain transfer (RAFT) and nitroxide-mediated polymerization (NMP) polymerizations of vinyl chloride (VC) and styrene (Sty). Methyl acrylate (MA) and vinyl acetate (VAc) were also successfully polymerized via RAFT using CPME. The kinetic data showed a linear increase of the molecular weight with the conversion for both polymerization methods. The k_p^{app} data obtained in CPME were in range of values reported for THF, DMSO, DCM and DMF, while the final conversions are higher. The polymer samples were comprehensively characterized by proton nuclear magnetic resonance spectroscopy (^{1}H NMR), ^{31}P NMR, matrix-assisted laser desorption ionization time-of-flight mass spectroscopy (MALDI-TOF-MS) and size exclusion chromatography (SEC). The "livingness" of the PVC macroinitiators prepared by RAFT and NMP were confirmed by chain-end characterization and successful reinitiation experiments. The data presented in this manuscript proves that CPME is an excellent green substitute to avoid the use of toxic solvents for RAFT and NMP.

3.2 Introduction

Reversible deactivation radical polymerization (RDRP) has revolutionized the field of macromolecular synthesis. On this matter, it is now possible to synthesize tailor made (co)polymers with controlled molecular weight, topology, architecture and functionalities. [1-6] The most popular RDRP methods are: atom transfer radical polymerization (ATRP) [5-7], nitroxide-mediated polymerization (NMP) [2, 8] and reversible addition-fragmentation transfer polymerization (RAFT) [3, 4, 9-12]. The intense research efforts of

the scientific community during the last two decades on their mechanistic understanding [2, 10, 13, 14] enabled to expand the range of monomers covered and to establish new reactions conditions that can be implemented in large scale production.

Although polymerizations in bulk and in dispersed media have been widely studied [15-17], solution polymerizations received less attention despite their numerous advantages (e.g., low viscosity of the reaction medium, possibility to dilute the reaction medium and avoid the gel effect, broad variety of solvents, etc.). [18-20] Even though water is the ideal solvent in terms of innocuousness, very few monomers/polymers are water-soluble. Therefore, alternative "green" organic solvents are highly desirable. The continuous search to find eco-friendly solvents for RDRP methods resulted in the use of water [21-24], water/alcohol mixtures [25-31], and ionic liquids. [32-36]

Recently, our research group introduced for the first time the use of CPME in the RDRP arena. [37] CPME presents several important features that are particularly relevant. It is highly hydrophobic and presents a good stability in acidic and basic conditions. [38] Moreover, it leads to a low formation of peroxides as by-products, results in negative skin sensitization [39], gives no genotoxicity or mutagenicity [40] and is approved by the Toxic Substances Control Act (TSCA) and the European List of Notified Chemical Substances (ELINCS). [37, 38] CPME was successfully employed as co-solvent in the supplemental activator reducing agent (SARA) ATRP of MA, glycidyl methacrylate (GMA), Sty and VC. [37] CPME is therefore very appealing to circumvent the toxicological drawbacks commonly associated with the use of DMSO, DMF, DCM and THF, which are very effective solvents for homogeneous RDRP methods of hydrophobic monomers such as VC [18, 41-44] and Sty [45-47]. Here, we demonstrate that CPME is a suitable (and nearly universal) solvent to perform RAFT and NMP of VC and Sty as well as RAFT of MA and VAc.

3.3 Experimental Section

The materials, analytical techniques and experimental procedures used in this chapter are described in detail on Appendix B.

3.4 Results and discussion

In a previous publication from our group, CPME was used for the first time in the SARA-ATRP [37] using $CuBr_2$/ligands (e.g., Me_6TREN, TPMA, Bpy, PMDETA and TREN). The poor solubility of metal complexes in CPME required the addition of co-solvents (e.g., H_2O and EtOH). For RAFT and NMP, it was considered to use CMPE as the only polymerization solvent.

3.4.1 RAFT Polymerization in CPME

Preliminary RAFT polymerization experiments were conducted using MA with DDMAT as chain transfer agent (CTA) in CPME for a DP_T of 222. The results presented in Figure 3-1 and Table 3-1 (entry 1) show first-order kinetics with respect to MA, a good agreement between theoretical and determined molecular weights and low $Đ$ values (below 1.1), indicating an excellent control of the polymerization even up to high conversions (~ 95%). These observations allowed us to conclude that CPME is a solvent compatible with RAFT systems.

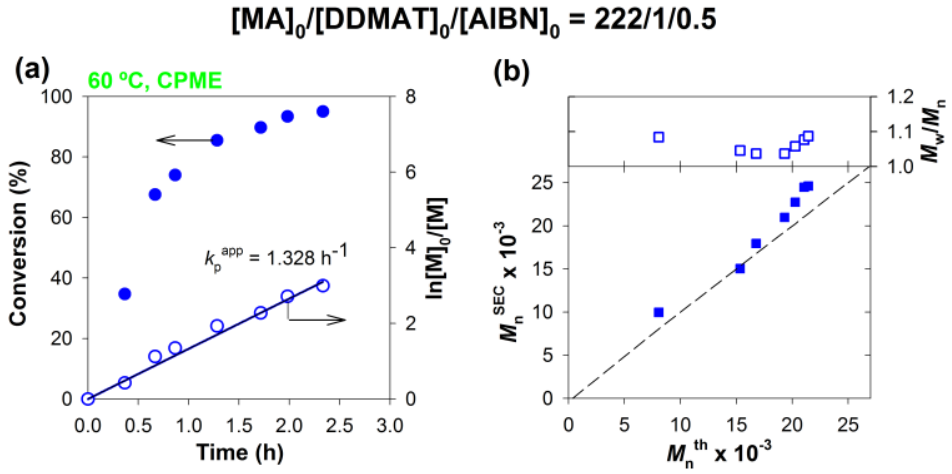

Figure 3-1: RAFT polymerization of MA in CPME at 60 °C mediated by DDMAT using AIBN as conventional initiator. (a) Conversion and $\ln[M]_0/[M]$ *vs.* time. (b) Number-average molecular weight (M_n^{SEC}) and dispersity (M_w/M_n) *vs.* theoretical number-average molecular weight (M_n^{th}). Reaction conditions: $[MA]_0/[DDMAT]_0/[AIBN]_0$ = 222/1/0.5; $[MA]_0/[CPME]$ = 2/1 (v/v).

The ability to polymerize Sty in CPME under identical experimental conditions was then evaluated. The resulting kinetic plot (see Figure 3-2 and entry 2 in Table 3-1) reveals a linear relationship between $\ln[M]_0/[M]$ values and time, and a nearly perfect match between experimentally determined MW values and theoretical ones, together with $Đ$ values of about 1.1, indicating a perfect control. In this respect, the actual RAFT system seems

to approach the ideal living polymerization conditions much better than the previously-reported SARA-ATRP counterpart. [45, 47, 48] Although low $Đ$ values were obtained by SARA-ATRP, a loss of chain-end functionality at high monomer conversions was observed, leading to a deviation of M_n^{SEC} from the theoretical ones [45], with an increase in $Đ$. This is not observed here, thus indicating that side reactions leading to a loss of functionality were minimized. Sty polymerizations (in bulk or in solution) usually require high temperatures (typically in the range of 70 to 110 °C) to reach reasonably high conversions and to overcome vitrification and potential catalyst solubility issues. [45] With the RAFT system in CPME reported in this study, it is possible to reach high monomer conversions (>95%) at 60 °C. This feature is particularly relevant because high temperatures (especially above 60 °C) can induce Sty autopolimerization reactions (by thermal self-initiation) [49] on the long term and result in a loss of molecular weight control (which also contributes for M_n^{SEC} deviation from theoretical values). RAFT polymerization of Sty usually takes place in a DMF solution or in bulk. [45] Our results demonstrate that the use of CPME is an excellent green alternative, allowing a rate of polymerization similar to that of systems in DMF and slightly better than bulk polymerizations. [50, 51] Therefore, CPME can replace DMF for the synthesis of well-defined PS.

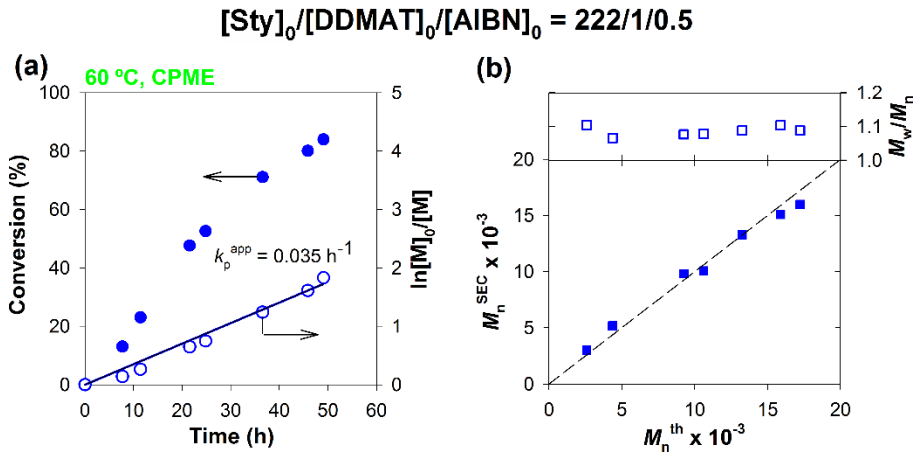

Figure 3-2: RAFT polymerization of Sty in CPME at 60 °C mediated by DDMAT using AIBN as conventional initiator. (a) Conversion *vs.* time and $\ln[M]_0/[M]$ *vs.* time. (b) M_n^{SEC} and M_w/M_n *vs.* M_n^{th}. Reaction conditions: $[Sty]_0/[DDMAT]_0/[AIBN]_0$ = 222/1/0.5; $[Sty]_0/[CPME]$ = 2/1 (v/v).

To demonstrate the versatility of this approach, VC polymerization in CPME was then investigated at a temperature of 42°C (based on a previous publication from our research group). [18] CMPCD was used as CTA and Trigonox was selected as a conventional initiator. Conversely to Sty, the plot of $\ln([M]_0/[M])$ *vs.* time for VC (Figure 3-3) appears to have two distinct linear zones. However, this behavior has already been reported in other

RAFT polymerizations of VC [18], and can be attributed to a difference in the rates of initiation by Trigonox-generated radicals, and reinitiation by the radical leaving groups •CH_2CN formed during the pre-equilibrium reaction of the RAFT mechanism. The apparent polymerization rate constants in CPME are slightly higher than those calculated in the previous work using THF as a solvent. [18] Higher conversions were obtained at the end of the reaction, while the level of control over the molecular weight appears to remain the same (with 1.8 > $Đ$ > 1.5 and a good agreement between M_n^{SEC} and M_n^{th}).

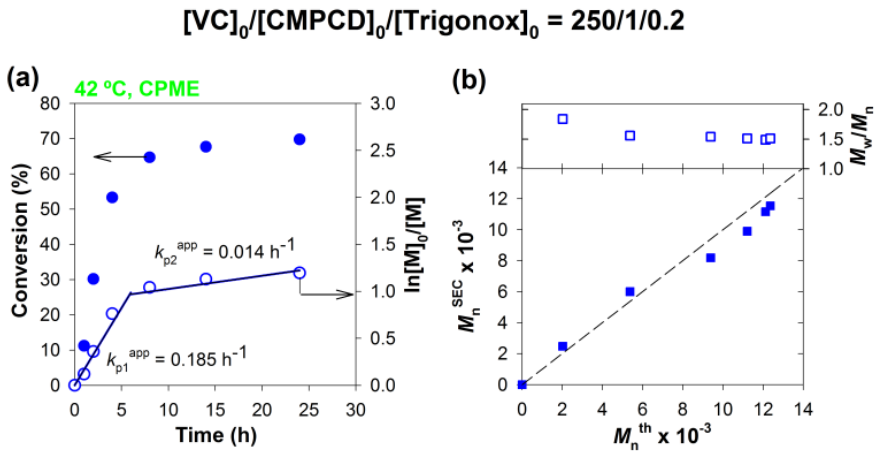

Figure 3-3: RAFT polymerization of VC in CPME at 42 °C mediated by CMPCD using Trigonox as conventional initiator. (a) Conversion and $\ln[M]_0/[M]$ vs. time. (b) M_n^{SEC} and M_w/M_n vs. M_n^{th}. Reaction conditions: $[VC]_0/[CMPCD]_0/[Trigonox]_0$ = 250/1/0.2; $[VC]_0/[CPME]$ = 1/1 (v/v).

The effect of the targeted number-average degree of polymerization (DP_T) on the reaction kinetics and the molecular weight control was then studied. Three different DP_n values were targeted: 100, 250 and 1000. As expected, the results featured in Table 3-1 (entries 4-6) show that the higher the targeted DP_n, the slower the reaction, as fewer radicals are present in the mixture at a given time. It is remarkable to note that for all the DP_T studied, better matches between the M_n^{SEC} and M_n^{th} values were obtained than those obtained in THF [18] despite similar $Đ$ values.

In addition to MA, Sty and VC, VAc was also tested using the CMPCD/Trigonox RAFT system (see Table 3-1, entry 3). An almost complete VAc conversion was achieved in less than 3 h, and the low $Đ$ value obtained by SEC analysis confirmed the growth of well-defined PVAc chains.

Table 3-1: Kinetic and control parameters obtained for RAFT polymerizations in CPME with different monomers. Conditions: reaction temperature = 42 °C; $[Monomer]_0/[Solvent]$ = 2/1 (v/v)

Entry	$[M]_0/[CTA]_0/[I]_0$	k_p^{app} (h^{-1})	Time (h)	Conv. (%)	$M_n^{th} \times 10^{-3}$	$M_n^{SEC} \times 10^{-3}$	$Đ$
1[a]	$[MA]_0/[DDMAT]_0/[AIBN]_0$ = 222/1/0.5	1.328	2	93	21.1	24.5	1.06
2[a]	$[Sty]_0/[DDMAT]_0/[AIBN]_0$ = 222/1/0.5	0.035	49	84	17.2	16.0	1.08
3	$[VAc]_0/[CMPCD]_0/[Trig.]_0$ = 100/1/0.5	-	2.3	99	8.7	9.0	1.18
4[b]	$[VC]_0/[CMPCD]_0/[Trig.]_0$ = 250/1/0.2	0.185	24	70	12.4	11.5	1.51
5[b]	$[VC]_0/[CMPCD]_0/[Trig.]_0$ = 100/1/0.2	-	5	59	4.5	4.2	1.54
6[b]	$[VC]_0/[CMPCD]_0/[Trig.]_0$ = 1000/1/0.2	-	48	34	22.7	17.7	1.72

[a]Reaction temperature: 60 °C. [b]$[Monomer]_0/[Solvent]$ = 1/1

In conclusion, the results presented in Table 3-1 confirm the robustness and the versatility of the RAFT polymerization in solution using CPME as a green solvent. The system allows the synthesis of different monomers in a wide range of molecular weights, while exhibiting a very high level of control that is better or at least similar to other reported solution polymerization systems.

Structural analysis of the RAFT-derived polymers

The structure of CTA-terminated PVC chains was determined by ^{1}H-NMR spectroscopy and MALDI-TOF-MS analysis. Both the ^{1}H-NMR spectrum (Appendix B, Fig. B1) and the MALDI-TOF-MS spectrum (Appendix B, Fig. B2) confirmed the well-defined structure predicted for the PVC chains. [18]

In addition, the structure of the RAFT-derived PVAc was also studied by ^{1}H-NMR (Figure 3-4). The peaks of the PVAc main chain, **d** and **e** (at 1.9 – 2.7 ppm and 4.2 – 4.8 ppm, respectively) were identified. [52] Furthermore, the characteristic peaks of CMPCD protons (**a**, **b** and **c**), corresponding to those found previously for PVC in Appendix B, Fig. B1, are also present in this spectrum, thereby confirming the presence of chain-end functionalities (from the initiator and the RAFT agent) in the PVAc chains. This conclusion is consistent with the very good control over the molecular weight that has been observed (Table 3-1, entry 3).

Evaluation of the RAFT-derived polymer livingness

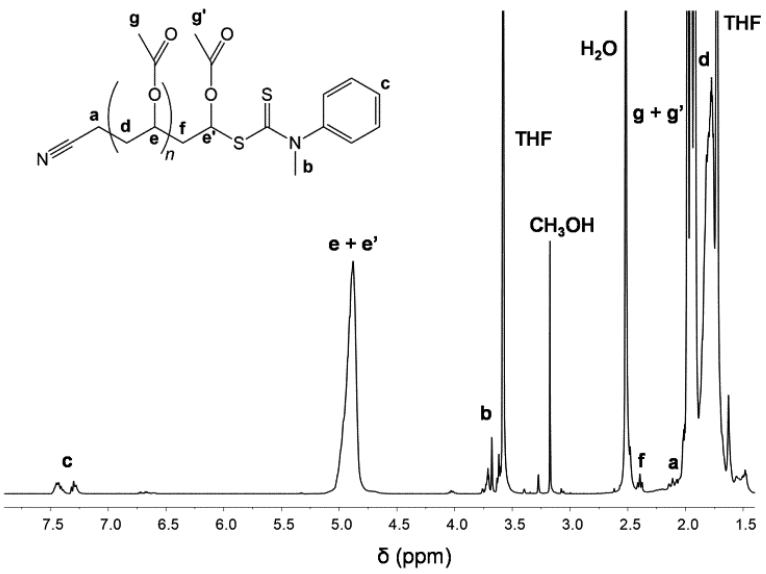

Figure 3-4: The ^{1}H NMR spectrum in d_8-THF of PVAc-CTA (M_n^{SEC} = 9000; $Đ$ = 1.18) obtained in Table 1, entry 3.

The living nature of the polymers was confirmed by carrying out successful chain extension experiments using PVC (Table 3-1, entry 5) and PVAc (Table 3-1, entry 3) macro-CTA (Fig. 3-5 and 3-6). As shown in Figure 3-5, a complete shift of the SEC trace during the "one-pot" chain extension experiment was achieved. Molecular weight of the starting PVC-CTA (p(VC) = 59%, M_n^{th} = 4500, M_n^{SEC} = 4200, $Đ$ = 1.54) has shifted toward higher molecular weight (p(VC) = 42%, M_n^{th} = 23800, M_n^{SEC} = 17300, $Đ$ = 1.53). Also, a PVAc-*b*-PVC diblock copolymer (p(VC) = 51%, M_n^{th} = 41100, M_n^{SEC} = 30200, $Đ$ = 1.59) was synthesized from a PVAc-CTA (p(VAc) = 99%, M_n^{th} = 8700, M_n^{SEC} = 9000, $Đ$ = 1.18) macroinitiator (Figure 3-6). The structure of this block copolymer was confirmed by ^{1}H NMR (Appendix B, Fig. B3).

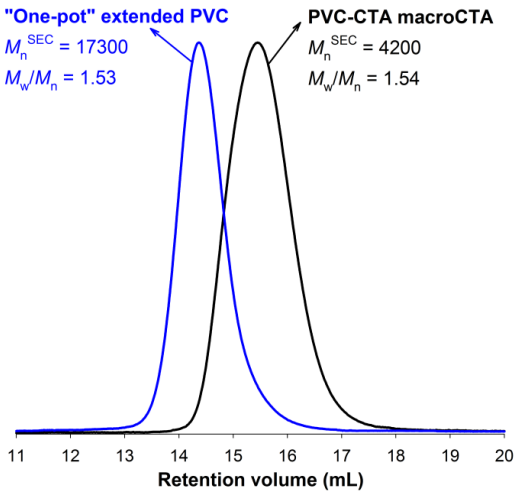

Figure 3-5: SEC traces of the PVC-CTA (p(VC) = 59%, M_n^{th} = 4500, M_n^{SEC} = 4200, $Đ$ = 1.54) macro-CTA (right curve), and the "one-pot" extended PVC (p(VC) = 42%, M_n^{th} = 23800, M_n^{SEC} = 17300, $Đ$ = 1.53) (left curve).

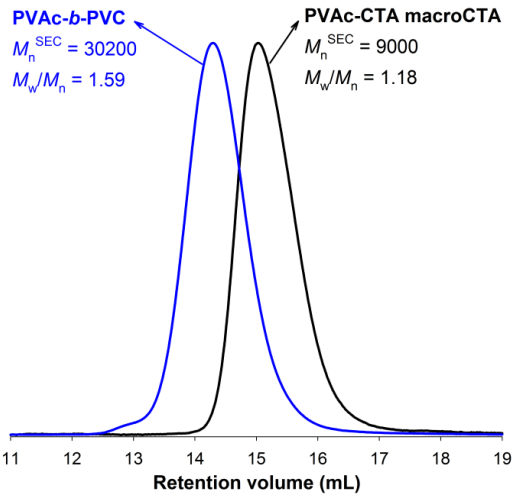

Figure 3-6: SEC traces of the PVAc-CTA (p(VAc) = 99%, M_n^{th} = 8700, M_n^{SEC} = 9000, $Đ$ = 1.18) macro-CTA (right curve), and the PVAc-*b*-PVC (p(VC) = 51%, M_n^{th} = 41100, M_n^{SEC} = 30200, $Đ$ = 1.59) block copolymer (left curve).

3.4.2 NMP in CPME

For the NMP of Sty and VC, the BlocBuilder® alkoxyamine, based on the nitroxide SG1, was selected. It is one of the most potent alkoxyamines developed so far and its use has conducted to significant advances in the control of bulk/solution and emulsion polymerizations, and the preparation of complex and functionalized architectures. [2]

The NMP of Sty using this alkoxyamine is usually performed in bulk at high temperatures; between 90 and 120 °C [2, 17, 53, 54], to enable reasonable polymerization rates. However, this range of temperatures is not fully compatible with the use of CPME (boiling point is 106 °C), unless a high pressure glassware is employed. In this context, a preliminary experiment of Sty polymerization was carried out at 60 °C. However, as expected, the polymerization was extremely slow as no polymer was formed even after 94 h. The temperature was then increased to 80 °C but the reaction proceeded rather slowly (Figure 3-7). Nevertheless, all the expected features of a RDRP system (e.g., first-order kinetic with respect to monomer conversion, linear increase of MW with monomer conversion, good match between M_n^{SEC} and M_n^{th} values and low $Đ$ values decreasing with monomer conversion) were obtained with a level of control comparable to that reported for NMP of Sty using BlocBuilder® at higher temperatures. [53-55] The use of a temperature lower than those reported in the literature may also contribute to a good control over the polymerization due to a lower rate of Sty autopolymerization, similarly to what was ear-

lier discussed with RAFT. Therefore, despite temperature limitations resulting in slow reactions, the very good control achieved over the polymerization of Sty validates the use of CPME as a solvent in the field of NMP.

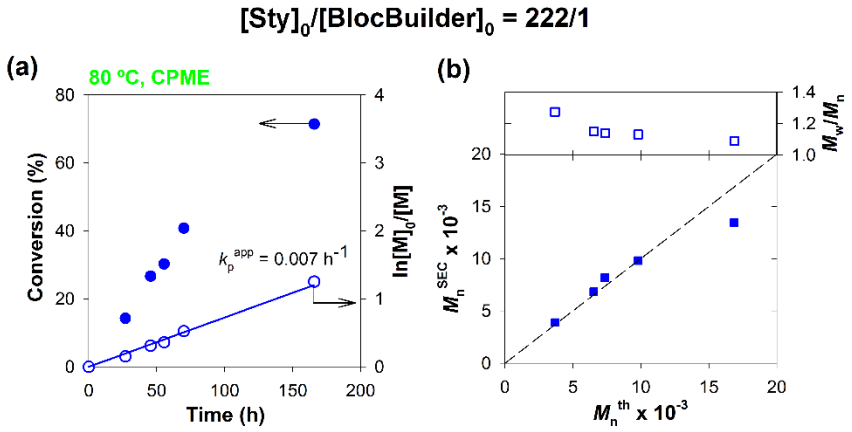

Figure 3-7: NMP of Sty in CPME at 80 °C initiated by SG1-based BlocBuilder® alkoxyamine. (a) Conversion and $\ln[M]_0/[M]$ *vs.* time. (b) M_n^{SEC} and M_w/M_n *vs.* M_n^{th}. Reaction conditions: $[Sty]_0/[BlocBluider]_0$ = 222/1; $[Sty]_0/[CPME]$ = 2/1 (v/v).

The NMP of VC initiated by the BlocBuilder® alkoxyamine in DCM or DMSO was recently proposed, and the results pointed out that a temperature of 42 °C provided the best compromise between a descent polymerization rate and a good control. [41] Based on this work, the NMP of VC was investigated with CPME as the solvent. The kinetic data show a first-order kinetic (Figure 3-8 (a)) and a good agreement between M_n^{SEC} and M_n^{th} values (Figure 3-8 (b)). The $Đ$ values follow those obtained in DCM under identical experimental conditions, approaching 1.5 at the end of the reaction [41], which suggests a similar level of control. However, the rate of polymerization in CPME (k_p^{app} = 0.042) was ~20% higher than that reported using DCM (k_p^{app} = 0.036) [41], which stresses another advantage of replacing DCM and DMSO by CPME.

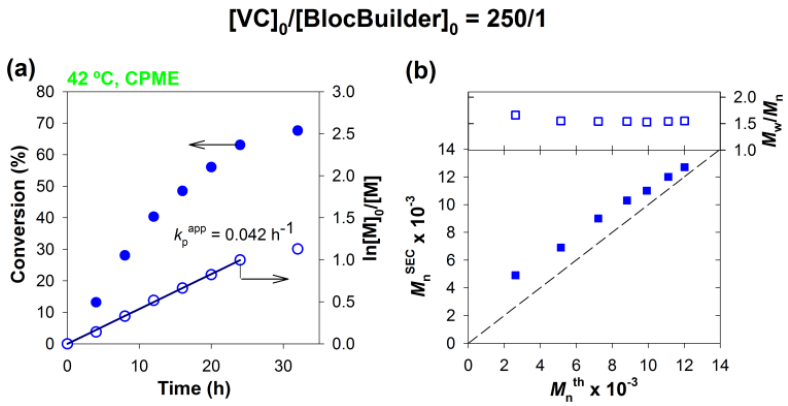

Figure 3-8: NMP of VC in CPME at 42 °C initiated by SG1-based BlocBuilder® alkoxyamine. (a) Conversion and $\ln[M]_0/[M]$ *vs.* time. (b) M_n^{SEC} and M_w/M_n *vs.* M_n^{th}. Reaction conditions: $[VC]_0/[BlocBuilder]_0$ = 250/1; $[VC]_0/[CPME]$ = 1/1 (v/v).

The influence of the monomer concentration in the reaction medium was then investigated for VC, by adjusting the monomer/solvent ratio and stopping the reaction after 24 h (Table 3-2, entries 1–3). It appears that a decrease in the $[VC]_0$/[CPME] ratio from 1/1 (entry 1) to 1/2 (entry 3) has a deleterious effect on the final monomer conversion, which is caused by a change of the reaction medium (polarity and/or viscosity) upon dilution, as previously observed for different NMP systems. [19, 56] Conversely, when the $[VC]_0$/[CPME] ratio increases from 1/1 (entry 1) to 2/1 (entry 2), dispersity increased slightly (1.54 *vs.* 1.69), similarly to solution NMP of oligo(ethylene glycol) methyl ether methacrylate (OEGMA) in ethanol. [56] With VC, the same observations were made in DCM system [41].

Finally the NMP system proposed here was further tested for different target DP_n's. Once again DP_T values of 100 and 1000 were tested and compared with a DP_T of 250 (Table 3-2, entries 1, 4 and 5). The results not only confirm the reduction of polymerization rate as DP_T increases but also the excellent control all across the DP_T range tested.

Table 3-2: NMP of VC initiated by the BlocBuilder alkoxyamine at 42 °C, using CPME as a solvent under different experimental conditions.

Entry	$[VC]_0$/ $[BlocBuilder]_0$	$[VC]_0$/ [CPME] (v/v)	Time (h)	Conv. (%)	$M_n^{th} \times 10^{-3}$	$M_n^{SEC} \times 10^{-3}$	$Đ$
1	250/1	1/1	24	63.1	11.1	12.0	1.54
2	250/1	2/1	24	58.1	10.3	11.1	1.69
3	250/1	1/2	24	42.3	7.8	8.5	1.59
4	100/1	1/1	10	52.2	3.8	4.3	1.55
5	1000/1	1/1	48	54.0	36.3	32.3	1.53

Structural analysis of the NMP-derived polymers

The evidences of the well-defined structure of the PVC were obtained by ^{1}H NMR spectroscopy (Appendix B, Fig. B4). The spectrum shows the expected peaks and in particular those from the starting alkoxyamine, thus proving the chain-end functionalization, in agreement with those reported in the literature for NMP-derived PVC prepared in other organic solvents. [41]

The end-group fidelity of the synthesized PVC was probed by performing ^{31}P NMR spectroscopy, which is a convenient and pretty accurate method for determination of the living chain fraction (LF) by quantifying the presence of the phosphorus-containing SG1 nitroxide end-group using diethyl phosphite (DEP) as an internal reference. [57, 58] The PVC-SG1 spectrum reported in Figure 3-9 gave a LF of ~87%, which is similar to LF values

reported for the NMP of styrenics and acrylates. This clearly demonstrates the living nature of the PVC obtained in CPME. It also enables the design of block copolymers by NMP containing PVC segments by chain extensions.

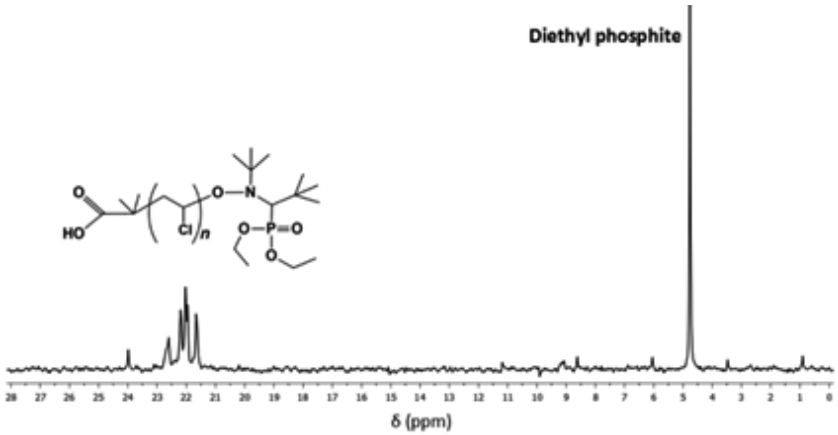

Figure 3-9: ^{31}P NMR spectra in d_8-THF of the purified PVC (M_n^{SEC} = 4300; $Đ$ = 1.55) obtained in Table 3-2, entry 4.

Evaluation of the NMP-derived polymer livingness

The living character of the PVC-SG1 obtained by NMP was confirmed by a successful "one-pot" chain extension experiment of VC from the SG1-terminated PVC (Table 3-2, entry 4) in CPME at 42 ºC. The SEC traces presented in Figure 3-10 showed the complete shift of the low molar mass SG1-terminated PVC macroinitiator (p(VC) = 52%, M_n^{th} = 3800, M_n^{SEC} = 4300, $Đ$ = 1.55) towards a higher molar mass polymer (p(VC)v = 47%, M_n^{th} = 29800, M_n^{SEC} = 23600, $Đ$ = 1.61), thus assessing the formation of a PVC-*b*-PVC diblock copolymer.

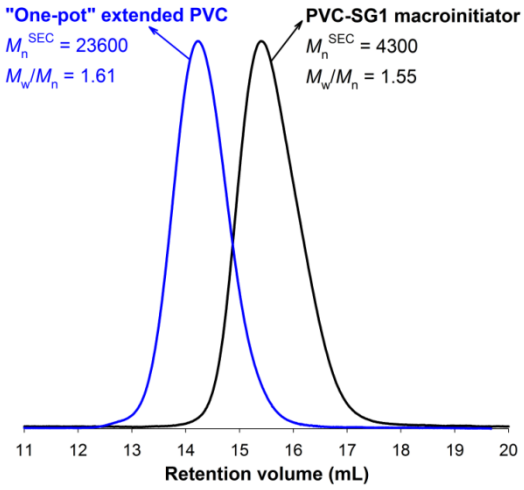

Figure 3-10: SEC chromatograms of the PVC-SG1 macroinitiator (p(VC) = 52.2%, M_n^{th} = 3800, M_n^{SEC} = 4300, $Đ$ = 1.55) (black line) and the PVC-*b*-PVC diblock copolymer (p(VC) = 47.2%, M_n^{th} = 29800, M_n^{SEC} = 23600, $Đ$ = 1.61) (blue line) after "one-pot" chain extension in CPME.

3.5 Conclusions

In conclusion this manuscript reports use of CPME for the NMP and RAFT polymerizations of VC and Sty as alternative to THF, DCM, DMSO and DMF. This eco-friendly solvent also allowed the RAFT polymerization of VAc and MA. The living character of the polymers was confirmed by ^{1}H-NMR, ^{31}P-NMR, MALDI-TOF-MS and by successful chain extension experiments. The results proved that CPME is a suitable "green" solvent to be employed in two of the most popular RDRP methods.

3.6 References

[1] Matyjaszewski, K., Tsarevsky, N. V., *Macromolecular Engineering by Atom Transfer Radical Polymerization*, Journal of the American Chemical Society, **2014**, 136, 6513-6533.

[2] Nicolas, J., Guillaneuf, Y., Lefay, C., Bertin, D., Gigmes, D., Charleux, B., *Nitroxide-mediated polymerization*, Progress in Polymer Science, **2013**, 38, 63-235.

[3] Moad, G., Rizzardo, E., Thang, S. H., *Living Radical Polymerization by the RAFT Process – A Third Update*, Australian Journal of Chemistry, **2012**, 65, 985-1076.

[4] Moad, G., Rizzardo, E., Thang, S. H., *Living Radical Polymerization by the RAFT Process – A Second Update*, Australian Journal of Chemistry, **2009**, 62, 1402-1472.

[5] Matyjaszewski, K., Xia, J., *Atom transfer radical polymerization*, Chemical reviews, **2001**, 101, 2921-2990.

[6] Kamigaito, M., Ando, T., Sawamoto, M., *Metal-catalyzed living radical polymerization*, Chemical Reviews, **2001**, 101, 3689-3745.

[7] Wang, J. S., Matyjaszewski, K., *Controlled/"living" radical polymerization. Atom transfer radical polymerization in the presence of transition-metal complexes*, Journal of the American Chemical Society, **1995**, 117, 5614-5615.

[8] Georges, M. K., Veregin, R. P. N., Kazmaier, P. M., Hamer, G. K., *Narrow Molecular Weight Resins By a Free Radical Polymerization Process*, Macromolecules, **1993**, 26, 2987-2988.

[9] Perrier, S., Takolpuckdee, P., *Macromolecular design via reversible addition-fragmentation chain transfer (RAFT)/Xanthates (MADIX) polymerization*, J. Polym. Sci. Pol. Chem., **2005**, 43, 5347-5393.

[10] Moad, G., Rizzardo, E., Thang, S. H., *Living Radical Polymerization by the RAFT Process*, Australian Journal of Chemistry, **2005**, 58, 379-410.

[11] Chiefari, J., Chong, B. Y. K., Ercole, F., Krstina, J., Jeffery, J., Le, T. P. T., et al., *Living Free-Radical Polymerization by Reversible Addition–Fragmentation Chain Transfer: The RAFT Process*, Macromolecules, **1998**, 31, 5559-5562.

[12] Moad, G., Rizzardo, E., Thang, S. H., *Toward living radical polymerization*, Accounts of Chemical Research, **2008**, 41, 1133-1142.

[13] Konkolewicz, D., Wang, Y., Krys, P., Zhong, M., Isse, A. A., Gennaro, A., et al., *SARA ATRP or SET-LRP. End of controversy?*, Polymer Chemistry, **2014**, 5, 4396-4417.

[14] Guliashvili, T., Mendonça, P. V., Serra, A. C., Popov, A. V., Coelho, J. F. J., *Copper-Mediated Controlled/"Living" Radical Polymerization in Polar Solvents: Insights into Some Relevant Mechanistic Aspects*, Chemistry - A European Journal, **2012**, 18, 4607-4612.

[15] Zetterlund, P. B., Kagawa, Y., Okubo, M., *Controlled/living radical polymerization in dispersed systems*, Chemical Reviews, **2008**, 108, 3747-3794.

[16] Cunningham, M. F., *Controlled/living radical polymerization in aqueous dispersed systems*, Progress in Polymer Science, **2008**, 33, 365-398.

[17] Charleux, B., Nicolas, J., *Water-soluble SG1-based alkoxyamines: A breakthrough in controlled/living free-radical polymerization in aqueous dispersed media*, Polymer, **2007**, 48, 5813-5833.

[18] Abreu, C. M. R., Mendonça, P. V., Serra, A. C., Coelho, J. F. J., Popov, A. V., Gryn'ova, G., et al., *Reversible addition-fragmentation chain transfer polymerization of vinyl chloride*, Macromolecules, **2012**, 45, 2200-2208.

[19] Chenal, M., Mura, S., Marchal, C., Gigmes, D., Charleux, B., Fattal, E., et al., *Facile Synthesis of Innocuous Comb-Shaped Polymethacrylates with PEG Side Chains by Nitroxide-Mediated Radical Polymerization in Hydroalcoholic Solutions*, Macromolecules, **2010**, 43, 9291-9303.

[20] Kuo, K. H., Chiu, W.-Y., Cheng, K.-C., *Influence of DMF on the polymerization of tert-butyl acrylate initiated by 4-oxo-TEMPO-capped polystyrene macroinitiator*, Polymer International, **2008**, 57, 730-737.

[21] Mendonça, P. V., Averick, S. E., Konkolewicz, D., Serra, A. C., Popov, A. V., Guliashvili, T., et al., *Straightforward ARGET ATRP for the Synthesis of Primary Amine Polymethacrylate with Improved Chain-End Functionality under Mild Reaction Conditions*, Macromolecules, **2014**, 47, 4615-4621.

[22] Konkolewicz, D., Krys, P., Góis, J. R., Mendonça, P. V., Zhong, M., Wang, Y., et al., *Aqueous RDRP in the Presence of Cu0: The Exceptional Activity of CuI Confirms the SARA ATRP Mechanism*, Macromolecules, **2014**, 47, 560-570.

[23] Simakova, A., Averick, S. E., Konkolewicz, D., Matyjaszewski, K., *Aqueous ARGET ATRP*, Macromolecules, **2012**, 45, 6371-6379.

[24] Konkolewicz, D., Magenau, A. J. D., Averick, S. E., Simakova, A., He, H., Matyjaszewski, K., *ICAR ATRP with ppm Cu Catalyst in Water*, Macromolecules, **2012**, 45, 4461-4468.

[25] Mendonça, P. V., Konkolewicz, D., Averick, S. E., Serra, A. C., Popov, A. V., Guliashvili, T., et al., *Synthesis of cationic poly ((3-acrylamidopropyl) trimethylammonium chloride) by SARA ATRP in ecofriendly solvent mixtures*, Polymer Chemistry, **2014**, 5, 5829-5836.

[26] Góis, J. R., Rocha, N., Popov, A. V., Guliashvili, T., Matyjaszewski, K., Serra, A. C., et al., *Synthesis of well-defined functionalized poly(2-(diisopropylamino)ethyl methacrylate) using ATRP with sodium dithionite as a SARA agent*, Polymer Chemistry, **2014**, 5, 3919-3919.

[27] Góis, J. R., Konkolewicz, D., Popov, A. V., Guliashvili, T., Matyjaszewski, K., Serra, A. C., et al., *Improvement of the control over SARA ATRP of 2-(diisopropylamino)ethyl methacrylate by slow and continuous addition of sodium dithionite*, Polymer Chemistry, **2014**, 5, 4617-4626.

[28] Huo, F., Wang, X., Zhang, Y., Zhang, X., Xu, J., Zhang, W., *RAFT Dispersion Polymerization of Styrene in Water/Alcohol: The Solvent Effect on Polymer Particle Growth during Polymer Chain Propagation*, Macromolecular Chemistry and Physics, **2013**, 214, 902-911.

[29] Cordeiro, R., Rocha, N., Mendes, J. P., Matyjaszewski, K., Guliashvili, T., Serra, A. C., et al., *Synthesis of well-defined poly(2-(dimethylamino)ethyl methacrylate) under mild conditions and its co-polymers with cholesterol and PEG using Fe(0)/Cu(ii) based SARA ATRP*, Polymer Chemistry, **2013**, 4, 3088-3088.

[30] Abreu, C. M. R., Serra, A. C., Popov, A. V., Matyjaszewski, K., Guliashvili, T., Coelho, J. F. J., *Ambient temperature rapid SARA ATRP of acrylates and methacrylates in alcohol-water solutions mediated by a mixed sulfite/Cu(ii)Br2 catalytic system*, Polymer Chemistry, **2013**, 4, 5629-5636.

[31] Abreu, C. M. R., Mendonça, P. V., Serra, A. C., Coelho, J. F. J., Popov, A. V., Guliashvili, T., *Accelerated Ambient-Temperature ATRP of Methyl Acrylate in Alcohol–Water Solutions with a Mixed Transition-Metal Catalyst System*, Macromolecular Chemistry and Physics, **2012**, 213, 1677-1687.

[32] Anastasaki, A., Nikolaou, V., Nurumbetov, G., Truong, N. P., Pappas, G. S., Engelis, N. G., et al., *Synthesis of Well-Defined Poly(acrylates) in Ionic Liquids via Copper(II)-Mediated Photoinduced Living Radical Polymerization*, Macromolecules, **2015**, 48, 5140-5147.

[33] Mendes, J. P., Branco, F., Abreu, C. M. R., Mendonça, P. V., Popov, A. V., Guliashvili, T., et al., *Synergistic Effect of 1-Butyl-3-methylimidazolium Hexafluorophosphate and DMSO in the SARA ATRP at Room Temperature Affording Very Fast Reactions and Polymers with Very Low Dispersity*, ACS Macro Letters, **2014**, 3, 544-547.

[34] Erdmenger, T., Guerrero-Sanchez, C., Vitz, J., Hoogenboom, R., Schubert, U. S., *Recent developments in the utilization of green solvents in polymer chemistry*, Chemical Society Reviews, **2010**, 39, 3317-3333.

[35] Biedroń, T., Kubisa, P., *Atom transfer radical polymerization of acrylates in an ionic liquid: Synthesis of block copolymers*, Journal of Polymer Science Part A: Polymer Chemistry, **2002**, 40, 2799-2809.

[36] Carmichael, A. J., Haddleton, D. M., Bon, S. A. F., Seddon, K. R., *Copper(I) mediated living radical polymerisation in an ionic liquid*, Chemical Communications, **2000**, 1237-1238.

[37] Maximiano, P., Mendes, J. P., Mendonça, P. V., Abreu, C. M. R., Guliashvili, T., Serra, A. C., et al., *Cyclopentyl methyl ether: A new green co-solvent for supplemental*

activator and reducing agent atom transfer radical polymerization, Journal of Polymer Science Part A: Polymer Chemistry, **2015**, DOI: 10.1002/pola.27736.

[38] Watanabe, K., Yamagiwa, N., Torisawa, Y., *Cyclopentyl Methyl Ether as a New and Alternative Process Solvent*, Organic Process Research & Development, **2007**, 11, 251-258.

[39] Watanabe, K., *The Toxicological Assessment of Cyclopentyl Methyl Ether (CPME) as a Green Solvent*, Molecules, **2013**, 18, 3183-3194.

[40] Antonucci, V., Coleman, J., Ferry, J. B., Johnson, N., Mathe, M., Scott, J. P., et al., *Toxicological Assessment of 2-Methyltetrahydrofuran and Cyclopentyl Methyl Ether in Support of Their Use in Pharmaceutical Chemical Process Development*, Organic Process Research & Development, **2011**, 15, 939-941.

[41] Abreu, C. M. R., Mendonca, P. V., Serra, A. C., Noble, B. B., Guliashvili, T., Nicolas, J., et al., *Nitroxide-Mediated Polymerization of Vinyl Chloride at Low Temperature: Kinetic Approach and Computational Studies*, **2015**, submitted to *Macromolecules*.

[42] Hatano, T., Rosen, B. M., Percec, V., *SET-LRP of Vinyl Chloride Initiated with CHBr3 and Catalyzed by Cu(0)-Wire/TREN in DMSO at 25 degrees C*, J. Polym. Sci. Pol. Chem., **2010**, 48, 164-172.

[43] Sienkowska, M. J., Rosen, B. M., Percec, V., *SET-LRP of Vinyl Chloride Initiated with CHBr3 in DMSO at 25 degrees C*, J. Polym. Sci. Pol. Chem., **2009**, 47, 4130-4140.

[44] Percec, V., Guliashvili, T., Ladislaw, J. S., Wistrand, A., Stjerndahl, A., Sienkowska, M. J., et al., *Ultrafast Synthesis of Ultrahigh Molar Mass Polymers by Metal-Catalyzed Living Radical Polymerization of Acrylates, Methacrylates, and Vinyl Chloride Mediated by SET at 25 °C*, Journal of the American Chemical Society, **2006**, 128, 14156-14165.

[45] Rocha, N., Mendonça, P. V., Mendes, J. P., Simões, P. N., Popov, A. V., Guliashvili, T., et al., *Facile Synthesis of Well-Defined Telechelic Alkyne-Terminated Polystyrene in Polar Media Using ATRP With Mixed Fe/Cu Transition Metal Catalyst*, Macromolecular Chemistry and Physics, **2013**, 214, 76-84.

[46] Abreu, C. M. R., Mendonça, P. V., Serra, A. C., Popov, A. V., Matyjaszewski, K., Guliashvili, T., et al., *Inorganic sulfites: Efficient reducing agents and supplemental activators for atom transfer radical polymerization*, ACS Macro Letters, **2012**, 1, 1308-1311.

[47] Mendonça, P. V., Serra, A. C., Coelho, J. F. J., Popov, A. V., Guliashvili, T., *Ambient temperature rapid ATRP of methyl acrylate, methyl methacrylate and styrene in polar solvents with mixed transition metal catalyst system*, European Polymer Journal, **2011**, 47, 1460-1466.

[48] Mendes, J. P., Branco, F., Abreu, C. M. R., Mendonça, P. V., Serra, A. C., Popov, A. V., et al., *Sulfolane: an Efficient and Universal Solvent for Copper-Mediated Atom Transfer Radical (co)Polymerization of Acrylates, Methacrylates, Styrene, and Vinyl Chloride*, ACS Macro Letters, **2014**, 3, 858-861.

[49] Mayo, F. R., *The dimerization of styrene*, Journal of the American Chemical Society, **1968**, 90, 1289-1295.

[50] Wu, Y., Zhang, W., Zhang, Z., Pan, X., Cheng, Z., Zhu, J., et al., *Initiator-chain transfer agent combo in the RAFT polymerization of styrene*, Chemical Communications, **2014**, 50, 9722-9724.

[51] Goto, A., Sato, K., Tsujii, Y., Fukuda, T., Moad, G., Rizzardo, E., et al., *Mechanism and kinetics of RAFT-based living radical polymerizations of styrene and methyl methacrylate*, Macromolecules, **2001**, 34, 402-408.

[52] Piette, Y., Debuigne, A., Bodart, V., Willet, N., Duwez, A.-S., Jerome, C., et al., *Synthesis of poly(vinyl acetate)-b-poly(vinyl chloride) block copolymers by Cobalt-Mediated Radical Polymerization (CMRP)*, Polymer Chemistry, **2013**, 4, 1685-1693.

[53] Grimaldi, S., Finet, J.-P., Le Moigne, F., Zeghdaoui, A., Tordo, P., Benoit, D., et al., *Acyclic β-Phosphonylated Nitroxides: A New Series of Counter-Radicals for "Living"/Controlled Free Radical Polymerization*, Macromolecules, **2000**, 33, 1141-1147.

[54] Benoit, D., Grimaldi, S., Robin, S., Finet, J.-P., Tordo, P., Gnanou, Y., *Kinetics and Mechanism of Controlled Free-Radical Polymerization of Styrene and n-Butyl Acrylate in the Presence of an Acyclic β-Phosphonylated Nitroxide†*, Journal of the American Chemical Society, **2000**, 122, 5929-5939.

[55] Nicolas, J., Charleux, B., Guerret, O., Magnet, S., *Novel SG1-Based Water-Soluble Alkoxyamine for Nitroxide-Mediated Controlled Free-Radical Polymerization of Styrene and n-Butyl Acrylate in Miniemulsion*, Macromolecules, **2004**, 37, 4453-4463.

[56] Nicolas, J., Couvreur, P., Charleux, B., *Comblike Polymethacrylates with Poly(ethylene glycol) Side Chains via Nitroxide-Mediated Controlled Free-Radical Polymerization*, Macromolecules, **2008**, 41, 3758-3761.

[57] Delplace, V., Harrisson, S., Ho, H. T., Tardy, A., Guillaneuf, Y., Pascual, S., et al., *One-Step Synthesis of Azlactone-Functionalized SG1-Based Alkoxyamine for Nitroxide-Mediated Polymerization and Bioconjugation*, Macromolecules, **2015**, 48, 2087-2097.

[58] Nicolas, J., Dire, C., Mueller, L., Belleney, J., Charleux, B., Marque, S. R. A., et al., *Living Character of Polymer Chains Prepared via Nitroxide-Mediated Controlled Free-Radical Polymerization of Methyl Methacrylate in the Presence of a Small Amount of Styrene at Low Temperature*, Macromolecules, **2006**, 39, 8274-8282.

CHAPTER 4

Ambient temperature "flash" SARA ATRP of methyl acrylate in water/ ionic liquid/glycols mixtures

*The contents of this chapter were submitted as part of the following paper: Costa, J., **Maximiano, P.**, Mendonça, P. V., Serra, A. C., Guliashvili, T., Coelho, J. F. J., "Ambient temperature "flash" SARA ATRP of methyl acrylate in water/ ionic liquid/glycols mixtures", 2015*

Chapter 4: Ambient temperature "flash" SARA ATRP of methyl acrylate in water/ ionic liquid/glycols mixtures

4.1 Abstract

The supplemental activator and reducing agent atom transfer radical polymerization (SARA ATRP) of methyl acrylate (MA) in DMSO/BMIM-PF_6/glycol mixtures (DMSO: dimethyl sulfoxide; BMIM-PF_6: 1-butyl-3-methylimidazolium hexafluorophosphate) near room temperature (30 °C), using different SARA agents, is reported. The unusual "hyperpolarity" effect within the solvent mixture allowed very fast and controlled polymerizations ($Đ$ < 1.1) during the entire reaction time. Remarkably, the replacement of DMSO by water in the reaction mixture led to a "flash" polymerization with monomer conversion reaching 92% in only 11 min (DP_T = 222), yet still affording good control over the polymer molecular weights ($Đ$ < 1.1)

4.2 Introduction

Reversible deactivation radical polymerization techniques are valuable tools for macromolecular engineering, since they allow the synthesis of tailor-made polymers with targeted molecular weight, composition, architecture, topology and narrow dispersity (Đ). [1] Atom transfer radical polymerization (ATRP) [2] is one of the most versatile and robust RDRP techniques, which has been successfully applied to the polymerization of a vast range of monomer families, such as (meth)acrylates [3], acrylamides [4], 4-vinylpyridine [5], styrene [6, 7] and vinyl chloride [8]. The major disadvantage associated with ATRP is attributed to the use of a high concentration of metal catalyst to mediate the polymerization. [2] New ATRP variation techniques, namely activators regenerated by electron transfer (ARGET) ATRP [9], supplemental activator and reducing agents (SARA) [3, 10], initiators for continuous activator regeneration (ICAR) ATRP [11] and electrochemically mediated ATRP (e-ATRP) [12], have been developed affording the use of a very

low concentration of metal catalyst. Recently, a metal-free ATRP process was also developed. [13, 14] All these contributions aimed to extend the range of application of ATRP by creating ecofriendly processes as much as possible.

SARA ATRP has been studied during the past 4 years and it has proved to be a very attractive technique from the environmental standpoint, since the polymerizations can be carried out with zero valent metals [3, 6, 10] or even with FDA-approved inorganic sulfites [15-18] as the SARA agents. An important step towards industrialization of this technology has been done recently with use of sulfolane as a "universal" solvent for SARA ATRP of acrylates, methacrylates, styrene and vinyl chloride. [8] In addition, the use of water or eco-friendly alcohol/water mixtures as the polymerization solvent has been successfully implemented. [4, 19] Recently, our research group has reported the use of an ionic liquid (BMIM-PF_6: 1-butyl-3-methylimidazolium hexafluorophosphate), in combination with dimethyl sulfoxide (DMSO), as the solvent mixture for the SARA ATRP of methyl acrylate (MA) at room temperature. [20] An unusual synergistic effect of BMIM-PF_6/DMSO mixture was found, which resulted in very fast polymerizations, while the $Đ$ remained always <1.05. It is known that BMIM-PF_6 can also exhibit synergistic effects with other solvents, particularly an unusual "hyperpolarity" effect with glycols. [21, 22] In this work, the influence of the presence of glycols in the BMIM-PF_6/DMSO mixtures for the SARA ATRP kinetics of MA at room temperature was investigated. To the best of our knowledge, this is the first time that ionic liquids/glycols are used as solvents in ATRP. The "hyperpolarity" effect within the BMIM-PF_6/DMSO/glycol mixture led to ultrafast and controlled polymerizations.

4.3 Experimental Section

The materials, analytical techniques and experimental procedures used in this chapter are described in detail on Appendix C.

4.4 Results and discussion

4.4.1 Influence of the glycol structure on the polymerization kinetics

In a previous work by our research group [20], an unusual synergistic solvent effect was found within DMSO/BMIM-PF_6 mixtures, as the solvent for the $Na_2S_2O_4$/$CuBr_2$/

Me_6TREN-catalyzed SARA ATRP of MA. This synergistic effect induced very fast polymerizations, in comparison to the use of pure DMSO as the reaction solvent, while maintaining an excellent control over the molecular weight ($Đ$ < 1.05) of the polymers. Interestingly, it is also known that BMIM-PF_6 can exhibit a particular "hyperpolarity" effect in the presence of glycols. [21] In this work, the "hyperpolarity" effect within DMSO/BMIM-PF_6/glycols mixtures was evaluated in the SARA ATRP of MA. Three different glycols were investigated (TEG, DEG and EG), in order to evaluate the influence of different chain lengths and the number of ether and hydroxyl groups (Figure 4-1) in this "hyperpolarity" effect and in polymerization kinetics. For instance, it is proposed in the literature [22] that both chemical groups are responsible for the tuning of the physicochemical properties of BMIM-PF_6/PEG mixtures (e.g hydrophilicity), in comparison to pure mixture components ("hyperpolarity" effect), due to hydrogen bonding. [23]

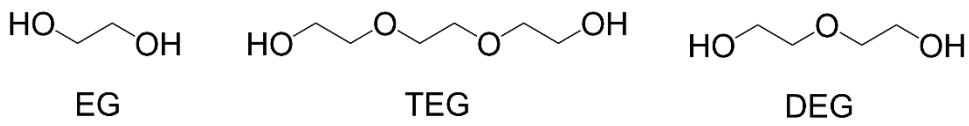

Figure 4-1: Chemical structure of the different glycols investigated.

The investigation started with the evaluation of the polarity of the solvent mixtures using the electronic transition energy parameter E_T (30), which is the most commonly used scale to measure the polarity of solvents. [23] As previously reported [20], this prediction was obtained by measuring the absorbance of BMIM-PF_6/DMSO/glycol ternary mixtures in the presence of the solvatochromic probe Reichardt's dye (30). The results from Figure 4-2 suggest that the BMIM-PF_6/DMSO/glycol mixtures exhibit a synergistic effect for all the molar percentages of glycols, as judged by the higher E_T (30) values when compared with expected ones (dashed line). Additionally, it was possible to observe a "hyperpolarity" effect for all glycols investigated, as confirmed by the higher E_T (30) values than the ones obtained for solutions with 0% and 100% of glycol. It was reported that the presence of ionic liquids induces an increase in the polymerization rate of methyl methacrylate due to both a decrease in the rate constant of termination (k_t) and an increase in the rate constant of propagation (k_p). [24-26] In addition, it is known that the ionic liquid BMIM-PF_6 decreases the propagation activation energy due to the increase in the polarity of the medium, allowing a higher contribution of charge-transfer structures (electron transference between the propagating radicals and the catalyst) and reducing the transition state energy. [25]

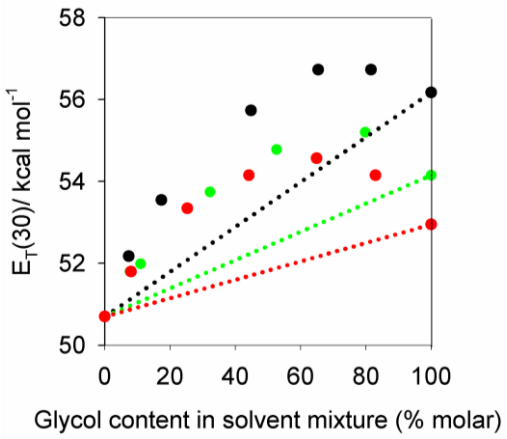

Figure 4-2: Experimental E_T (30) values as a function of the glycol molar fraction in BMIM-PF_6/DMSO/glycol mixtures with Reichardt's dye 30 (concentration = 50 µM). Glycols: TEG (red symbols); EG (black symbols) and DEG (green symbols).

In order to compare the influence of the synergistic effect on the SARA ATRP of MA for the three glycols investigated (TEG, EG and DEG), different polymerizations were carried out using the same molar ratio (8%) in the solvent mixture. The content of the remaining solvents was adjusted to achieve DMSO/BMIM-PF_6 = 50/50 (v/v), since this ratio provided the fastest polymerization of MA by SARA ATRP in the binary mixture, as previously reported. [20] The results (Figure 4-3 (a)) showed that, regardless the nature of the glycol used, the DMSO/BMIM-PF_6/glycol ternary mixtures allowed faster reactions when compared with the binary DMSO/BMIM-PF_6 = 50/50 (v/v) mixture [20], suggesting that a synergistic effect within the components of the solvent mixtures could have a direct influence in polymerization rate. Additionally, Figure 4-3 (a) shows linear first-order kinetic in respect to monomer conversion, which is typical of a controlled polymerization. Remarkably, even with the high polymerization rate and monomer conversions near 100%, the level of control obtained was excellent ($Đ$ < 1.1 during the entire polymerization) (Figure 4-3 (b)). These results clearly demonstrate that the polarity of the solvent mixture has a direct influence on the polymerization process. However, it seems that this is not the only parameter influencing the polymerization rate, since the three glycols present similar E_T (30) values (see Figure 4-2 for 8% molar fraction) but yet led to polymerizations with different rates, particularly when DEG was used in the solvent mixture (Figure 4-3 (a)). Other factors such as the change in the catalyst solubility, catalyst activity, interaction with monomer or even the possible complexation of glycols with sodium Na^+ (derived from $Na_2S_2O_4$ catalyst) [27] might have also contributed for the differences observed.

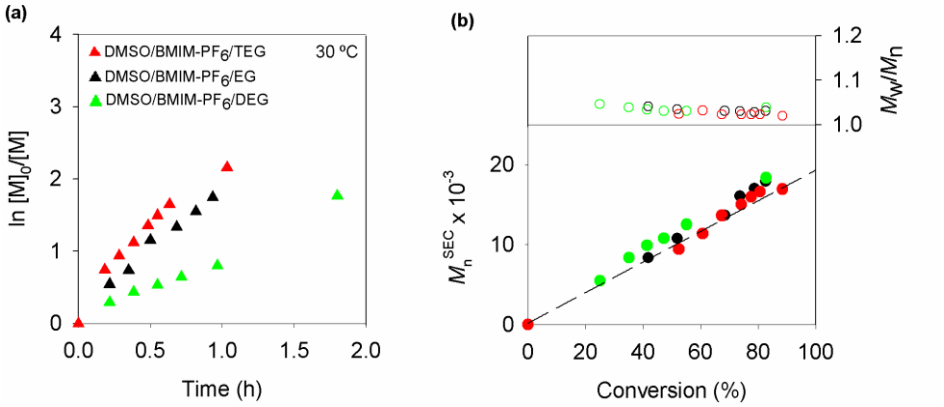

Figure 4-3: (a) Kinetic plots of conversion and ln$[M]_0/[M]$ vs. time and (b) plot of number-average molecular weights (M_n^{SEC}) and $Đ$ (M_w/M_n) vs. monomer conversion for the SARA ATRP of MA in DMSO/BMIM-PF_6/TEG = 45/45/10 (v/v/v), DMSO/BMIM-PF_6/EG = 48/48/4 (v/v/v) and DMSO/BMIM-PF_6/DEG = 46/46/8 (v/v/v) at 30 °C: TEG (red symbols); EG (black symbols) and DEG (green symbols). Reaction conditions: $[MA]_0/[solvent]$ = 2/1 (v/v); $[MA]_0/[EBiB]_0/[Na_2S_2O_4]_0/[CuBr_2]_0/[Me_6TREN]_0$= 222/1/1/0.1/0.2.

4.4.2 Influence of the SARA agent nature

Additionally to the synergetic effect studied in the above mentioned SARA ATRP agent ($Na_2S_2O_4$), the use of other SARA agents (Fe(0) and Cu(0)) was investigated with the DMSO/BMIM-PF_6/TEG mixture, once it provided the fastest polymerization. The experiments with both SARA ATRP agents (Figure 4-4 (a)) displayed a similar effect in the polymerization rate and level of control as for sodium dithionite. For the Fe(0) catalytic system, the polymerization rate was 13 times faster than that observed in pure DMSO. [3] The Cu(0)-mediated polymerization was faster than the Fe(0)-mediated one, which is in agreement with other results reported in the literature on the SARA ATRP of MA. [3, 28, 29] Nevertheless, regardless the SARA agent used, the monomer reached high conversion

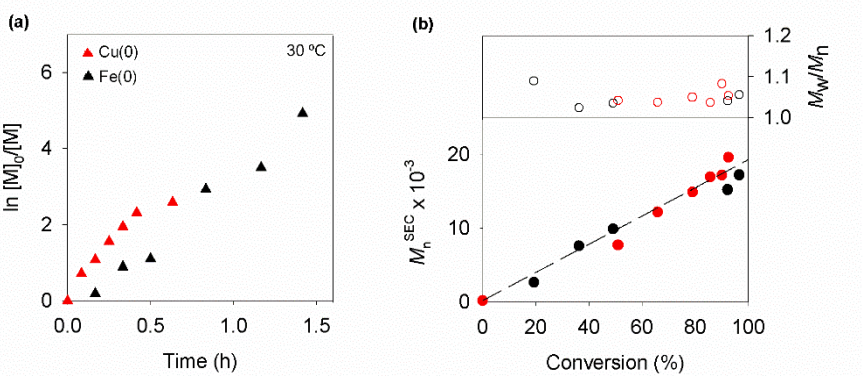

Figure 4-4: (a) Kinetic plots of conversion and ln$[M]_0/[M]$ vs. time and (b) plot of number-average molecular weights (M_n^{SEC}) and $Đ$ (M_w/M_n) vs. monomer conversion for the SARA ATRP of MA in DMSO/BMIM-PF_6/TEG = 45/45/10 (v/v/v) at 30 °C, using different SARA agents. Reaction conditions: $[MA]_0/[solvent]$ = 2/1 (v/v); $[MA]_0/[EBiB]_0/$SARA agent$/[CuBr_2]_0/[Me_6TREN]_0$= 222/1/1/0.1/1.1.

and the control over the molecular weight was excellent (Figure 4-4 (b)). The Cu(0)-mediated SARA ATRP was also tested using the three different glycols (EG, DEG and TEG) and the results were similar in terms of polymerization features (Appendix C, Figure C2), proving the versatility of the system.

4.4.3 "Flash" SARA ATRP in water/BMIM-PF_6/TEG mixtures

Since an increase in the polarity of the medium appeared to contribute for faster polymerizations, DMSO was replaced by water in the solvent reaction mixture in order to investigate its influence on the polymerization. The replacement of DMSO is also attractive, considering the growing concerns about the environmental hazards derived from organic solvents and due to the raising interest in polymerizations using ecofriendly solvents. The SARA ATRP of MA was performed using a water/BMIM-PF_6/TEG = 10/45/45 (v/v) mixture. The content of water was limited to 10% to afford a homogeneous homopolymerization, considering that water is not miscible with BMIM-PF_6 and PMA is insoluble in water. The kinetic results presented in Figure 4-5 (a) (black symbols) show an extremely fast polymerization, with monomer reaching near 100% of conversion in less than 15 min for a DP = 222. Despite the very high polymerization rate, the $Đ$ of the polymers was below 1.1 during the entire reaction (Figure 4-5 (b)), which is remarkable. To the best of our knowledge, this is the fastest controlled polymerization of MA obtained by ATRP related processes. The system proved to be quite robust, as a well-defined PMA with high molecular weight ($M_n^{SEC} \approx 60\,000$) was obtained in 1 h of reaction, using 100 ppm of copper (green symbols in Figure 4-5).

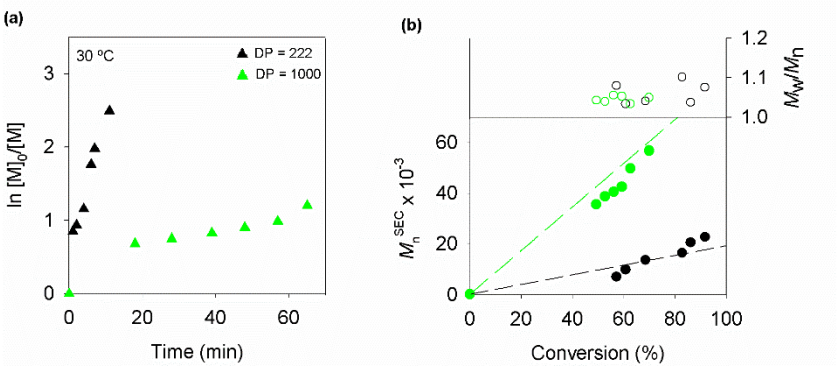

Figure 4-5: (a) Kinetic plots of conversion and ln[M]$_0$/[M] vs. time and (b) plot of number-average molecular weights (M_n^{SEC}) and $Đ$ (M_w/M_n) vs. monomer conversion for the SARA ATRP of MA in water/BMIM-PF_6/TEG = 10/45/45 (v/v/v) at 30 °C. Reaction conditions: [MA]$_0$/[solvent] = 2/1 (v/v); [MA]$_0$/[EBiB]$_0$/[$Na_2S_2O_4$]$_0$/[$CuBr_2$]$_0$/[Me_6TREN]$_0$= 1000 or 222/1/1/0.1/0.2; DP = [MA]$_0$/[EBiB]$_0$.

The E_T (30) experimental values were also determined for this H_2O/BMIM-PF_6/TEG solvent mixture, in order to confirm a possible "hyperpolarity" effect. Since the BMIM-PF_6 and water are immiscible, it was not possible to determine the E_T (30) value when the TEG content was 0%. Alternatively, MA was added to the mixture, with the same ratio solvent/monomer used for the polymerizations, to provide homogenous solutions and to allow the determination of the E_T (30) value. Figure 4-6 shows that there is a synergistic effect within the H_2O/BMIM-PF_6/TEG mixtures, as the E_T (30) values were always higher than the theoretical ones (dashed line). However, no "hyperpolarity" effect was observed since the E_T (30) values were always lower than the ones of the separated components, regardless the content of TEG in the mixture. Therefore, as previously suggested, the dramatic increase on the polymerization rate should be a consequence of a combination of factors and not only due to the existence of a "hyperpolarity" effect. Additional studies revealed that there was also an increase of medium polarity with the increase of the monomer conversion during the polymerization (Appendix C, Figure C3). In the case of this H_2O/BMIM-PF_6/TEG mixture, besides the evident synergistic effect (Figure 4-6), one might expect that the activity of Cu(I) could also be very high due to the presence of water, leading to ultra-fast reactions. Another explanation for the observed ultrafast polymerization (Figure 4-5) might be the increased solubility of the SARA agent ($Na_2S_2O_4$) in the reaction mixture due to the presence of water and TEG. The confirmation of these hypotheses requires further investigation, namely the determination of the k_{act} value. Regarding the DMSO/BMIM-PF_6/TEG mixtures, the addition of monomer did not affect the "hyperpolarity" effect (Appendix C, Figure C4).

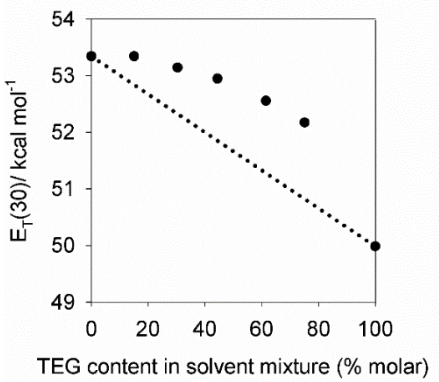

Figure 4-6: Experimental E_T (30) values of water/BMIM-PF_6/TEG mixtures with Reichardt's dye 30 (concentration = 50 μM). Dashed line represents the theoretical E_T (30) values for each solvent mixture.

4.4.4 "Livingness" of the PMA-Br chains

A "one-pot" chain extension experiment was performed to prove the "living" character of the PMA-Br obtained by "flash" SARA ATRP. The SEC trace of the PMA-Br macroinitiator (Figure 4-7, black line) exhibit a slight shoulder for higher molecular weights, which was attributed to the occurrence of some side reactions due to the very high monomer conversion at the time of the second monomer addition (> 97 %). This resulted in a tailing effect for low molecular weights in SEC trace of the extended polymer (Figure 4-7, red line).

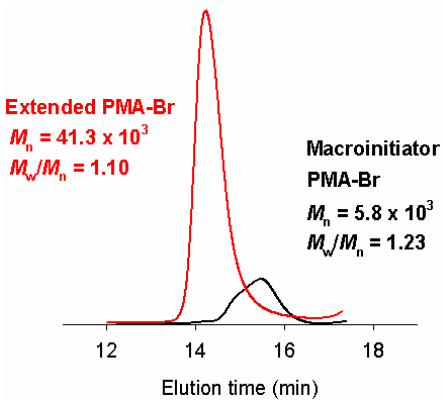

Figure 4-7: SEC traces of the PMA-Br macroinitiator before (right curve) and after the chain extension experiment (left curve).

Nevertheless, the clear shift in the molecular weight distribution from the PMA-Br (M_{nSEC} = 5.8 x 10^3; $Đ$ = 1.23) macroinitiator to the extended PMA-Br (M_{nSEC} = 41.3 x 10^3; $Đ$ = 1.10) confirms the "living" character of the polymer. The presence of the active chain-end and the chemical structure of the polymer were confirmed by ^{1}H NMR spectroscopy (Figure 4-8).

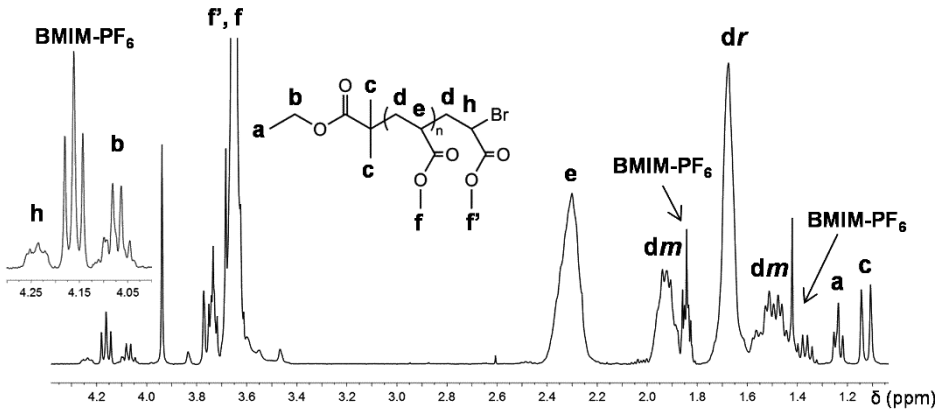

Figure 4-8: ^{1}H NMR spectrum ($CDCl_3$) of a PMA-Br (M_{nSEC} = 4.7 x 10^3; $Đ$ = 1.11) obtained by "flash" SARA ATRP in water/BMIM-PF_6/TEG = 10/45/45 (v/v).

4.5 Conclusions

A "hyperpolarity" effect within the DMSO/BMIM-PF_6/glycol (glycol: TEG, DEG or EG) ternary mixtures allowed the increase of the overall polymerization rate, in comparison with DMSO/BMIM-PF_6 binary mixtures, for the SARA ATRP of MA at 30 °C. The molecular weight of the resultant PMA is well controlled during the entire polymerization time ($Đ$ < 1.1) and the polymer presented "living" features. The change of the DMSO by water in a water/BMIM-PF_6/TEG mixture dramatically accelerated the polymerization, providing the fastest ATRP of MA reported in the literature, which was named "flash" SARA ATRP.

4.6 References

[1] Braunecker, W., Matyjaszewski, K., *Controlled/living radical polymerization: Features, developments, and perspectives*, Progress in Polymer Science, **2007**, 32, 93-146.

[2] Matyjaszewski, K., *Atom Transfer Radical Polymerization (ATRP): Current status and future perspectives*, Macromolecules, **2012**, 45, 4015-4039.

[3] Mendonça, P. V., Serra, A. C., Coelho, J. F. J., Popov, A. V., Guliashvili, T., *Ambient temperature rapid ATRP of methyl acrylate, methyl methacrylate and styrene in polar solvents with mixed transition metal catalyst system*, European Polymer Journal, **2011**, 47, 1460-1466.

[4] Mendonça, P. V., Konkolewicz, D., Averick, S. E., Serra, A. C., Popov, A. V., Guliashvili, T., et al., *Synthesis of cationic poly ((3-acrylamidopropyl) trimethylammonium chloride) by SARA ATRP in ecofriendly solvent mixtures*, Polymer Chemistry, **2014**, 5, 5829-5836.

[5] Rocha, N., Mendes, J., Duraes, L., Maleki, H., Portugal, A., Geraldes, C. F. G. C., et al., *Poly(ethylene glycol)-block-poly(4-vinyl pyridine) as a versatile block copolymer to prepare nanoaggregates of superparamagnetic iron oxide nanoparticles*, Journal of Materials Chemistry B, **2014**, 2, 1565-1575.

[6] Rocha, N., Mendonça, P. V., Mendes, J. P., Simões, P. N., Popov, A. V., Guliashvili, T., et al., *Facile Synthesis of Well-Defined Telechelic Alkyne-Terminated Polystyrene in Polar Media Using ATRP With Mixed Fe/Cu Transition Metal Catalyst*, Macromolecular Chemistry and Physics, **2013**, 214, 76-84.

[7] Tom, J., Hornby, B., West, A., Harrisson, S., Perrier, S., *Copper(0)-mediated living radical polymerization of styrene*, Polymer Chemistry, **2010**, 1, 420-422.

[8] Mendes, J. P., Branco, F., Abreu, C. M. R., Mendonça, P. V., Serra, A. C., Popov, A. V., et al., *Sulfolane: an Efficient and Universal Solvent for Copper-Mediated Atom Transfer Radical (co)Polymerization of Acrylates, Methacrylates, Styrene, and Vinyl Chloride*, ACS Macro Letters, **2014**, 3, 858-861.

[9] Jakubowski, W., Matyjaszewski, K., *Activators Regenerated by Electron Transfer for Atom-Transfer Radical Polymerization of (Meth)acrylates and Related Block Copolymers*, Angewandte Chemie, **2006**, 118, 4594-4598.

[10] Zhang, Y., Wang, Y., Matyjaszewski, K., *ATRP of methyl acrylate with metallic zinc, magnesium, and iron as reducing agents and supplemental activators*, Macromolecules, **2011**, 44, 683-685.

[11] Matyjaszewski, K., Jakubowski, W., Min, K., Tang, W., Huang, J., Braunecker, W. A., et al., *Diminishing catalyst concentration in atom transfer radical polymerization with reducing agents*, Proceedings of the National Academy of Sciences of the United States of America, **2006**, 103, 15309-15314.

[12] Magenau, A. J. D., Strandwitz, N. C., Gennaro, A., Matyjaszewski, K., *Electrochemically Mediated Atom Transfer Radical Polymerization*, Science, **2011**, 332, 81-84.

[13] Treat, N. J., Sprafke, H., Kramer, J. W., Clark, P. G., Barton, B. E., Read de Alaniz, J., et al., *Metal-Free Atom Transfer Radical Polymerization*, Journal of the American Chemical Society, **2014**, 136, 16096-16101.

[14] Pan, X., Lamson, M., Yan, J., Matyjaszewski, K., *Photoinduced Metal-Free Atom Transfer Radical Polymerization of Acrylonitrile*, ACS Macro Letters, **2015**, 4, 192-196.

[15] Abreu, C. M. R., Serra, A. C., Popov, A. V., Matyjaszewski, K., Guliashvili, T., Coelho, J. F. J., *Ambient temperature rapid SARA ATRP of acrylates and methacrylates in alcohol-water solutions mediated by a mixed sulfite/Cu(ii)Br2 catalytic system*, Polymer Chemistry, **2013**, 4, 5629-5636.

[16] Góis, J. R., Konkolewicz, D., Popov, A. V., Guliashvili, T., Matyjaszewski, K., Serra, A. C., et al., *Improvement of the control over SARA ATRP of 2-(diisopropylamino)ethyl methacrylate by slow and continuous addition of sodium dithionite*, Polymer Chemistry, **2014**, 5, 4617-4626.

[17] Góis, J. R., Rocha, N., Popov, A. V., Guliashvili, T., Matyjaszewski, K., Serra, A. C., et al., *Synthesis of well-defined functionalized poly(2-(diisopropylamino)ethyl methacrylate) using ATRP with sodium dithionite as a SARA agent*, Polymer Chemistry, **2014**, 5, 3919-3919.

[18] Abreu, C. M. R., Mendonça, P. V., Serra, A. C., Popov, A. V., Matyjaszewski, K., Guliashvili, T., et al., *Inorganic sulfites: Efficient reducing agents and supplemental activators for atom transfer radical polymerization*, ACS Macro Letters, **2012**, 1, 1308-1311.

[19] Cordeiro, R., Rocha, N., Mendes, J. P., Matyjaszewski, K., Guliashvili, T., Serra, A. C., et al., *Synthesis of well-defined poly(2-(dimethylamino)ethyl methacrylate) under mild conditions and its co-polymers with cholesterol and PEG using Fe(0)/Cu(ii) based SARA ATRP*, Polymer Chemistry, **2013**, 4, 3088-3088.

[20] Mendes, J. P., Branco, F., Abreu, C. M. R., Mendonça, P. V., Popov, A. V., Guliashvili, T., et al., *Synergistic Effect of 1-Butyl-3-methylimidazolium Hexafluorophosphate and DMSO in the SARA ATRP at Room Temperature Affording Very Fast Reactions and Polymers with Very Low Dispersity*, ACS Macro Letters, **2014**, 3, 544-547.

[21] Sarkar, A., Trivedi, S., Pandey, S., *Unusual Solvatochromism within 1-Butyl-3-methylimidazolium Hexafluorophosphate + Poly(ethylene glycol) Mixtures*, The Journal of Physical Chemistry B, **2008**, 112, 9042-9049.

[22] Sarkar, A., Trivedi, S., Baker, G. A., Pandey, S., *Multiprobe Spectroscopic Evidence for "Hyperpolarity" within 1-Butyl-3-methylimidazolium Hexafluorophosphate Mixtures with Tetraethylene Glycol*, The Journal of Physical Chemistry B, **2008**, 112, 14927-14936.

[23] Beniwal, V., Kumar, A., *Synergistic Effects and Correlating Polarity Parameters in Binary Mixtures of Ionic Liquids*, ChemPhysChem, **2015**, 16, 1026-1034.

[24] Harrisson, S., Mackenzie, S. R., Haddleton, D. M., *Unprecedented solvent-induced acceleration of free-radical propagation of methyl methacrylate in ionic liquids*, Chemical Communications, **2002**, 2850-2851.

[25] Harrisson, S., Mackenzie, S. R., Haddleton, D. M., *Pulsed Laser Polymerization in an Ionic Liquid: Strong Solvent Effects on Propagation and Termination of Methyl Methacrylate*, Macromolecules, **2003**, 36, 5072-5075.

[26] Percec, V., Grigoras, C., *Catalytic effect of ionic liquids in the Cu2O/2,2′-bipyridine catalyzed living radical polymerization of methyl methacrylate initiated with arenesulfonyl chlorides*, Journal of Polymer Science Part A: Polymer Chemistry, **2005**, 43, 5609-5619.

[27] Yanagida, S., Takahashi, K., Okahara, M., *Metal-ion Complexation of Noncyclic Poly(oxyethylene) Derivatives. II. PMR Studies of the Complexation with Alkali and Alkaline-earth Metal Cations*, Bulletin of the Chemical Society of Japan, **1978**, 51, 1294-1299.

[28] Guliashvili, T., Mendonça, P. V., Serra, A. C., Popov, A. V., Coelho, J. F. J., *Copper-Mediated Controlled/"Living" Radical Polymerization in Polar Solvents: Insights into Some Relevant Mechanistic Aspects*, Chemistry - A European Journal, **2012**, 18, 4607-4612.

[29] Maximiano, P., Mendes, J. P., Mendonça, P. V., Abreu, C. M. R., Guliashvili, T., Serra, A. C., et al., *Cyclopentyl methyl ether: A new green co-solvent for supplemental activator and reducing agent atom transfer radical polymerization*, Journal of Polymer Science Part A: Polymer Chemistry, **2015**, n/a-n/a.

CHAPTER 5

Conclusions and future work

Chapter 5: Conclusions and Future Work

Reversible deactivation radical polymerization methods are extremely versatile and robust techniques which make possible the preparation of polymers with well-defined structures and composition, therefore reaching specific target applications that free radical polymerization cannot cover. Each of the 3 main RDRP techniques – ATRP, NMP and RAFT – have unique mechanistic, control and kinetic features, which can be fine-tuned by changing the nature and/or concentration of the components of the system, as well as other parameters (e.g. temperature). However, it was found that most of the literature on these methods still involves harmful organic solvents (e.g DMSO, THF, DCM, DMF, and so on), therefore preventing any use of the polymers synthesized on biomedical applications. Only recently green solvents (like water, alcohols, ionic liquids and supercritical CO_2) have found their place in RDRP systems.

In the study conducted on Chapter 2 about the use of CPME in SARA ATRP systems it was concluded that CPME can be used successfully in MA polymerizations, provided that a co-solvent is present (due to solubility issues of the catalytic Cu complexes in CPME). Both a mixture of CPME/DMSO (70/30 (v/v)) and of CPME/EtOH/H_2O (70/28/2 (v/v/v)) have conducted to low $Đ$ values and reasonable rates of polymerization during the synthesis of PMA. The robustness of this system was confirmed first by testing different SARA agents (Cu(0), $Na_2S_2O_4$ and Fe(0)) and then different DP_T's (100, 222 and 1000), on the basis of the CPME/EtOH/H_2O mixture tested (due to its greener character relative to DMSO). Despite differences in the kinetics of the process (which, in the case of DP_T variations, were expected due to different radical concentrations) the level of control over the polymerization remained very good in all cases, with values of $Đ$ close to 1.1 and the values of M_n^{GPC} close to M_n^{th}. Furthermore, Sty, GMA and VC were also successfully polymerized via SARA-ATRP in CPME based mixtures with a control that is comparable to that exhibited by systems using only organic solvents, thus establishing the versatility of CPME for SARA ATRP. The livingness of the PVC chains prepared by this process was confirmed by a "one-pot" copolymerization experiment, yielding a PMA-PVC-PMA triblock copolymer (and revealing a shift in the GPC curve from the macroinitiator towards the copolymer). However it should be noted that, in the case of Sty and GMA, DMF was still employed as a co-solvent, and in the case of VC, DMSO was used, and so the possibility of

replacing these toxic organic solvents by other green solvents should be studied in future works.

The ability to polymerize both MA and Sty in a RAFT system (using DDMAT as a CTA) using pure CPME as a solvent was demonstrated in Chapter 3, with both processes achieving values of $Đ$ very close to 1.1. Two key features of this new RAFT system for Sty were the ability to completely replace DMF by CPME and also to use lower temperatures (60 °C) than those typically reported for Sty polymerizations. This last factor is important to mitigate the known autopolymerization reactions that result in a loss of chain end functionalities. In addition to MA and Sty, VAc and VC were also tested in pure CPME (this time using CMPCD as the CTA). The performance of CPME in the case of VC polymerization was very similar to that reported for THF, but CPME seems to provide slightly higher reaction rates, with better agreement between M_n^{GPC} and M_n^{th} values. The robustness and versatility of these new systems were further confirmed by the successful polymerizations of VC at different targeted DP's. The living nature and well defined structure of the PVC chains synthetized were verified by a chain extension experiment and ^{1}H-NMR spectra analysis, respectively.

The nitroxide mediated polymerization of Sty, using the BlocBuilder® alkoxyamine, was performed at 80 °C (since the usual temperatures used are very close to the boiling point of CPME) which resulted in a rather slow reaction. Despite this, a good control was achieved (evidenced by linear kinetics, low Đ values and close agreement of M_n^{GPC} and M_n^{th}), therefore proving the feasibility of CPME in NMP systems. This study was extended to VC, revealing that the new CPME system provides values of $Đ$ that are very similar to those reported for DCM. However the NMP of VC in CPME was, remarkably, 20% faster than in DCM. The structural analysis of PVC-SG1 chains by ^{31}P NMR (showing an 87% living chain fraction) and a "one pot" chain extension experiment corroborated their living nature.

Following existing reports on a synergistic effect between BMIM-PF_6 and DMSO and a "hyperpolarity" effect between this ionic liquid and glycols, the polarity of BMIM-PF_6/DMSO/Glycol mixtures (where Glycol = EG, DEG or TEG) was investigated using values of E_T (30) (polarity parameter of the solvatochromic probe Reichardt's Dye (30)) determined via UV/vis spectroscopy. It was observed that mixtures with either three glycols exhibited synergistic and hyperpolarity effects, over a wide range of glycol concentrations, and both effects decrease from EG to DEG and from DEG to TEG. Experiments of

SARA ATRP of MA (with $Na_2S_2O_4$ as the SARA agent) using mixtures based on the three glycols (with glycol content equal to 8 % molar) indicated that this synergistic effects between the ionic liquid and the glycols can increase the overall rate of polymerization, when compared to a system without glycols (i.e. BMIM-PF_6/DMSO in a 50/50 proportion). This fact may be due to an increase in the medium polarity, thus reducing the activation energy needed for propagation. Remarkably, the effects of TEG and EG were much more noticeable than those of DEG (contrary to the results of the polarity tests), suggesting that there are other factors influencing the system (e.g. changes in catalyst solubility, catalyst activity or even glycol complexation reactions), which need to be clarified in future investigations. The versatility of this new glycol based system was proved by testing other SARA agents (namely Cu(0) and Fe(0), using the BMIM-PF_6/DMSO/TEG mixture), as the ensuing polymerization processes were well controlled and faster than the BMIM-PF_6/DMSO mixture.

With the aim of finding a greener system and taking the polarity effects even further, the harmful DMSO was replaced with water (H_2O/BMIM-PF_6/TEG = 10/45/45 (v/v/v)) and a MA polymerization experiment was conducted. Astonishingly, the polymerization proceeded to almost 100% monomer conversion in under 15 min, and with values of $Đ$ below 1.1 (for DP_T = 222), which is an unprecedented result in ATRP of MA. This system also proved to be quite robust, as an increase in the DP_T to 1000 seemed to have no effect on the values of $Đ$. The high reaction rates and the excellent green character of this new "flash" SARA ATRP system are highly attractive advantages for possible industrial applications of this process. Besides this, another possibility to consider for future investigations is the expansion of this system to other monomers as well. It should be noted that E_T (30) measurements for the solvent mixture used revealed no hyperpolarity effect (although the polarity of the mixture increased with conversion), therefore proving that polarity is not the only factor affecting the reaction rate. In particular, the presence of water, which is known to increase the activity of the Cu catalyst and the solubility of $Na_2S_2O_4$, may also be responsible for this result. However, at this point, no conclusion could be drawn regarding this subject, and so further research is needed, especially to measure the values of k_{act} and K_{ATRP} so as to determine the influence of water in the catalytic activity.

APPENDICES

Appendix A: Supporting Information for "Cyclopentyl methyl ether: a new green co-solvent for supplemental activator and reducing agent atom transfer radical polymerization"

Experimental section

Materials

Methyl acrylate (MA, Acros, 99% stabilized), glycidyl methacrylate (GMA, Sigma-Aldrich, 97% stabilized) and Sty were passed through a sand/alumina column before use to remove the radical inhibitor. $CuBr_2$ (Acros, 99+% extra pure, anhydrous), deuterated chloroform ($CDCl_3$) (Euriso-top, +1% TMS), DMF (Sigma-Aldrich, +99.8%), CPME (Sigma-Aldrich, inhibitor-free, anhydrous, +99.9%), DMSO (Acros, 99.8+% extra pure), ethyl α-bromoisobutyrate (EBiB) (Sigma-Aldrich, 98%), bromoform ($CHBr_3$) (+ 99 % stabilized; Acros), ethanol (EtOH, Panreac, 99.5%), PS standards (Polymer Laboratories), iron powder (Fe(0) (Acros, 99%, ~70 mesh), 2-(4-hydroxyphenylazo)benzoic acid (HABA) (Sigma–Aldrich, 99.5%), 2,5-dihydroxybenzoic acid (DHB) (Sigma–Aldrich, >99%), N,N,N′,N′′,N′′-pentamethyldiethylenetriamine (PMDETA, Aldrich, 99%), tris(2-aminoethyl)amine (TREN) (96 %; Sigma-Aldrich), 2,2'-bipyridine (Bpy) (Sigma-Aldrich, +99.8%) and sodium dithionite ($Na_2S_2O_4$, 85 %, technical grade; Aldrich) were used as received.

Metallic copper (Cu(0), d = 1 mm, Sigma Aldrich) was washed with HCl in methanol and subsequently rinsed with methanol and dried under a stream of nitrogen following the literature procedures. [1]

Purified water (Milli-Q®, Millipore, resistivity >18 MΩ.cm) was obtained by reverse osmosis.

THF (Panreac, HPLC grade) was filtered under reduced pressure before use.

Tris[2-(dimethylamino)ethyl]amine (Me_6TREN) [2] and tris(2-pyridylmethyl)amine (TPMA) [3] were synthesized according the procedures described in the literature.

VC (99 %) was kindly supplied by CIRES Lda, Portugal.

Techniques

The chromatographic parameters of the samples were determined using high performance size exclusion chromatography HPSEC; Viscotek (Viscotek TDAmax) with a differential viscometer (DV); right-angle laser-light scattering (RALLS, Viscotek); low-angle laser-light scattering (LALLS, Viscotek); and refractive index (RI) detectors. The column set consisted of a Viscotek Tguard column (8mm) followed by one Viscotek T2000 column (6mm), one MIXED-E PLgel column (3 mm), and one MIXED-C PLgel column (5mm). HPLC dual piston pump was set with a flow rate of 1 mL/min. The eluent (THF) was previously filtered through a 0.2 μm filter. The system was also equipped with an on-line degasser. The tests were done at 30 °C using an Elder CH-150 heater. Before the injection (100 μL), the samples were filtered through a polytetrafluoroethylene (PTFE) membrane with 0.2 μm pore. The system was calibrated with narrow PS standards. The dn/dc was determined as 0.063 for PMA, 0.105 for PVC, 0.087 for PGMA and 0.185 for PS. Molecular weight (M_n^{GPC}) and $Đ$ of the synthesized polymers were determined by multidetectors calibration using the OmniSEC software version: 4.6.1.354.

400 MHz ^{1}H NMR spectra of reaction mixture samples were recorded on a Bruker Avance III 400 MHz spectrometer, with a 5-mm TIX triple resonance detection probe, in $CDCl_3$ with tetramethylsilane (TMS) as an internal standard. Conversions of the monomer were determined by integration of monomer and polymer signals using MestRenova software version: 6.0.2-5475.

For the MALDI-TOF-MS analysis, the PMA samples were dissolved in THF at a concentration of 10 mg/mL. DHB and HABA (0.05 M in THF) were used as matrix. The dried droplet sample preparation technique was used to obtain 1:1 ratio (sample/matrix); an aliquot of 1 mL of each sample was directly spotted on the MTP AnchorChip TM 600/384 TF MALDI target, Bruker Daltonik (Bremen Germany) and, before the sample dry, 1 mL of matrix solution in THF was added and allowed to dry at room temperature, to allow matrix crystallization. External mass calibration was performed with a peptide calibration standard (PSCII) for the range 700–3000 (9 mass calibration points), 0.5 mL of the calibration solution and matrix previously mixed in an Eppendorf tube (1:2, v/v) were applied directly on the target and allowed to dry at room temperature. Mass spectra were recorded using an Autoflex III smartbeam1 MALDI-TOF-MS mass spectrometer Bruker Daltonik (Bremen, Germany) operating in the linear and reflection positive ion mode. Ions were formed upon irradiation by a smartbeam laser using a frequency of 200 Hz. Each mass spectrum was produced by averaging 2500 laser shots collected across the whole

sample spot surface by screening in the range *m/z* 500–10,000. The laser irradiance was set to 35–40% (relative scale 0–100) arbitrary units according to the corresponding threshold required for the applied matrix systems

Procedures

Typical procedure for the $[Cu(0)]_0/[CuBr_2]_0/[Me_6TREN]_0$ = Cu(0) wire/0.1/1.1 catalyzed SARA ATRP of MA

Cu(0) wire (5 cm, 450 mg) and a solution of $CuBr_2$ (3.51 mg, 0.016 mmol) and Me_6TREN (39.76 mg, 0.173 mmol) in CPME (1.1 mL), water (31.6 μL) and ethanol (0.44 mL) were placed in a Schlenk tube reactor. A mixture of MA (3.16 mL, 34.85 mmol) and EBiB (30.62 mg, 0.157 mmol) was added to the reactor that was sealed, using a glass stopper, and frozen in liquid nitrogen. The Schlenk tube reactor containing the reaction mixture was deoxygenated with four freeze-vacuum-thaw cycles and purged with nitrogen. The reactor was placed in a water bath at 30 ºC with stirring (700 rpm). During the polymerization, different reaction mixture samples were collected by using an airtight syringe and purging the side arm of the Schlenk tube reactor with nitrogen. The samples were analyzed by ^{1}H NMR spectroscopy to determine the monomer conversion and by GPC to determine M_n^{GPC} and $Đ$ of the polymers.

Typical procedure for the $[Cu(0)]_0/[CuBr_2]_0/[PMDETA]_0$ = Cu(0) wire/0/1.1 catalyzed SARA ATRP of Sty

A mixture of Cu(0) wire (5 cm, 450 mg), $CuBr_2$ (2.89 mg, 0.013 mmol), PMDETA (24.73 mg, 0.14 mmol), CPME (1.2 mL) and DMF (0.5 mL) was placed in a Schlenk tube reactor. A solution of EBiB (25.31 mg, 0.13 mmol) in Sty (3.30 mL, 28.81 mmol) was added to the reactor that was sealed, by using a glass stopper, and frozen in liquid nitrogen. The Schlenk tube reactor containing the reaction mixture was deoxygenated with four freeze-vacuum-thaw cycles and purged with nitrogen. The reactor was placed in a water bath at 60 ºC with stirring (700 rpm). During the polymerization, different reaction mixture samples were collected by using an airtight syringe and purging the side arm of the Schlenk tube reactor with nitrogen. The samples were analyzed by ^{1}H NMR spectroscopy to determine the monomer conversion and by GPC, to determine the M_n^{GPC} and $Đ$ of the polymers.

Typical procedure for the $[Cu(0)]_0/[CuBr_2]_0/[TREN]_0$ = Cu(0) wire/0.1/1.1 catalyzed SARA ATRP of VC

A 50 mL Ace glass 8645#15 pressure tube, equipped with bushing and plunger valve, was charged with a mixture of $CHBr_3$ (86.43 mg, 0.33 mmol), TREN (55.03 mg, 0.36 mmol), $CuBr_2$ (7.34 mg, 0.033 mmol), Cu(0) wire (5 cm, 450 mg), CPME (3.5 mL) and DMSO (1.5 mL) (previously bubbled with nitrogen for about 15 min). The precondensed VC (5 mL, 72.8 mmol) was added to the tube. The exact amount of VC was determined gravimetrically. The tube was closed, placed in liquid nitrogen and degassed through the plunger valve by applying reduced pressure and filling the tube with N_2 about 20 times. The valve was closed, and the tube reactor was placed in a water bath at 42 °C with stirring (700 rpm). The reaction was stopped by plunging the tube into ice water. The tube was slowly opened, the excess of VC was distilled, and the mixture was precipitated into methanol. The polymer was separated by filtration and dried in a vacuum oven until constant weight was observed. The monomer conversion was determined gravimetrically. GPC was used for the determination of PVC´s M_n^{GPC} and $Đ$.

Typical procedure for the synthesis of PMA-b-PVC-b-PMA block copolymer by "one-pot" $[Cu(0)]_0/[CuBr_2]_0/[TREN]_0$ = Cu(0) wire/0.1/1.1 catalyzed SARA ATRP

A 50 mL Ace glass 8645#15 pressure tube, equipped with bushing and plunger valve, was charged with a mixture of $CHBr_3$ (115.07 mg, 0.44 mmol), TREN (73.24 mg, 0.48 mmol), $CuBr_2$ (9.76 mg, 0.044 mmol), Cu(0) wire (5 cm, 450 mg), CPME (2.1 mL) and DMSO (0.9 mL) (previously bubbled with nitrogen for about 15 min). The precondensed VC (3.0 mL, 43.7 mmol) was added to the tube. The exact amount of VC was determined gravimetrically. The tube was closed, submerged in liquid nitrogen and degassed through the plunger valve by applying reduced pressure and filling the tube with nitrogen about 20 times. The valve was closed, and the tube reactor was placed in a water bath at 42 °C with stirring (700 rpm). After 10 h, the reaction was stopped by plunging the tube into ice water. The tube was slowly opened and the excess VC was distilled. The monomer conversion were determined gravimetrically (61.8%), and the M_n^{GPC} = 6100 and $Đ$ = 1.57 were determined by GPC analysis in THF. A mixture of CPME (8.4 mL), DMSO (3.6 mL) and MA (12 mL, 132.4 mmol) was added to the same 50 mL Ace glass 8645#15 pressure tube (without any purification of the α,ω-di(bromo)PVC macroinitiator). The tube was

closed, submerged in liquid nitrogen and degassed through the plunger valve by applying reduced pressure and filling the tube with nitrogen about 20 times. The valve was closed, and the tube reactor was placed in a water bath at 42 °C with stirring (700 rpm). The reaction was stopped after 32 h and the mixture was analysed by ^{1}H NMR spectroscopy in order to determine the MA conversion and by GPC, to determine the M_n^{GPC} and $Đ$ of the PMA-*b*-PVC-*b*-PMA block copolymer.

Kinetic data

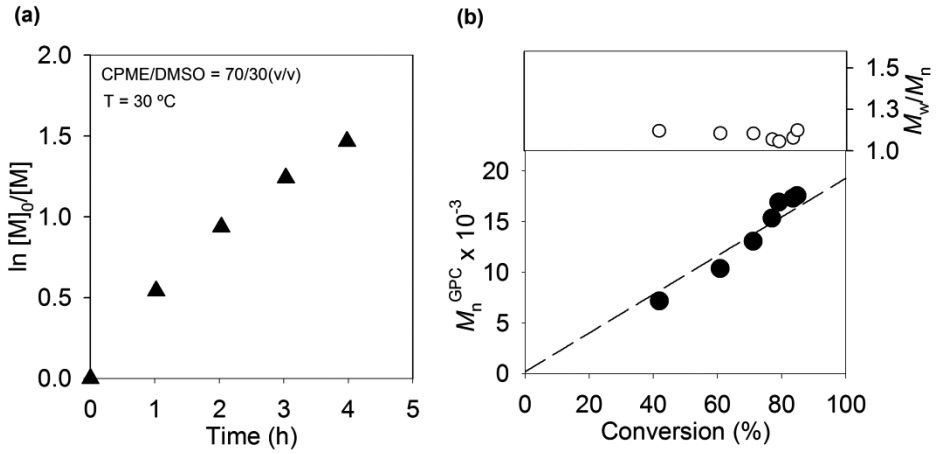

Figure A1: (a) Kinetic plots of conversion and ln$[M]_0/[M]$ *vs.* time and (b) plot of number-average molecular weights (M_n^{GPC}) and $Đ$ (M_w/M_n) *vs.* monomer conversion for the SARA ATRP of MA in CPME/DMSO = 70/30 (v/v) at 30 °C. Reaction conditions: $[MA]_0$/[solvent] = 2/1 (v/v); $[MA]_0/[EBiB]_0/Cu(0)/[CuBr_2]_0/[Me_6TREN]_0$ = 222/1/Cu(0) wire/0.1/1.1.

Chain extension

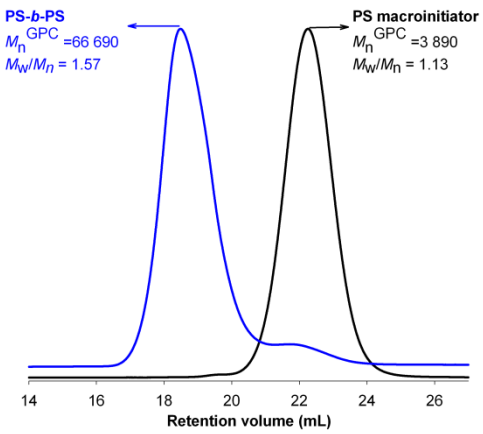

Figure A2: GPC chromatograms of a PS-Br macroinitiator (black line) and self-extended PS (blue line) by SARA ATRP.

^{1}H NMR spectra

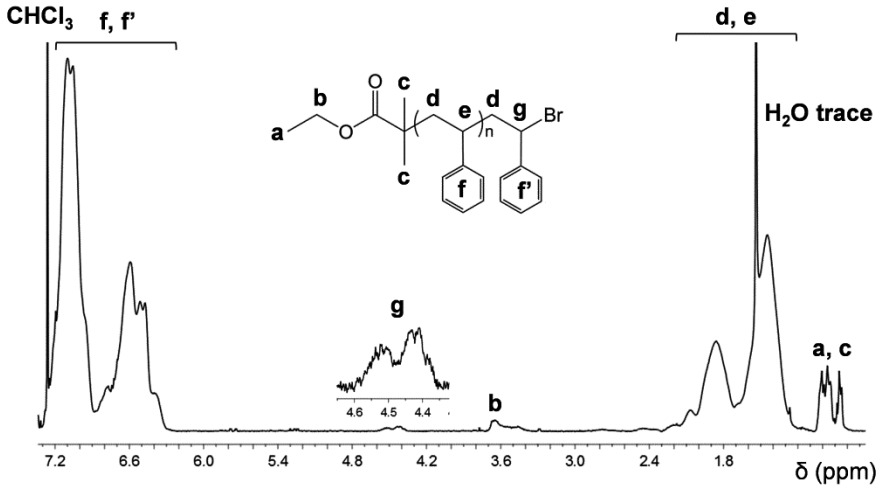

Figure A3: ^{1}H NMR spectrum of a PS sample (M_n^{GPC} = 3800 ; $Đ$ =1.14) obtained by SARA ATRP; solvent: $CDCl_3$.

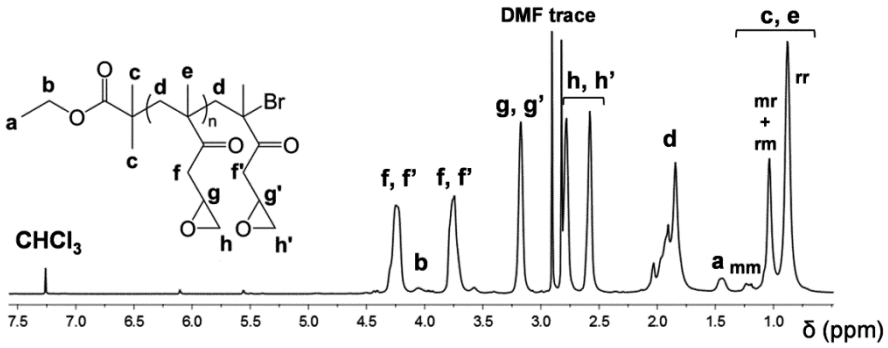

Figure A4: ^{1}H NMR spectrum of a PGMA sample (M_n^{GPC} = 46600; $Đ$ = 1.39) obtained by SARA ATRP; solvent: $CDCl_3$.

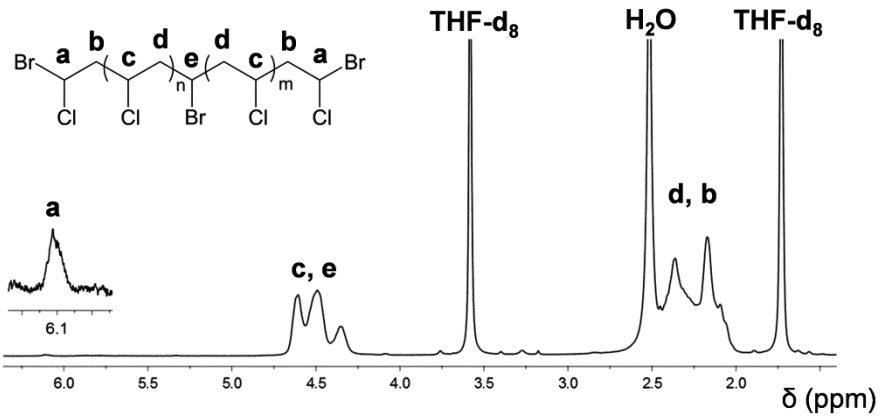

Figure A5: ^{1}H NMR spectrum of a PVC sample (M_n^{GPC} = 6100; $Đ$ =1.57) obtained by SARA ATRP; solvent: d_8-THF.

MALDI spectrum

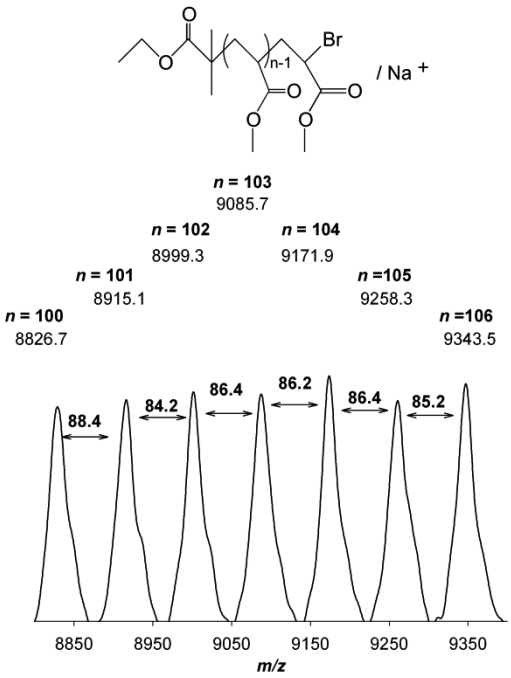

Figure A6: Enlargement of the MALDI-TOF-MS from m/z 8800 to 9400 in the linear mode (using HABA as matrix) of PMA-Br (M_n^{GPC} = 10600, $Đ$ =1.28).

References

[1] Zhang, Y., Wang, Y., Peng, C.-h., Zhong, M., Zhu, W., Konkolewicz, D., et al., *Copper-Mediated CRP of Methyl Acrylate in the Presence of Metallic Copper: Effect of Ligand Structure on Reaction Kinetics*, Macromolecules, **2012**, 45, 78-86.

[2] Ciampolini, M., Nardi, N., *Five-Coordinated High-Spin Complexes of Bivalent Cobalt, Nickel, andCopper with Tris(2-dimethylaminoethyl)amine*, Inorganic Chemistry, **1966**, 5, 41-44.

[3] Britovsek, G. J. P., England, J., White, A. J. P., *Non-heme Iron(II) Complexes Containing Tripodal Tetradentate Nitrogen Ligands and Their Application in Alkane Oxidation Catalysis*, Inorganic Chemistry, **2005**, 44, 8125-8134.

Appendix B: Supporting Information for "Cyclopentyl Methyl Ether As A Green Solvent for Reversible-Addition Fragmentation Chain Transfer and Nitroxide-Mediated Polymerizations"

Experimental Section

Materials

VC (99.9%) was kindly supplied by CIRES Lda, Portugal. MA (99% stabilized; Acros), Sty (+ 99 %; Sigma-Aldrich) and VAc (+ 99 %; Sigma-Aldrich) were passed over a basic alumina column before use to remove the radical inhibitors. The BlocBuilder alkoxyamine was obtained from Arkema. Cyanomethyl methyl(phenyl)carbamodithioate (CMPCD) (Sigma–Aldrich, 98 %), 2-(dodecylthiocarbonothioylthio)-2-methylpropionic acid (DDMAT) (Sigma–Aldrich, 98 %), Trigonox 187-W40 (40 % water and methanol emulsion of diisobutyryl peroxide - DIBPO), deuterated tetrahydrofuran (d_8-THF) (Euriso-top, 99.5%), deuterated chloroform ($CDCl_3$) (+ 1 % tetramethylsilane (TMS); Euriso-top), 2-(4-hydroxyphenylazo)benzoic acid (HABA) (Sigma–Aldrich, 99.5%), CPME (Sigma-Aldrich, inhibitor-free, anhydrous, +99.9%), methanol (Labsolve, 99,5%), hexane (Fisher Chemical, 95%), and polystyrene (PS) standards (Polymer Laboratories) were used as received. Azobisisobutyronitrile (AIBN) (Fluka, 98 %) was recrystallized three times from ethanol before use. High-performance liquid chromatography (HPLC) grade THF (Panreac) was filtered (0.2 μm filter) under reduced pressure before use.

Techniques

400 MHz ^{1}H NMR spectra of samples were recorded on a Bruker Avance III 400 MHz spectrometer, with a 5-mm TIX triple resonance detection probe, in d_8-THF and $CDCl_3$ with tetramethylsilane (TMS) as an internal standard.

The chromatographic parameters of the samples were determined using a size exclusion chromatography set-up from Viscotek (Viscotek TDAmax) equipped with a differential viscometer (DV) and right-angle laser-light scattering (RALLS, Viscotek), low-angle laser-light scattering (LALLS, Viscotek) and refractive index (RI) detectors. The column set consisted of a PL 10 mm guard column (50 × 7.5 mm^2) followed by one Viscotek T200

column (6 µm), one MIXED-E PLgel column (3 µm) and one MIXED-C PLgel column (5 µm). A dual piston pump was set with a flow rate of 1 mL/min. The eluent (THF) was previously filtered through a 0.2 µm filter. The system was also equipped with an on-line degasser. The analyses were performed at 30 °C using an Elder CH-150 heater. Before injection (100 µL), the samples were filtered through a polytetrafluoroethylene (PTFE) membrane with 0.2 µm pore. The system was calibrated with narrow PS standards. The dn/dc value was determined as 0.105 for PVC and 0.185 for PS. Molecular weight (M_n^{SEC}) and dispersity ($Đ = M_w/M_n$) of synthesized polymers were determined by triple detection calibration using the OmniSEC software version: 4.6.1.354.

For the MALDI-TOF-MS analysis, the PVC samples were dissolved in THF at a concentration of 10 mg/mL. HABA (0.05 M in THF) was used as matrix. The dried-droplet sample preparation technique was used to obtain 1/1 ratio (sample/matrix); an aliquot of 1 µL of each sample was directly spotted on the MTP AnchorChip TM 600/384 TF MALDI target, Bruker Daltonik (Bremen Germany) and, before the sample dry, 1 µL of matrix solution in THF was added and allowed to dry at room temperature, to allow matrix crystallization. External mass calibration was performed with a peptide calibration standard (PSCII) for the range 700-3000 (9 mass calibration points), 0.5 µL of the calibration solution and matrix previously mixed in an Eppendorf tube (1/2, v/v) were applied directly on the target and allowed to dry at room temperature. Mass spectra were recorded using an Autoflex III smartbeam1 MALDI-TOF-MS mass spectrometer Bruker Daltonik (Bremen, Germany) operating in the linear and reflectron positive ion mode. Ions were formed upon irradiation by a smartbeam1 laser using a frequency of 200 Hz. Each mass spectrum was produced by averaging 2500 laser shots collected across the whole sample spot surface by screening in the range *m/z* 400-10000. The laser irradiance was set to 35-40% (relative scale 0-100) arbitrary units according to the corresponding threshold required for the applied matrix systems.

Procedures

The VC polymerizations were carried out in a 50 mL glass high-pressure tube equipped with a magnetic stir bar. In the kinetic studies each point represents a single experiment.

Typical procedure for the RAFT polymerization of VC in CPME at 42 °C with $[VC]_0/[CMPCD]_0/[Trigonox]_0 = 250/1/0.2$

A 50-mL Ace Glass 8645#15 pressure tube, equipped with a bushing and a plunge valve, was charged with a mixture of CMPCD (66 mg, 0.29 mmol), Trigonox 187 W40 (25 mg, 0.058 mmol) and CPME (5.0 mL) (previously bubbled with nitrogen for 5 min). The precondensed VC (5 mL, 73 mmol) was added to the tube. The exact amount of VC was determined gravimetrically. The tube was sealed, submerged in liquid nitrogen and degassed through the plunger valve by applying reduced pressure and filling the tube with nitrogen about 20 times. The valve was closed and the tube reactor was placed in a water bath at 42 °C ± 0.5 °C under stirring (700 rpm). After 24 h, the reaction was stopped by plunging the tube into ice water. The tube was slowly opened, the excess VC was distilled, and the mixture was precipitated into 250 mL of methanol. The polymer was separated by filtration and dried in a vacuum oven until constant weight, yielding 3.66 g (69.8 %) of PVC (M_n^{SEC} = 11500, $Đ$ = 1.51).

Typical procedure for the RAFT polymerization of Sty in CPME at 60 °C with $[Sty]_0/[DDMAT]_0/[AIBN]_0 = 222/1/0.5$

A mixture of DDMAT (59 mg, 0.16 mmol), AIBN (13 mg, 0.08 mmol) and CPME (2.0 mL) (previously bubbled with nitrogen for 5 min) was placed in a Schlenk tube reactor. Sty (4.0 mL, 35 mmol) was added to the reactor that was sealed, by using a glass stopper, and frozen in liquid nitrogen. The Schlenk tube reactor containing the reaction mixture was deoxygenated with four freeze-vacuum-thaw cycles and purged with nitrogen. The reactor was placed in an oil bath at 60 ºC with stirring (700 rpm). During the polymerization, different reaction mixture samples were collected by using an airtight syringe and purging the side arm of the Schlenk tube reactor with nitrogen. The samples were analyzed by ^{1}H NMR spectroscopy to determine the monomer conversion and by SEC, to determine the M_n^{SEC} and $Đ$ of the polymers (e.g.: t_{rx} = 49 h, conv = 84%, M_n^{SEC} = 16000, $Đ$ = 1.09).

Typical procedure for the "one-pot" chain extension experiment from a CTA-terminated PVC

A 50-mL Ace Glass 8645#15 pressure tube, equipped with a bushing and a plunger valve, was charged with a mixture CMPCD (99 mg, 0.44 mmol), Trigonox 187 W40 (38 mg, 0.087 mmol) and CPME (3.0 mL) (previously bubbled with nitrogen for 5 min). The precondensed VC (3.0 mL, 44 mmol) was added to the tube. The exact amount of VC was

determined gravimetrically. The tube was sealed, submerged in liquid nitrogen and degassed through the plunger valve by applying reduced pressure and filling the tube with nitrogen about 20 times. The valve was closed, and the tube reactor was placed in a water bath at 42 °C under stirring (700 rpm). After 5 h, the reaction was stopped by plunging the tube into ice water. The tube was slowly opened and the excess VC was distilled. The monomer conversion were determined gravimetrically (58.6 %), and the M_n^{SEC} = 4200 and $Đ$ = 1.54 were determined by SEC. CPME (18.0 mL) (previously bubbled with nitrogen for 5 min), Trigonox 187 W40 (31 mg, 0.07 mmol) and the precondensed VC (18.0 mL, 262 mmol) were added in the medium without any purification of the previously obtained PVC-CTA macroCTA. The tube was sealed, submerged in liquid nitrogen and degassed through the plunger valve by applying reduced pressure and filling the tube with nitrogen about 20 times. The valve was closed, and the tube reactor was placed in a water bath at 42 °C under stirring (700 rpm). The reaction was stopped after 48 h by plunging the tube into ice water. The tube was slowly opened and the excess VC was distilled. The monomer conversion were determined gravimetrically (41.8 %), and the M_n^{SEC} = 17300 and $Đ$ = 1.53 of the resulting extended PVC-*b*-PVC were determined by SEC.

Typical procedure for the NMP of VC in CPME at 42 °C with $[VC]_0/[BlocBuilder]_0$= 250/1

A 50-mL Ace Glass 8645#15 pressure tube, equipped with a bushing and a plunge valve, was charged with a mixture of BlocBuilder alkoxyamine (111 mg, 0.29 mmol) and CPME (5.0 mL) (previously bubbled with nitrogen for 5 min). The precondensed VC (5 mL, 73 mmol) was added to the tube. The exact amount of VC was determined gravimetrically. The tube was sealed, submerged in liquid nitrogen and degassed through the plunger valve by applying reduced pressure and filling the tube with nitrogen about 20 times. The valve was closed and the tube reactor was placed in a water bath at 42 °C ± 0.5 °C under stirring (700 rpm). After 24 h, the reaction was stopped by plunging the tube into ice water. The tube was slowly opened, the excess VC was distilled, and the mixture was precipitated into 250 mL of methanol. The polymer was separated by filtration and dried in a vacuum oven until constant weight, yielding 3.30 g (63.1 %) of PVC (M_n^{SEC} = 12000, $Đ$ = 1.54).

Typical procedure for the NMP of Sty in CPME at 80 °C with $[Sty]_0/[BlocBuilder]_0$ = 222/1

A mixture of BlocBuilder alkoxyamine (60 mg, 0.16 mmol) and CPME (2.0 mL) (previously bubbled with nitrogen for 5 min) was placed in a Schlenk tube reactor. Sty (4.0 mL, 35 mmol) was added to the reactor that was sealed, by using a glass stopper, and frozen in liquid nitrogen. The Schlenk tube reactor containing the reaction mixture was deoxygenated with four freeze-vacuum-thaw cycles and purged with nitrogen. The reactor was placed in an oil bath at 80 ºC with stirring (700 rpm). During the polymerization, different reaction mixture samples were collected by using an airtight syringe and purging the side arm of the Schlenk tube reactor with nitrogen. The samples were analyzed by ^{1}H NMR spectroscopy to determine the monomer conversion and by SEC, to determine the M_n^{SEC} and $Đ$ of the polymers (e.g.: t_{rx} = 166 h, conv = 71%, M_n^{SEC} = 13500, $Đ$ = 1.09).

Typical procedure for the "one-pot" chain extension experiment from SG1-terminated PVC

A 50-mL Ace Glass 8645#15 pressure tube, equipped with a bushing and a plunger valve, was charged with a mixture of BlocBuilder alkoxyamine (167 mg; 0.44 mmol) and CPME (3.0 mL) (previously bubbled with nitrogen for 5 min). The precondensed VC (3.0 mL, 43.7 mmol) was added to the tube. The exact amount of VC was determined gravimetrically. The tube was sealed, submerged in liquid nitrogen and degassed through the plunger valve by applying reduced pressure and filling the tube with nitrogen about 20 times. The valve was closed, and the tube reactor was placed in a water bath at 42 °C under stirring (700 rpm). After 10 h, the reaction was stopped by plunging the tube into ice water. The tube was slowly opened and the excess VC was distilled. The monomer conversion were determined gravimetrically (52.2 %), and the M_n^{SEC} = 4300 and $Đ$ = 1.55 were determined by SEC. CPME (18.0 mL) (previously bubbled with nitrogen for 5 min) and the precondensed VC (18.0 mL, 262 mmol) were added in the medium without any purification of the previously obtained PVC-SG1 macroinitiator. The tube was sealed, submerged in liquid nitrogen and degassed through the plunger valve by applying reduced pressure and filling the tube with nitrogen about 20 times. The valve was closed, and the tube reactor was placed in a water bath at 42 °C under stirring (700 rpm). The reaction was stopped after 48 h by plunging the tube into ice water. The tube was slowly opened and the excess VC was distilled. The monomer conversion were determined gravimetrically (47.2 %), and the M_n^{SEC} = 23600 and $Đ$ = 1.61 of the resulting extended PVC-*b*-PVC were determined by SEC.

Results

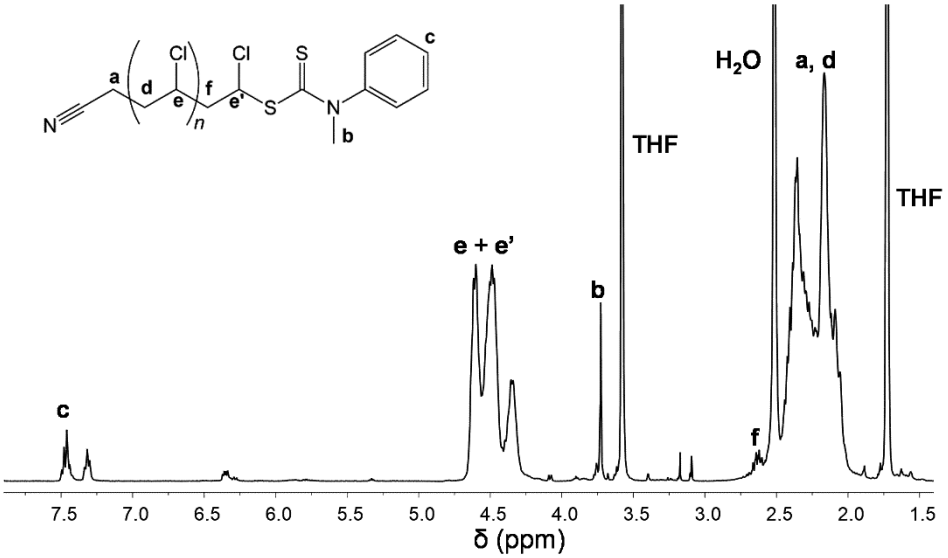

Fig. B1: The ^{1}H NMR spectrum in d_8 -THF of PVC-CTA (M_n^{SEC} = 4200; $Đ$ = 1.54) obtained in Table 3-1, entry 5.

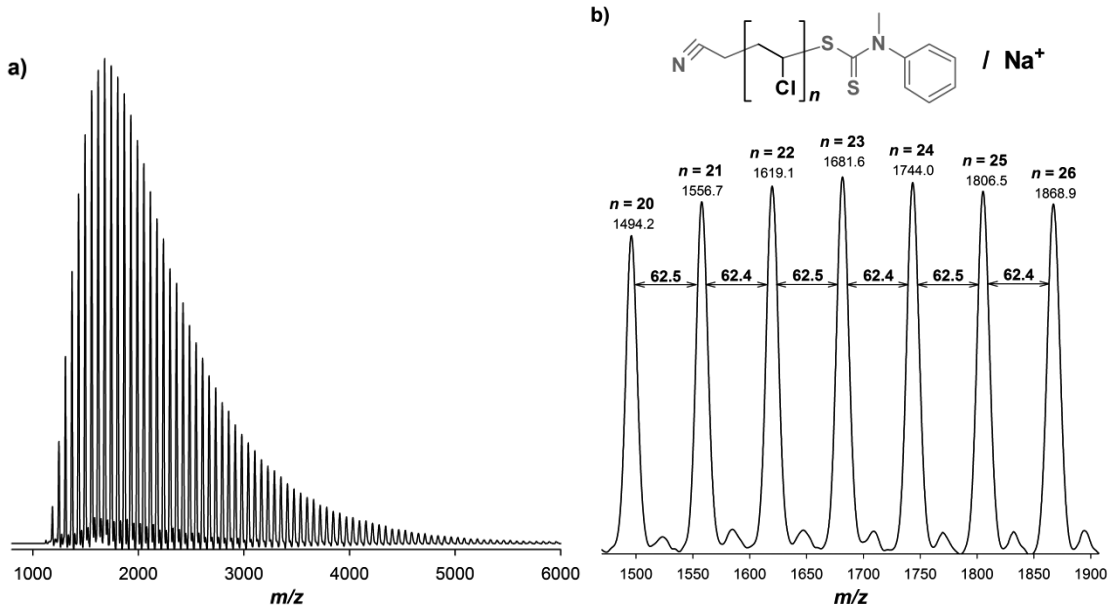

Fig. B2 (a) MALDI-TOF-MS in the linear mode (using HABA as matrix) of PVC-CTA (M_n^{SEC} = 4200, $Đ$ = 1.54) obtained in Table 3-1, entry 5; (b) Enlargement of the MALDI-TOF-MS from m/z 1500 to 1900 of PVC-CTA.

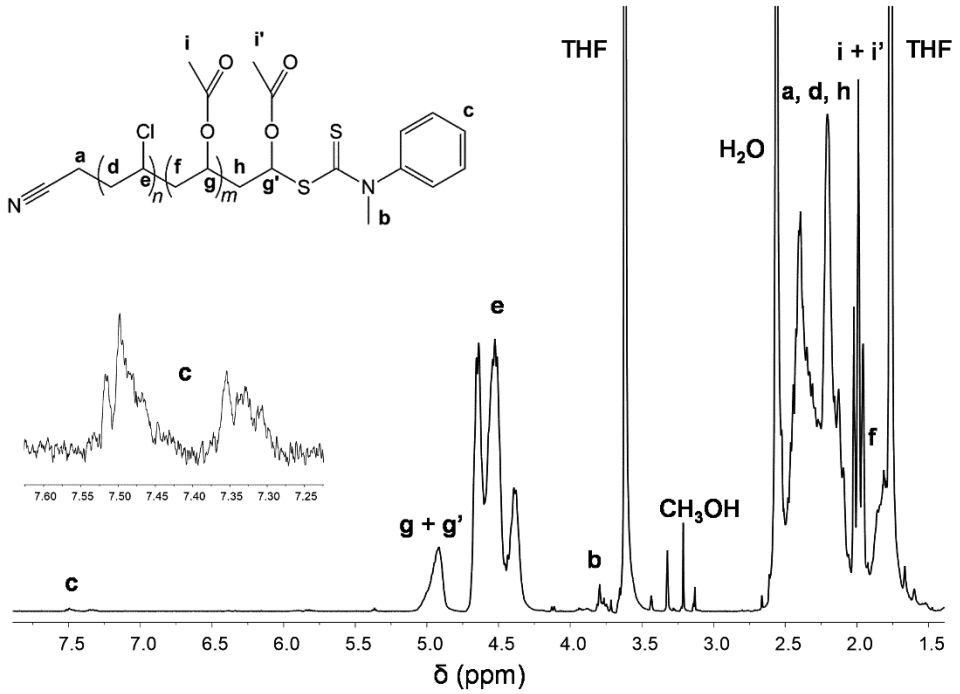

Fig. B3: ^{1}H NMR spectrum of the PVAc-*b*-PVC diblock copolymer (M_n^{SEC} = 30200; $Đ$ = 1.59) in d_8-THF.

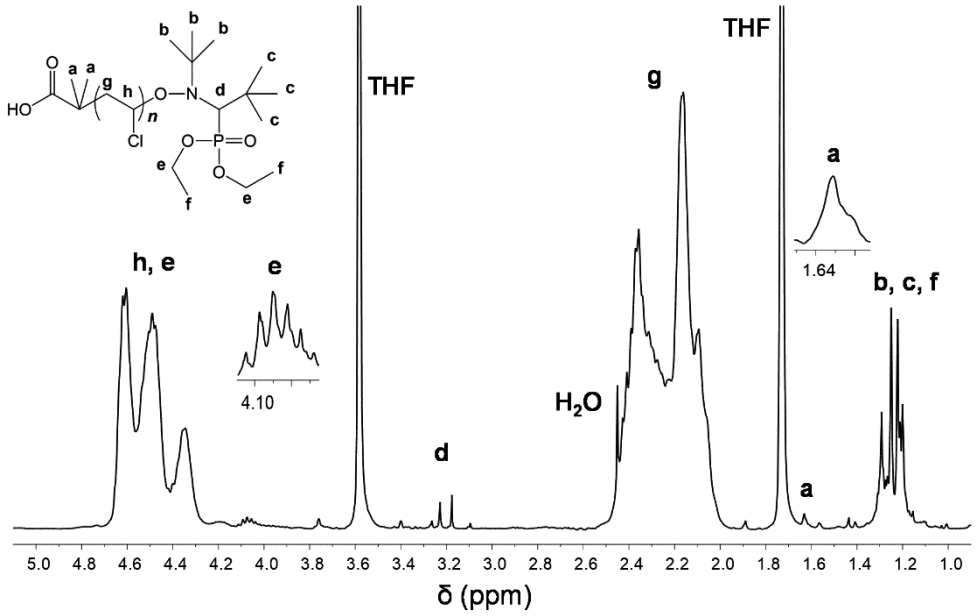

Fig. B4: ^{1}H NMR spectra in d_8-THF of a purified PVC (M_n^{SEC} = 4300; $Đ$ = 1.55) obtained in Table 3-2, entry 4.

Appendix C: Supporting Information for "Ambient temperature «flash» SARA ATRP of methyl acrylate in water/ionic liquid/glycols mixtures"

Experimental Section

Materials

1-Butyl-3-methylimidazolium hexafluorophosphate (BMIM-PF6, >98%; TCI (Tokyo Chemical Industry Co. LTD)), copper(II) bromide ($CuBr_2$, +99% extra pure, an-hydrous; Acros), deuterated chloroform (CDCl3, +1% tetramethylsilane (TMS); Euriso-top), DMSO (+99.8% extra pure; Acros), diethylene glycol (DEG, 99%, Sigma-Aldrich), ethyl 2-bromoisobutyrate (EBiB, 98 %; Aldrich), ethylene glycol (EG, ≥ 99%, Sigma-Aldrich), iron powder (Fe(0) (Acros, 99%, ~70 mesh), polystyrene (PS) standards (Polymer Laboratories), Reichardt's dye (30) (90 %, Sigma-Aldrich), sodium hydrosulfite also known as sodium dithionite ($Na_2S_2O_4$, 85%, technical grade; Aldrich) and triethylene glycol (TEG, 99%, Acros) were used as received.

MA (99% stabilized; Acros) was passed over a sand/alumina column before use to remove the radical inhibitor.

Metallic copper (Cu(0) wire, d = 1 mm, Sigma Aldrich) was washed with HCl in methanol and subsequently rinsed with methanol and dried under a stream of nitrogen following the literature procedures. [1]

Me_6TREN was synthesized according the procedure described in the literature. [2]

Purified water (Milli-Q®, Millipore, resistivity >18 MΩ.cm) was obtained by reverse osmosis.

Tetrahydrofuran (THF, high-performance liquid chromatography (HPLC) grade; Panreac) was filtered (0.2 μm filter) under reduced pressure before use.

Techniques

The chromatographic parameters of the samples were determined using high performance size exclusion chromatography (HPSEC); Viscotek (Viscotek TDAmax) with a differential viscometer (DV); right-angle laser-light scattering (RALLS) (Viscotek); low-

angle laser-light scattering (LALLS) (Viscotek) and refractive index (RI) detectors. The column set consisted in a Tguard column (8 μm) followed by one Viscotek T2000 column (6 μm), one MIXED-E PLgel column (3 μm) and one MIXED-C PLgel column (5 μm). A HPLC dual piston pump was set at a flow rate of 1 mL/min. The eluent, THF, was previously filtered through a 0.2 μm filter. The system was also equipped with an on-line degasser. The tests were done at 30 °C using an Elder CH-150 heater. Before the injection (100 μL), the samples were filtered through a polytetrafluoroethylene (PTFE) membrane with 0.2 μm pore. The system was calibrated with narrow polystyrene (PS) standards. The dn/dc of PMA was determined as 0.063. The number-average molecular weight (M_{nSEC}) and dispersity ($Đ$) of synthesized polymers were determined by multidetectors calibration using OmniSEC software version: 4.6.1.354.

400 MHz 1H NMR spectra of the reaction mixture samples were recorded on a Bruker Avance III 400 MHz spectrometer, with a 5-mm TIX triple resonance detection probe, in $CDCl_3$ with TMS as an internal standard. Conversion of the monomer was determined by integration of monomer and polymer peaks using MestRenova software version: 6.0.2-5475.

The UV/Vis studies were performed with a Jasco V-530 spectrophotometer. The analyses were carried out in the 350–1100 nm range at room temperature.

Fundamentals of solvatochromic probe polarity tests [3, 4]

A solvatochromic probe is a substance that is capable of changing its color in the presence of solvents with different polarities. This is due to the solvatochromic effect: a shift in the absorption spectra of the substance as the medium polarity changes. The betaine dye 4-(2,4,6-triphenylpyridinium-1-yl)-2,6-diphenylphenolate, also known as Reichardt's Dye (30), represented in Figure C1, is an example of a solvatochromic probe. In its ground state (Figure C1 (a)) this molecule is zwitterionic (i.e. it has simultaneously a partial positive charge and a partial negative charge) and highly polar. However, upon absorption of light with a certain amount of energy ($E = h\nu = hc/\lambda$), a transition occurs to a nonpolar excited state (Figure C1 (b)), corresponding to an electron being transferred from the phenoxide to the pyridinium moieties.

The energy required to cause this transition to the excited state depends heavily on the polarity of the solvent present in the medium. If the solvent has high polarity, it will stabilize the polar ground state and therefore the energy required for the transition will

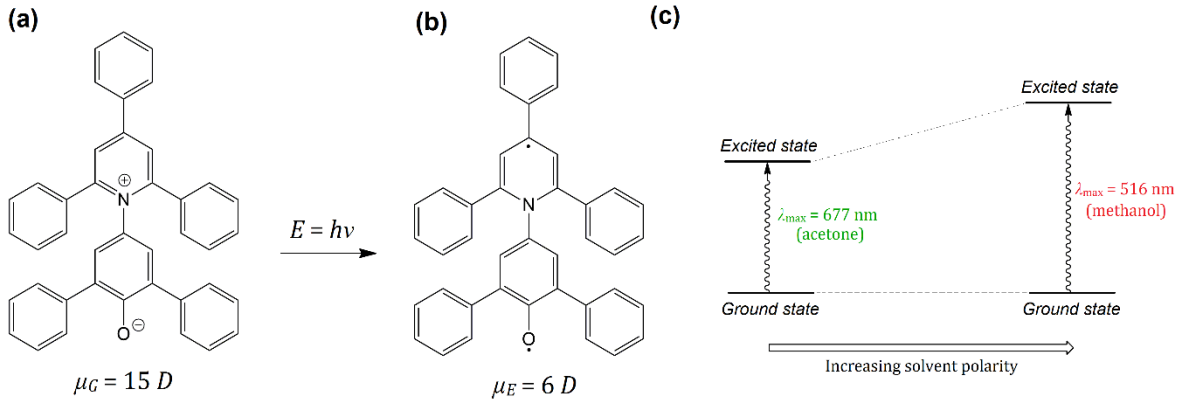

Figure C1: Representations of the ground state (a) and excited state (b) of Reichardt's Dye (30). The values underneath each structure are their respective electric dipole moments, μ, in Debye (D) units. (c) – Scheme illustrating the change in transition energy with solvent polarity, with the examples of acetone and methanol. Adapted from ref. 3 (see below).

be higher (and so the wavelength of absorbed light will be smaller). On the other hand, if the solvent has low polarity it will tend to stabilize the excited state, resulting in lower energies required for transition (correspondent to higher wavelengths of absorbed light). This behavior is known as the negative solvatochromic effect (λ decreases with increasing polarity) but the opposite (positive) effect is also possible with other solvatochromic probes.

For Reichardt's Dye (30) this transitions usually occur in the region of visible light, and so a change in solvent polarity is usually accompanied by a change in the color of the solution. By measuring the absorption spectra of the solution on a UV/Vis spectrophotometer, the wavelength corresponding to the maximum in the spectrum (λ_{max}) can be determined and, with it, the molar transition energy can be calculated. This energy, represented by $E_T(30)$, is therefore a measure of a solvent's polarity and can be calculated by the following expression:

$$E_T(30) \quad (kcal \cdot mol^{-1}) = h\nu_{\max} N_A = \frac{hcN_A}{\lambda_{\max}} = \frac{28591}{\lambda_{\max}(nm)}$$

Sometimes this values are normalized using two reference solvents (tetramethylsilane and water), according to the formula:

$$E_T^N = \frac{E_T(30)\big|_{solvent} - E_T(30)\big|_{TMS}}{E_T(30)\big|_{water} - E_T(30)\big|_{TMS}} = \frac{E_T(30)\big|_{solvent} - 30.7}{32.4}$$

thus creating a scale from 0 (TMS) to 1 (water). It should be emphasized that E_T (30) is a specific polarity parameter associated with the Reichardt's Dye (30) probe. Other probes will give other parameters.

UV/Vis spectroscopy of BMIM-PF_6/DMSO/glycols and BMIM-PF_6/H_2O/TEG

Typically, the Reichardt's Dye (30) betaine (1 mg, 50μM) was weighted to a vial, followed by BMIM-PF_6 and subject to vigorous agitation until the complete dissolution of the dye. Then, a glycol/ DMSO mixture (or TEG/water) was added to the vial and the resulting mixture was stirred leading to a homogeneous solution. From these solutions, samples with different molar fractions of glycols were prepared with a final volume of 3 mL. Each sample solution was then added to a quartz UV/Vis cuvette and placed in the spectrophotometer for spectra acquisition. The absorbance was measured in the 350-1100 nm range at room temperature.

Procedures

Typical Procedure for the [$Na_2S_2O_4$]/[$CuBr_2$]/[Me_6TREN] = 1/0.1/0.2 catalyzed SARA ATRP of MA (DP=222) in BMIM-PF_6/DMSO/TEG = 45/45/10 (v/v)

In a typical SARA ATRP polymerization of MA, $Na_2S_2O_4$ (40.984 mg, 0.2 mmol) was placed in a Schlenk reactor. A mixture of $CuBr_2$ (4.47 mg, 0.02 mmol), Me_6TREN (9.22 mg, 0.04 mmol), DMSO (0.900 mL), TEG (0.200 mL) and BMIM-PF_6 (0.900 mL) was added to the reactor. Finally, a mixture of MA (4 mL, 44.42 mmol) and EBiB (39.82 mg, 0.2 mmol) was also added to the Schlenk reactor, which was sealed and frozen in liquid nitrogen. The Schlenk reactor containing the reaction mixture was deoxygenated with four freeze-vacuum-thaw cycles and purged with nitrogen. The reactor was placed in a water bath at 30 °C with stirring (700 rpm). During the polymerization, different reaction mixture samples were collected by using an airtight syringe and purging the side arm of the Schlenk reactor with nitrogen. The samples were analyzed by ^{1}H NMR spectroscopy to determine the monomer conversion and by SEC, to determine the $M_{n,SEC}$ and $Đ$ of the polymers.

Typical "one-pot" chain extension of PMA-Br

MA (1.0 mL, 11.0 mmol), EBiB (54.9 mg, 0.28 mmol), $CuBr_2$ (6.2 mg, 27.6 µmol), Me_6TREN (12.7 mg, 55.2 µmol), water (50 µL), BMIM-PF_6 (230 µL) and TEG (230 µL) were added to a 25 mL Schlenk flask equipped with a magnetic stirrer bar. Next, $Na_2S_2O_4$ (56.5 mg, 0.28 mmol) was added to the Schlenk flask, which was sealed with a glass stopper, deoxygenated with four freeze-vacuum-thaw cycles and purged with nitrogen. The reaction was allowed to proceed with stirring (700 rpm) at 30 °C. When the monomer conversion reached more than 95%, a degassed mixture of MA (11.9 mL, 0.14 mol), water (440 µL), BMIM-PF_6 (2.0 mL) and TEG (2.0 mL) was added to the Schlenk flask under nitrogen. The monomer conversion was determined by ^1H NMR spectroscopy and the $M_{n,SEC}$ and Đ were determined by SEC.

Results

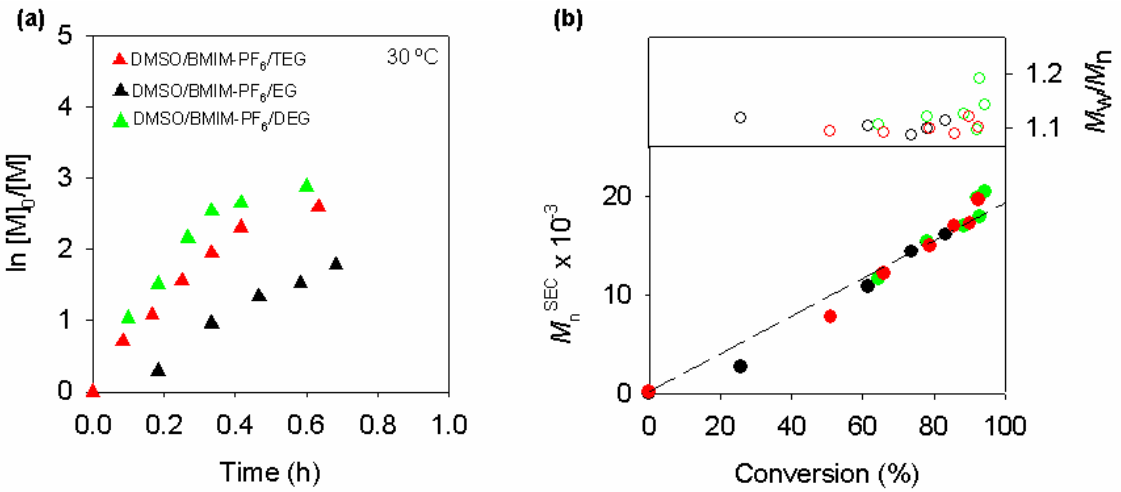

Figure C2. (a) Kinetic plots of conversion and $\ln[M]_0/[M]$ *vs.* time and (b) plot of number-average molecular weights (M_n^{SEC}) and *Đ* (M_w/M_n) *vs.* monomer conversion for the SARA ATRP of MA in DMSO/BMIM-PF_6/glycol = 45/45/10 (v/v/v) at 30 °C, using different glycols: TEG (red symbols); EG (black symbols) and DEG (green symbols). Reaction conditions: $[MA]_0/[solvent]$ = 2/1 (v/v); $[MA]_0/[EBiB]_0/Cu(0)/[CuBr_2]_0/[Me_6TREN]_0$= 222/1/Cu(0) wire/0.1/1.1.

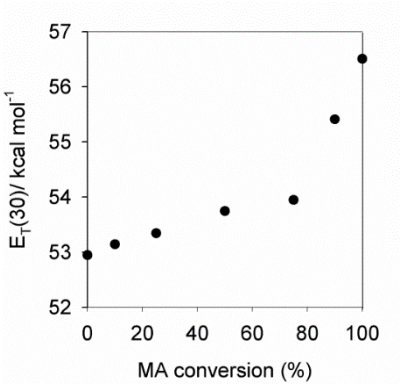

Figure C3. Experimental E_T (30) values of H_2O/BMIM-PF_6/TEG mixtures containing different amounts of MA in order to simulate the monomer conversion during a typical "flash" SARA ATRP of MA. Conditions: Reichardt's dye (30) concentration = 50 μM.

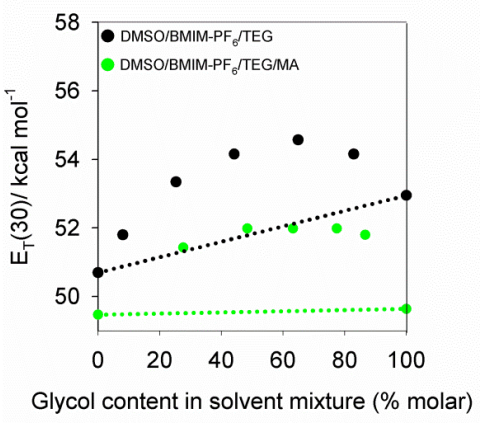

Figure C4. Experimental E_T (30) values of DMSO/BMIM-PF_6/TEG (black symbols) and DMSO/BMIM-PF_6/TEG/MA (green symbols) mixtures with Reichardt's dye (30) (concentration = 50 μM). Dashed line represents the theoretical E_T (30) values for each solvent mixture.

References

[1] Zhang, Y., Wang, Y., Peng, C.-h., Zhong, M., Zhu, W., Konkolewicz, D., et al., *Copper-Mediated CRP of Methyl Acrylate in the Presence of Metallic Copper: Effect of Ligand Structure on Reaction Kinetics*, Macromolecules, **2012**, 45, 78-86.

[2] Ciampolini, M., Nardi, N., *Five-Coordinated High-Spin Complexes of Bivalent Cobalt, Nickel, andCopper with Tris(2-dimethylaminoethyl)amine*, Inorganic Chemistry, **1966**, 5, 41-44.

[3] Reichardt, C., *Pyridinium N-phenolate betaine dyes as empirical indicators of solvent polarity: Some new findings*, Pure and applied chemistry, **2004**, 76, 1903-1919.

[4] Reichardt, C., Welton, T., *Solvents and Solvent Effects in Organic Chemistry*. 3rd ed. John Wiley & Sons, New York, 2003.